THE HIGHLY PREORGANIZED LIGANDS 8-(2-PYRIDYL)QUINOLINE, 2,2'-DIPYRIDYL AMINE AND 1,10-PHENANTHROLINE-2, 9-DICARBOXYLIC ACID, AND THEIR COMPLEXING PROPERTIES WITH METAL IONS

Charles Richard Gaver Jr.

A Thesis Submitted to the
University of North Carolina Wilmington in Partial Fulfillment
of the Requirements for the Degree of
Master of Science

Department of Chemistry

University of North Carolina Wilmington

2008

Approved by

Advisory Committee

Dr Bart Jones Dr John Tyrell

Dr Robert Hancock
Chair

Accepted by

DN: cn=Robert D. Roer, o=UNCW, ou=Dean of the Graduate School & Research, email=roer@uncw.edu, c=US
Date: 2009.02.16 11:59:42 -05'00'

Dean, Graduate School

TABLE OF CONTENTS

ABSTRACT

Highly preorganized ligands are those that are constrained as the free ligands to be in the conformation required to complex the target metal ion. Such ligands have been shown to form more stable complexes, and display higher metal ion selectivity than less preorganized analogs. These ligands have become of particular interest in a variety of different areas, including biomedical, environmental, nuclear and industrial applications. The preorganized ligands 8-(2-pyridyl)Quinoline (8PQ), 2,2'-dipyridyl amine (DIPY), and 1,10-phenanthroline-2, 9-dicarboxylic acid (PDA) and their complexing properties with metal ions are explored in this project.

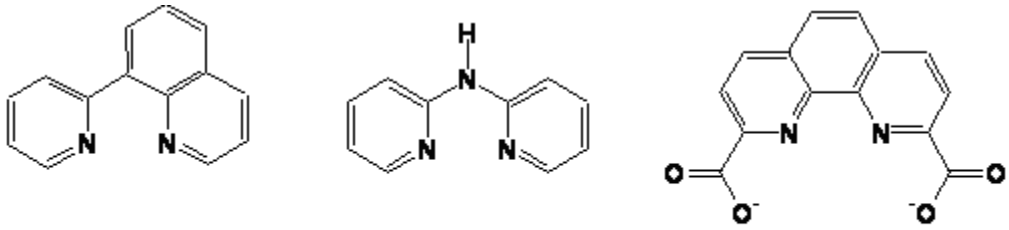

8PQ DIPY PDA

The interest in 8PQ and DIPY is that they form six-membered chelate rings on complex-formation. Following rules on ligand design[1], ligands that form six-membered chelate rings should show selectivity for smaller metal ions as compared to analogs such as 2,2'-bipyridyl that form five-membered chelate rings.

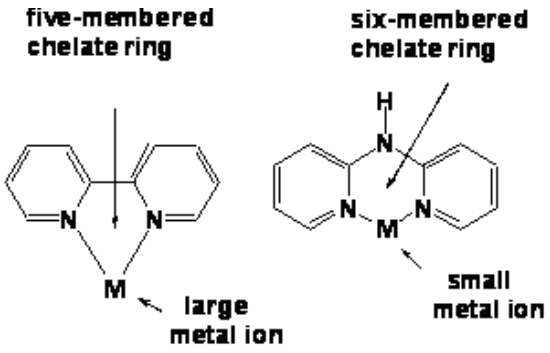

Thus, 8PQ and DIPY can be compared in this regard to BIPY, which forms a five-membered chelate ring. Titration experiments were carried out on aqueous solutions of these ligands and metal ions in order to determine their formation constants. UV-Vis spectrophotometry was used to monitor the equilibria involved in the formation of metal-ligand complexes. The log K_1 values for the formation of metal-ligand complexes were determined from UV absorbance data as a function of pH, and are reported in 0.1 *M* $NaClO_4$ at 25.0ºC. Formation constants (log K_1, in parentheses) for 8PQ with Cd(II) (2.19), Ca(II) (≈0), Cu(I) (4.66), Cu(II) (4.37), Ni(II) (3.3), and Zn(II) (3.48); DIPY with Al(III) (≈0), Cd(II) (2.67), Co(II) (4.36), Cu(II) (7.34), Ga(III) (≈0), Ni(II) (6.15), and Zn(II) (3.52); and PDA with In(III) (19.78) and UO_2^{2+} (≈19.78) are reported. The results are discussed in terms of the role of chelate ring geometry in controlling metal ion selectivity.

ACKNOWLEDGEMENTS

I would like to thank my advisor Dr. Robert Hancock for allowing me the opportunity of working with him and for all of his help and guidance with my research project. I would also like to thank my committee members, Dr. Bart Jones and Dr. John Tyrell for their willingness to help me with any questions or problems I came upon. Research would not have been possible without the fine facilities provided to me by UNCW and the Chemistry department.

I would like to thank my parents Charlie and Jackie Gaver for all their love and support. They have always been there for me when ever I needed them. I really appreciate all that they have done and continue to do for me. Finally, I'd like to that my friends for their support and making my experience here more enjoyable.

LIST OF TABLES

LIST OF FIGURES

INTRODUCTION

The study of metal-ligand interactions is currently of considerable importance in the field of medicinal chemistry, since metal ions have been found to control vital processes in the human body. After largely focusing on the foundation of 24 fundamental elements in the body, research has expanded to encompass the usage of non-essential elements as well. Figure 1 depicts a periodic table labeling some if the usages for these nonessential elements. Some of the medical applications based on these inorganic relationships range from chelation therapy, for the removal of metal ions such as Pb(II) from the body, to magnetic resonance imaging (MRI)[1] and radiopharmacology.[2] Gd(III), which is used extensively as an MRI contrast agent, is a key example of a nonessential element with applications in medicinal chemistry. Gd(III) has the toxic effect of displacing Zn(II) within the body which is why ligand design fills an important role in selectively chelating Gd(III). Gd(III) has 7 unpaired electrons and long relaxation time that allows it to coordinate H_2O molecules to its inner sphere.[3] This produces a contrast between the ^{1}H-signal of H_2O coordinated to Gd(III) and the ^{1}H-signal of H_2O found naturally in biological fluids. As Gd(III) is highly toxic, Gd(III) is usually bound to a metal ion selective chelating agent such as diethylenetriamine pentaacetic acid (DTPA) before it is introduced into the body. The chemical structure of this complex is shown in Figure 2. This complex is used because DTPA forms a strong complex with Gd^{3+} (log K_1 22.39) (NIST).

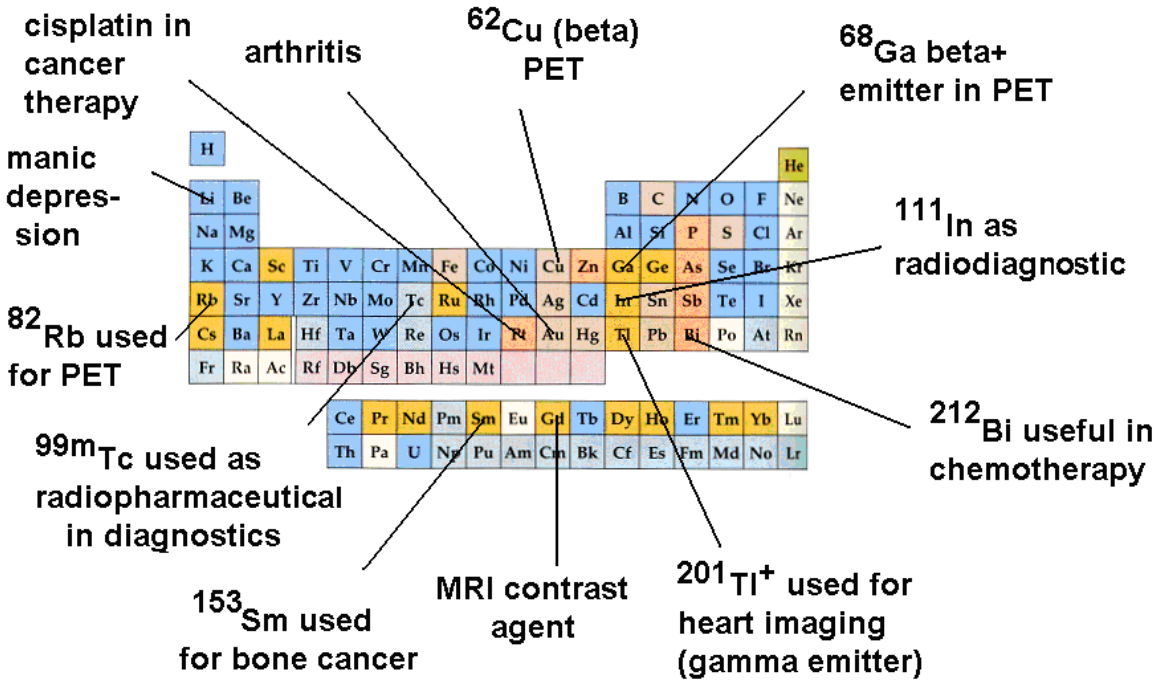

Figure 1: A diagram of some common uses of metal ions in medicinal chemistry.

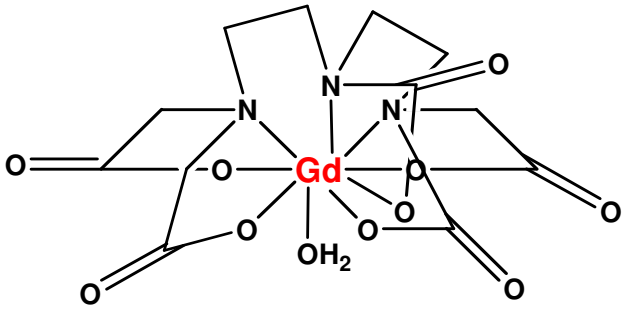

Figure 2: Chemical structure of the $[Gd(DTPA)OH_2]^{2-}$ complex used as a MRI contrast agent

Other applications for metal complexes include sequestration of radioactive isotopes such as ^{212}Bi for treatment of cancer[4] and in the development of sensors, known as chemosensors, for monitoring the distribution and movement of metal ions in living cells.[5] Chemosensors are molecules that transform chemical information, such as the presence of a specific metal ion, into an analytically useful signal.[6] These sensors take advantage of their ability to undergo chelation-enhanced fluorescence (CHEF). This means that metal binding triggers intense fluorescence of the sensor and the unbound molecule is non-fluorescent.[6] The goal of ligand design is to develop ligands which are highly selective for a desired metal ion, and that form complexes of high thermodynamic stability when bound to them. The selective chelation of a metal ion by a ligand can be enhanced by the degree of preorganization of the chelate structure. Donald J. Cram was the first to define the concept of preorganization.[7] A ligand is considered to be more preorganized when it is more constrained to be in the conformation needed to complex with a metal ion.

The ligands that are the subject of this research are 8PQ, DIPY, and PDA, shown below.

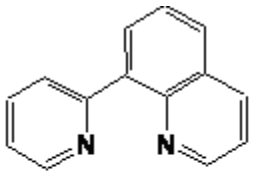

8PQ

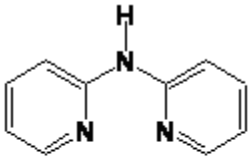

DIPY

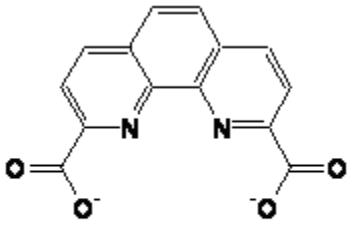

PDA

These ligands are of interest because of a variety of structural features that should lead to interesting metal ion complexing properties. One important property is that of

preorganization. Crown ethers[8,9] and cryptands[10,11] are the most common and widely studied highly preorganized ligands that form complexes of high thermodynamic stability with metal ions, due to their preorganized conformations. The enhanced complex stability of these ligands, the macrocyclic[12] and cryptate[13] effects, has led to the discovery of other chelating agents with similar binding properties. These macrocycles are able to selectively complex certain metal ions over others due to their structural rigidity. Ligands such as 8PQ, DIPY, and PDA above all have extended aromatic systems that should lead to considerable rigidity, and hence enhanced levels of preorganization. The ability of macrocycles to selectively complex various metal ions is also based on their chelating ring size. A rule of ligand design has been formulated that states that the changing of a chelate ring from five-membered to six-membered in a given ligand will shift selectivity in the direction of smaller metal ions.[14] This can be summarized as in Figure 3. In Figure 3 one sees that six-membered chelate rings favor complex-formation with very small metal ions, and 8-PQ and DIPY studied here should show selectivity for small metal ions because of their formation of six-membered chelate rings.

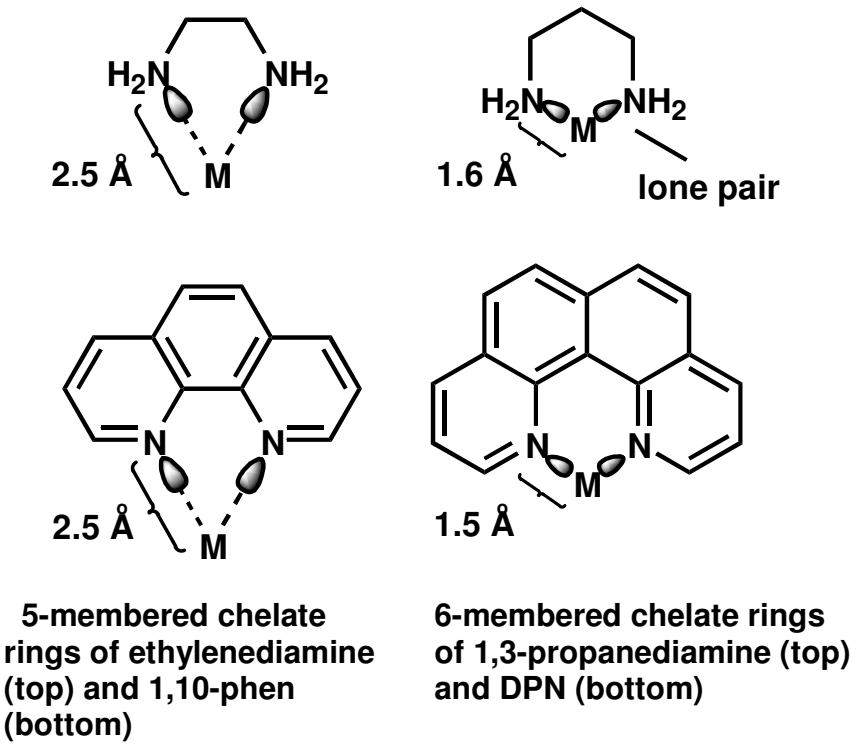

Figure 3: A diagram of the best-fit M-N lengths for metal ions required to form a minimum-stain chelate ring with ethylenediamine and 1,10-phen (five-membered chelate ring) or 1,3-propanediamine and DPN (dipyridonaphthalene) (six-membered chelate ring).

The smallest metal ion Be^{2+}, which has an ionic radius of 0.27 Å (all metal ion radii were obtained from reference 15), is comparable in size to the bond lengths between carbon atoms in a cyclohexane ring so that it forms a more stable complex in six-membered chelate rings. Carbon atoms are equidistant from each other in a cyclohexane ring and the hydrogen atoms are all in a staggered formation. Cyclopentane, a five-membered ring, is not nearly as stable because the axial hydrogens partially eclipse each other. When a smaller metal ion is introduced into a five-membered chelate ring, a strained ring results, and a weaker complex is formed. However, when a large metal ion

is introduced into a five-membered chelate ring, the hydrogen atoms adjust to become staggered from the change in metal to ligand bond length making complexation more favorable.[16] In each case, for five and six membered chelate rings, there is a rapid rise in ring strain energy as the metal ion becomes less ideal in size and geometry, and there is a lowering of complex stability. This effect can be seen in Figure 4, where there is a greater decrease in complex stability for large metal ions with an increase in chelate ring size in two different open chain ligands.[1] Using this approach it is possible to accurately predict the changes that occur in the formation constant, log K_1. This is summarized in Fig. 5, where it can be seen that there is a strong correlation of complex stability with the ionic radius of the metal ions and chelate ring size.

One would expect a similar change in selectivity in comparing 8PQ and DIPY to BIPY, shown in Figure 3 above. The six-membered chelate rings formed by 8PQ and DIPY should lead to a strong preference for smaller metal ions such as Cu(II), as compared to larger metal ions such as Cd(II). In contrast, PDA forms exclusively five-membered chelate rings, and so should show preference for larger metal ions such as Cd(II), Gd(III), or Th(IV), as previous studies have already demonstrated.[17,18]

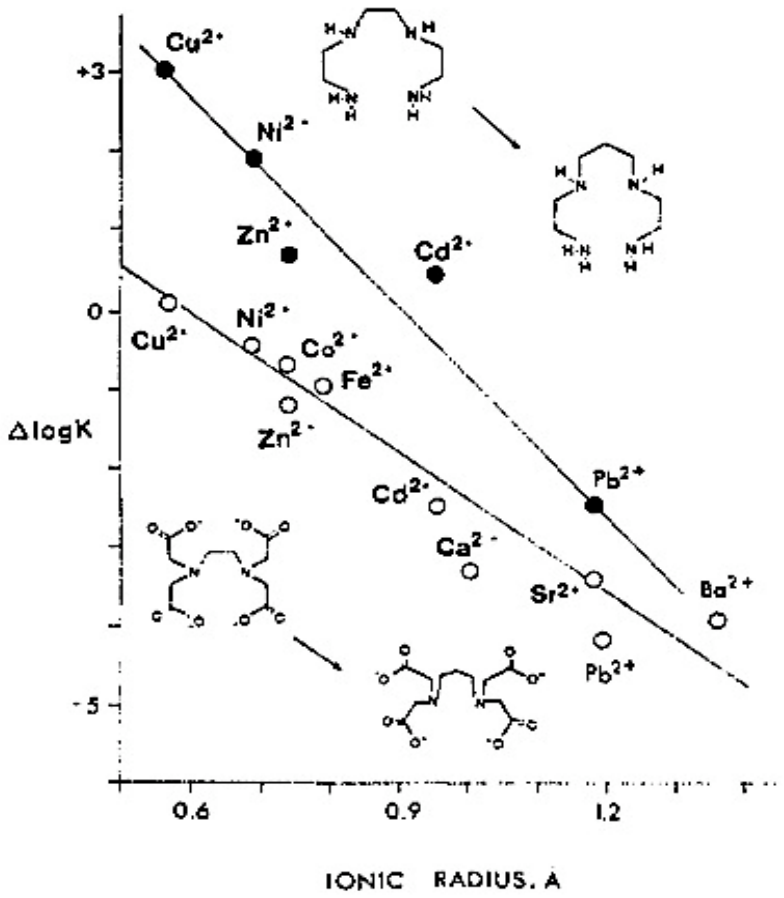

Figure 4: Plot of Δ log *K* versus ionic radius (Å) for two different open chain ligands to illustrate the effect on complex stability with an increase of chelate ring size from a five membered ring to a six membered ring. Δ log *K* in each case is log K_1 for the ligand that forms a six-membered chelate ring (e.g. 2,3,2-tet) minus log K_1 for the analogue that forms a five-membered chelate ring (e.g. 2,2,2-tet). At bottom Δ log *K* is log K_1 for the TMDTA complex minus log K_1 for the EDTA complex.[15]

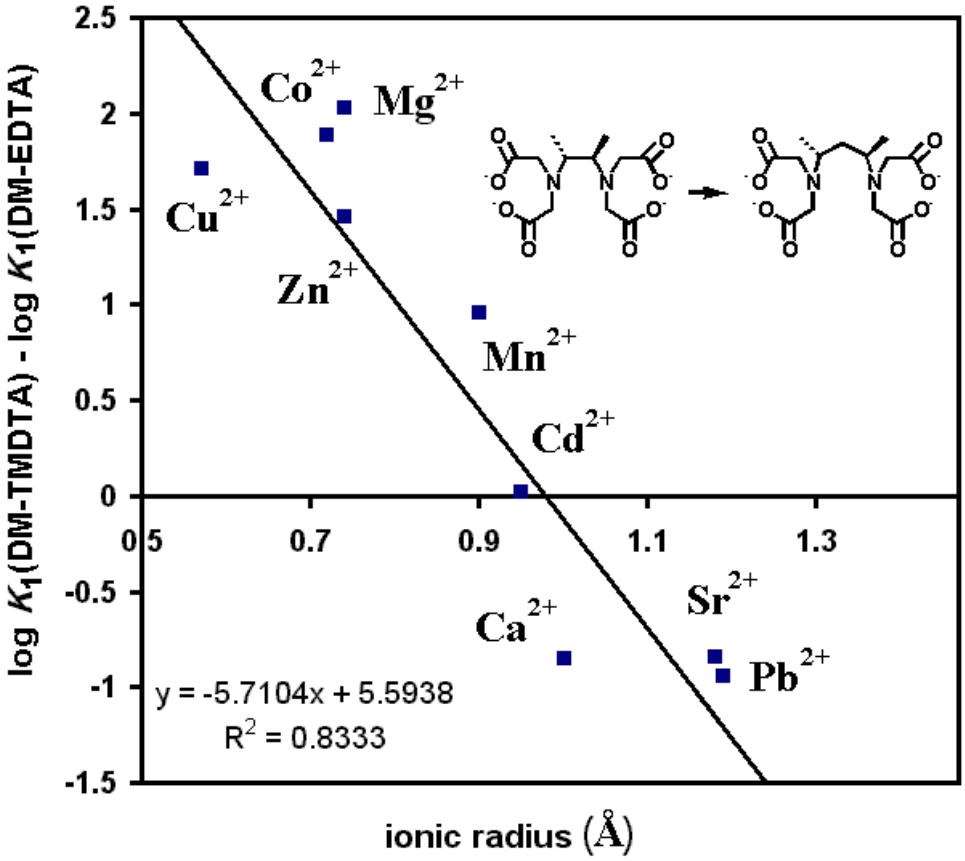

Figure 5: A diagram illustrating the linear free energy relationship (LFER) that shows metal ion size-related change in selectivity (Δlog *K*) as a function of metal ion radius for *trans*-DM-EDTA (5-membered chelate ring involving the two N-donors) relative to DM-TMDTA (6-membered chelate ring involving the two N-donors) complexes. Of interest here is the way in which the small Zn(II) ion benefits from the presence of a six-membered chelate ring in its DM-TMDTA complex.[15]

The coordination number of a target metal ion is an important factor to consider when designing a ligand. The coordination number determines the number of binding sites that the metal ion contains. Denticity is defined as being the number of donor atoms that a ligand has to offer. Increasing the denticity to the point where the number of donor atoms is equal to the coordination number of the metal ion increases the stability of the complex formed. This effect is shown in Table 1 in which the stability constant of Ni^{2+} increases as the denticity increases in a series of polyamine ligands.

Polyamine	EN	DIEN	TRIEN	TETREN	PENTEN
denticity, n	2	3	4	5	6
log β_n (NH_3)	5.08	6.85	8.12	8.93	9.08
log K_1 (polyamine)	7.47	10.7	14.4	17.4	19.1

Ionic Strength =	0.5 *M*
EN	$NH_2CH_2CH_2NH_2$
DIEN	$NH_2(CH_2CH_2NH)_2H$
TRIEN	$NH_2(CH_2CH_2NH)_3H$
TETREN	$NH_2(CH_2CH_2NH)_4H$
PENTEN	$NH_2(CH_2CH_2NH)_5H$
Log $\beta_n(NH_3)$ =	$\log(K_1 \times K_2$ ----- $\times K_n)$

Table 1: Stability constants of Ni^{2+} complexes in a series of polyamine ligands to show the effect of increasing ligand denticity.

A further important factor in ligand design is the nature of the metal-ligand bond, the extent of covalence or ionicity in the bond. After observing a pattern of variation of log K_1 values for the formation of metal-ligand complexes, Pearson proposed the principle of hard and soft acids and bases (HSAB) in 1963.[19] The principle of HSAB states that hard acids prefer hard bases and soft acids prefer soft bases.[19] A soft base is defined as a donor atom that has high polarizability, low electro negativity, and is easily oxidized. A hard base is a donor atom that has low polarizability, high electro negativity, and is not easily oxidized. A soft acid is defined as an acceptor atom that has a low positive charge, large size and outer electrons that are easily excited. A hard acid is an acceptor atom that has a large positive charge, small size, and lacks easily excited outer electrons. This is an important principle to consider when designing a ligand, as the donor atoms will affect the binding strength. The classification of Lewis acids as hard, soft or intermediate can be seen in Figure 6. The classification of hard and soft acids and bases is shown in Table 2.

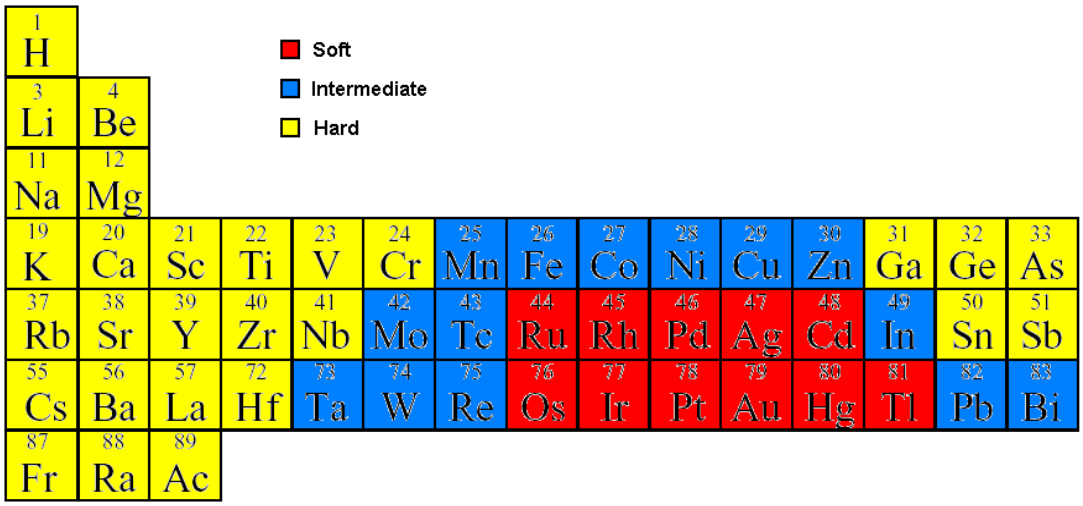

Figure 6: Classification of metals according to the HSAB principle[19] and illustration of trends in the periodic table.

Classification of Lewis Acids	
Class (a)/Hard	Class (b)/Soft
H^+, Li^+, Na^+, K^+	Cu^+, Ag^+, Au^+, Tl^+, Hg^+, Cs^+
Be^{2+}, Mg^{2+}, Ca^{2+}, Sr^{2+}, Sn^{2+}	Pd^{2+}, Cd^{2+}, Pt^{2+}, Hg^{2+}
Al^{3+}, Se^{3+}, Ga^{3+}, In^{3+}, La^{3+}	CH_3Hg^+
Cr^{3+}, Co^{3+}, Fe^{3+}, As^{3+}, Ir^{3+}	Tl^{3+}, $Tl(CH_3)_3$, RH_3
Si^{4+}, Ti^{4+}, Zr^{4+}, Th^{4+}, Pu^{4+}, VO^{2+}	RS^+, RSe^+, RTe^+
UO_2^{2+}, $(CH_3)_2Sn^{2+}$	I^+, Br^+, HO^+, RO^+
$BeMe_2$, BF_3, BCl_3, $B(OR)_3$	I_2, Br_2, INC, etc.
$Al(CH_3)_3$, $Ga(CH_3)_3$, $In(CH_3)_3$	Trinitrobenzene, etc.
RPO_2^+, $ROPO_2^+$	Chloranil, quinones, etc.
RSO_2^+, $ROSO_2^+$, SO_3	Tetracyanoethylene, etc.
I^{7+}, I^{5+}, Cl^{7+}	O, Cl, Br, I, R_3C
R_3C^+, RCO^+, CO_2, NC^+	M^0 (metal atoms)
	Bulk metals
HX (hydrogen-bonding molecules)	
Borderline	
Fe^{2+}, Co^{2+}, Ni^{2+}, Cu^{2+}, Zn^{2+}, Pb^{2+}	
$B(CH_3)_3$, SO_2, NO^+	

Classification of Lewis Bases	
Hard	Soft
H_2O, OH^-, F^-	R_2S, RSH, RS^-
CH_3CO_2, PO_4^{3-}, SO_4^{2-}	I^-, SCN^-, $S_2O_3^{2-}$
Cl^-, CO_3^{2-}, ClO_4, NO_3^-	R_3P, R_3As, $(RO)_3P$
ROH, RO^-, R_2O	CN^-, RNC, CO
NH_3, RNH_2, N_2H_4	C_2H_4, C_6H_6
	H^-, R^-
Borderline	
$C_6H_5NH_2$, C_5H_5N, N_3^-, Br^-, NO_2^-, SO_3^{2-}, N_2	

Table 2: Classification of hard and soft acids and bases by Pearson's HSAB principle.[19]

The ligands 8PQ and DIPY contain only nitrogen-donor ligands, which makes them of interest in that they should bind only weakly with metal ions such as Mg^{2+}, which are widely present in nature, and might interfere with sensing of the softer Zn^{2+} or Cd^{2+} ions.

METHODS

All chemicals and reagents used were of analytical grade and purchased from commercial sources. All solutions were made up in deionized water (Milli-Q, Waters Corp.) of > 18 $M\Omega.cm^{-1}$ resistivity. UV/Vis absorbance spectra were recorded for aqueous metal-ligand titration experiments using a double beam Cary 1E UV/Vis spectrophotometer (Varian, Inc.) and WinUV Version 2.00(25) software. A 1.0 cm quartz flow cell, fitted with a variable flow peristaltic pump, was used to refresh the metal-ligand aqueous solution after each titrant addition was made to the sample. A schematic of the flow cell apparatus is shown in Figure 7(a). Equilibration times after each titrant addition varied between 5 to10 minutes but could range up to several hours depending on the kinetics of complex-formation of the metal ion being studied. Absorbance scan ranges were from 200 to 350 nm, or 350 to 800nm at a rate of 600 nm/min. All absorbance spectra were referenced by placing a 1.0 cm quartz cell filled with deionized H_2O in the path of the reference beam.

All pH values for the titration experiments were recorded using a SympHony SR60IC pH meter (VWR Scientific, Inc.), which was calibrated prior to each titration experiment by acid-base titration. Typically, 25.0 mL of 0.01 *M* $HClO_4$ in 0.09 *M*

$NaClO_4$ was placed in the cell, and titrated with 50 mL of 0.01 *M* NaOH in 0.09 *M* $NaClO_4$. The cell emf in mV was recorded for each titration point. A least-squares line was fitted to the relationship between emf and pH calculated for each titration point, which gave a slope corresponding to the Nernstian slope, with an intercept equal to E^o for the cell. A typical plot for the determination of E (cell) is seen in Figure 7(b).

Aqueous metal-ligand samples used in the titration experiments were in 0.1 *M* $NaClO_4$ for maintenance of a constant ionic strength, and the temperature was maintained at a constant 25.0 ± 0.1 °C throughout the experiment.

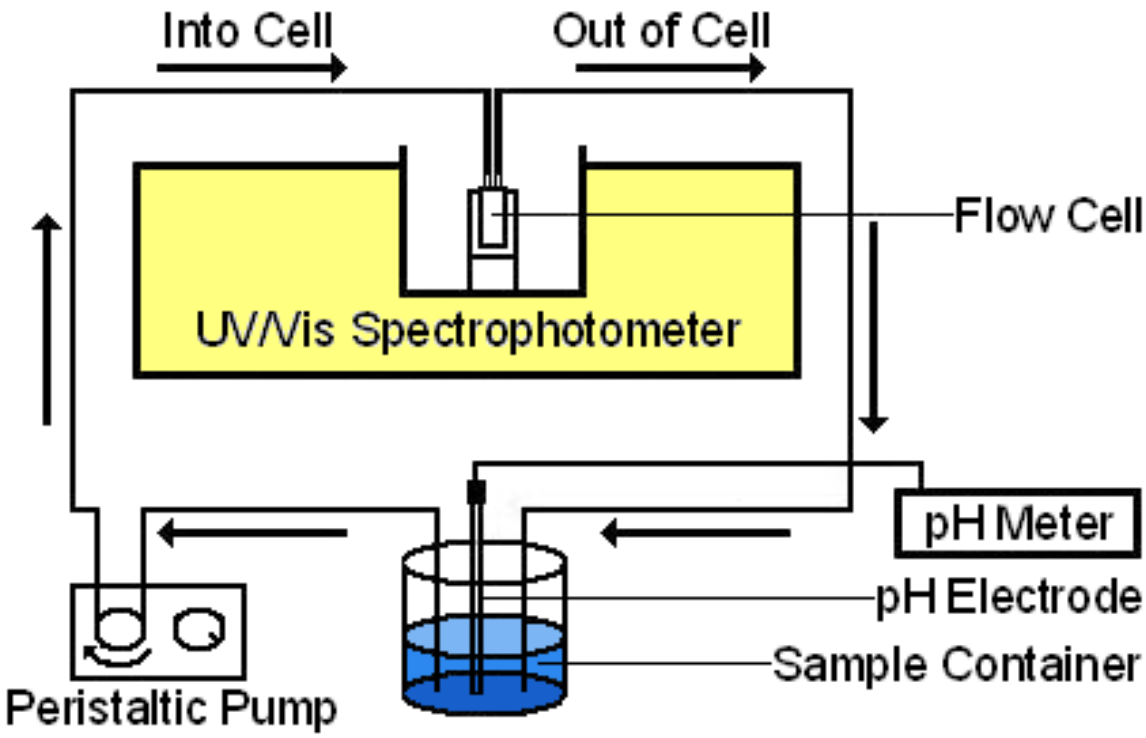

Figure 7(a): A schematic of the flow cell apparatus used in the titration experiments.

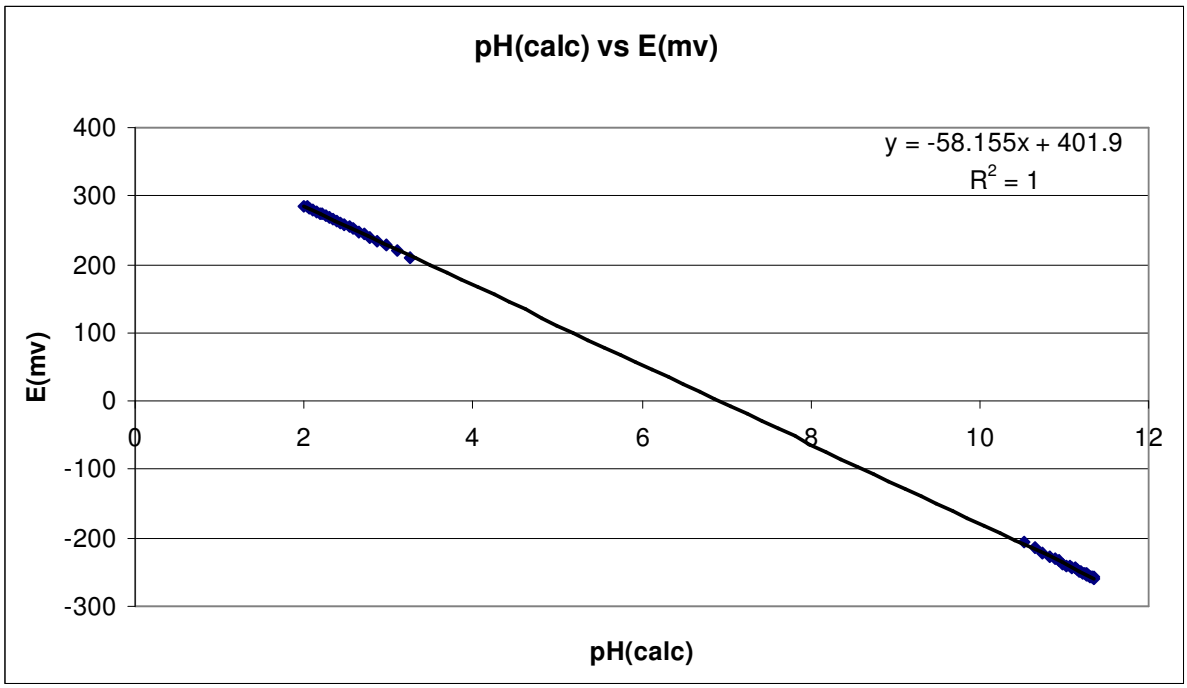

Figure 7(b): Plot for the calibration of the cell in a typical titration, where the measured potential for the cell (E) in mV is plotted against the pH calculated for the acid-base titration. The slope is seen to be 58.16 mV/decade, and the intercept, which is E^o for the cell, is 401.9 mV. The coefficient of determination (R^2) for the fit of the line to the experimental data is excellent at a value of 1.

Titrations Involving 8PQ

Acid-base titrations of aqueous metal ion/8PQ solutions were monitored using UV/Vis spectrophotometry. A stock solution of 2 x 10^{-5} *M* 8PQ in 0.01 *M* $HClO_4$ and 0.09 *M* $NaClO_4$ was used in the titration experiments.

Solutions for titration of 8PQ

In order to determine the protonation constants for 8PQ, 1L of 2 x 10^{-5} *M* 8PQ (4.1mg, synthesized by Dr. Randolph Thummel as described in the literature [20]) in 0.01 *M* $HClO_4$ (862 µl, 11.6 *M*, Alfa Aesar, 70%) and 0.09 *M* $NaClO_4$ (11.021 g, Alfa Aesar, 98-102%) was prepared. A 50.0 ± 0.05 mL aliquot of this solution was placed in the flow cell apparatus described above and titrated with 0.01 *M* NaOH (100 µl, 10 *M*, VWR, in 100 mL H_2O). Absorbance spectra, pH, and mV values were recorded after each addition.

Solution for Titration of 8PQ with Cadmium(II)

A stock solution of 0.1 *M* $Cd(ClO_4)_2 \cdot 6H_2O$ (2.097 g, Aldrich, in 50 mL H_2O) was prepared for use in this titration experiment. For the 500:1 Cd(II) and 8PQ titration experiment, the concentrations were 1 x 10^{-2} *M* and 2 x 10^{-5} *M* respectively. A solution of 5 mL 0.1 *M* $Cd(ClO_4)_2$ and 45 mL ± 0.05 mL of 2 x 10^{-5} *M* 8PQ in 0.01 *M* $HClO_4$ and 0.09 *M* $NaClO_4$ was prepared. This solution was placed in the flow cell apparatus described above and titrated with NaOH recording absorbance spectra and pH after each addition.

Solution for Titration of 8PQ with Calcium(II)

A stock solution of 0.0333 *M* $Ca(ClO_4)_2 \cdot 4H_2O$ (0.5178 g, Aldrich, 99%, in 50 mL H_2O) was prepared for use in this titration experiment. A 50.0 ± 0.05mL aliquot of 2 x 10^{-5} *M* 8PQ in 0.01 *M* $HClO_4$ and 0.09 *M* $NaClO_4$ was placed in the flow cell apparatus described above. This solution was then titrated with NaOH to reach an approximate pH of 6. Then this solution was titrated with varying amounts of the 0.0333 *M* $Ca(ClO_4)_2$ solution, recording absorbance spectra and pH values after each addition.

Solutions for Titrations of 8PQ with Copper(I)

A stock solution of 0.001 *M* $Cu(CH_3CN)_4PF_6$ (0.0186 g, synthesized by C. M. Whaley, in 50 mL H_2O) solution was prepared for use in the first titration experiment. For the first 1:1 Cu(I) and 8PQ titration experiment the concentrations were both 2 x 10^{-5} *M*. A solution of 1 mL of the 0.001 *M* Cu(I) solution and 49 ± 0.05 mL of 2 x 10^{-5} *M* 8PQ in 0.01 *M* $HClO_4$ and 0.09 *M* $NaClO_4$ was placed in the flow cell apparatus described above and N_2 bubbled through it. This solution was then titrated with NaOH and absorbance spectra and pH values were recorded after each addition. For the second 1:1 Cu(I) and 8PQ titration a stock solution of 1 x 10^{-4} *M* 8PQ in 0.01 *M* $HClO_4$ and 0.09 *M* $NaClO_4$ was prepared. Then 1.9 mg of $Cu(CH_3CN)_4PF_6$ was dissolved into 50 ± 0.05 mL of this 1 x 10^{-4} *M* 8PQ solution. This solution was of the concentration 1 x 10^{-4} *M* with respect to both 8PQ and Cu(I). This solution was then placed in the flow cell apparatus described above and N_2 bubbled through it. This

solution was then titrated with NaOH and absorbance spectra and pH values were recorded after each addition.

Solution for Titrations of 8PQ with Copper(II)

A stock solution of 0.304 *M* $Cu(ClO_4)_2 \cdot 6H_2O$ (5.63 g, Aldrich, 98%, in 50 mL H_2O) was prepared for these titration experiments. For the 100:1 Cu(II) and 8PQ titration experiment the concentrations were $2 \times 10^{-3} M$ and $2 \times 10^{-5} M$ respectively. A 50.0 ± 0.05 mL aliquot of $2 \times 10^{-5} M$ 8PQ in 0.01 *M* $HClO_4$ and 0.09 *M* $NaClO_4$ was taken and 330 µl of 0.304 *M* $Cu(ClO_4)_2$ was added to it. This solution was then placed in the flow cell apparatus described above. This solution was then titrated with NaOH and absorbance spectra, pH, and mV values were recorded after each addition. For the 10:1 Cu(II) and 8PQ titration experiment the concentrations were $2 \times 10^{-4} M$ and $2 \times 10^{-5} M$ respectively. A 50.0 ± 0.05 mL aliquot of $2 \times 10^{-5} M$ 8PQ in 0.01 *M* $HClO_4$ and 0.09 *M* $NaClO_4$ was taken and 33 µl of 0.304 *M* $Cu(ClO_4)_2$ was added to it. This solution was then placed in the flow cell apparatus described above. This solution was then titrated with NaOH and absorbance spectra, pH, and mV values were recorded after each addition.

Solutions for Titrations of 8PQ with Nickel(II)

A stock solution of 0.1 *M* $Ni(ClO_4)_2 \cdot 6H_2O$ (1.828 g, Alfa Aesar, in 50 mL H_2O) was prepared for use in the first titration experiment. For the 1665:1 Ni(II) and 8PQ titration experiment the concentrations were 0.0333 *M* and $2 \times 10^{-5} M$ respectively. A

50.0 ± 0.05 mL aliquot of 2 x 10^{-5} *M* 8PQ in 0.01 *M* $HClO_4$ and 0.09 *M* $NaClO_4$ was taken and 16.65 mL of 0.1 *M* $Ni(ClO_4)_2$ added to it. This solution was then placed in the flow cell apparatus described above and N_2 bubbled through it. This solution was then titrated with NaOH and absorbance spectra and pH values were recorded after each addition. For the following titration experiments a stock solution of 0.0333 *M* $Ni(ClO_4)_2 \cdot 6H_2O$ (0.6087 g, Alfa Aesar, in 50 mL H_2O) was prepared. For the 500:1 Ni(II) and 8PQ titration experiment, the concentrations were 0.01 *M* and 2 x 10^{-5} *M* respectively. A 35 ± 0.05 mL aliquot of 2 x 10^{-5} *M* 8PQ in 0.01 *M* $HClO_4$ and 0.09 *M* $NaClO_4$ was taken and 15 mL of 0.0333 *M* $Ni(ClO_4)_2$ added to it. This solution was then placed in the flow cell apparatus described above. This solution was then titrated with NaOH and absorbance spectra and pH values were recorded after each addition. For the 50:1 Ni(II) and 8PQ titration experiment the concentrations were 1 x 10^{-3} *M* and 2 x 10^{-5} *M* respectively. A 50.0 ± 0.05 mL aliquot of 2 x 10^{-5} *M* 8PQ in 0.01 *M* $HClO_4$ and 0.09 *M* $NaClO_4$ was taken and 1.5 mL of 0.0333 *M* $Ni(ClO_4)_2$ added to it. This solution was then placed in the flow cell apparatus described above. This solution was then titrated with NaOH and absorbance spectra and pH values were recorded after each addition.

Solutions for Titrations of 8PQ with Palladium(II)

A stock solution of 0.0209 *M* $Pd(NO_3)_2$ (0.2408 g, Aldrich, 97%, in 50 mL H_2O) was prepared for use both sets of titration experiments. For the 1:1 Pd(II) and 8PQ titration experiment the concentrations were both at 2 x 10^{-5} *M*. A 50.0 ± 0.05 mL

aliquot of 2 x 10^{-5} *M* 8PQ in 0.01 *M* $HClO_4$ and 0.09 *M* $NaClO_4$ was taken and 48 µl of 0.0209 *M* $Pd(NO_3)_2$ was added to it. This solution was then placed in the flow cell apparatus described above. This solution was then titrated with NaOH and absorbance spectra and pH values were recorded after each addition.

Solution for the Titration of 8PQ with Sodium(I)

A stock solution of 0.1 *M* $NaClO_4$ (1.22 g, Alfa Aesar, 98-102%, in 100 mL H_2O) was prepared for use in this titration experiment. A 50.0 ± 0.05 mL aliquot of 2 x 10^{-5} *M* 8PQ in 0.01 *M* $HClO_4$ and 0.09 *M* $NaClO_4$ was placed in the flow cell apparatus described above. This solution was then titrated with NaOH to reach an approximate pH of 6. Then this solution was titrated with varying amounts of the 0.1 *M* $NaClO_4$ solution, recording absorbance spectra and pH values after each addition.

Solutions for Titrations of 8PQ with Zinc(II)

A stock solution of 0.0999 *M* $Zn(ClO_4)_2 \cdot 6H_2O$ (1.86 g, Aldrich, in 50 mL H_2O) was prepared for use in the following titration experiment. For the 1665:1 Zn(II) and 8PQ titration experiment the concentrations were 0.0333 *M* and 2 x 10^{-5} *M* respectively. A 50.0 ± 0.05 mL aliquot of 2 x 10^{-5} *M* 8PQ in 0.01 *M* $HClO_4$ and 0.09 *M* $NaClO_4$ was taken and 16.67 mL of 0.0999 *M* $Zn(ClO_4)_2$ added to it. This solution was then placed in the flow cell apparatus described above and N_2 bubbled through it. This solution was then titrated with NaOH and absorbance spectra and pH values were recorded after each addition. For the following titration experiment a stock solution of 0.0333 *M*

$Zn(ClO_4)_2 \cdot 6H_2O$ (0.6199 g, Aldrich, in 50 mL H_2O) was prepared. For the 100:1 Zn(II) and 8PQ titration experiment the concentrations were 2 x 10^{-3} *M* and 2 x 10^{-5} *M* respectively. A 50.0 ± 0.05 mL aliquot of 2 x 10^{-5} *M* 8PQ in 0.01 *M* $HClO_4$ and 0.09 *M* $NaClO_4$ was taken and 3 mL of 0.0333 *M* $Zn(ClO_4)_2$ added to it. This solution was then placed in the flow cell apparatus described above. This solution was then titrated with NaOH and absorbance spectra and pH values were recorded after each addition.

Titrations Involving DIPY

Acid-base titrations of aqueous metal-DIPY solutions were monitored using UV/Vis spectrophotometry. Stock solutions (1L) of 2x10^{-5} *M* DIPY (3.4mg, TCI America, 99%) in 0.01 *M* $HClO_4$ (862µl, 11.6M, Alfa Aesar, 70%) and 0.09 *M* $NaClO_4$ (11.021g, Alfa Aesar, 98-102%), 2x10^{-4} *M* DIPY (0.0342g) in 0.01 *M* $HClO_4$ and 0.09 *M* $NaClO_4$, 2x10^{-3} *M* DIPY (0.342g) in 0.01 *M* $HClO_4$ and 0.09 *M* $NaClO_4$, 1x10^{-2} *M* DIPY (1.71g) in 0.01 *M* $HClO_4$ and 0.09 *M* $NaClO_4$ and were used in the titration experiments. A stock solution of 0.01 *M* $HClO_4$ in 0.09 *M* $NaClO_4$ and a 0.01 *M* NaOH (100µl, 10M, VWR, in 100 mL H_2O) solution were also prepared for use in pH-mV calibrations done prior to every titration experiment. These calibrations were done by taking a 25.0 ± 0.05 mL aliquot of the 0.01 *M* $HClO_4$ in 0.09 *M* $NaClO_4$ solution and making fifty 1mL additions of 0.01 *M* NaOH recording pH and mV readings after every addition.

Solutions for Titration of DIPY

In order to determine the protonation constants for DIPY a 50.0 ± 0.05 mL aliquot of the 2 x 10^{-5} *M* DIPY in 0.01 *M* $HClO_4$ and 0.09 *M* $NaClO_4$ solution was placed in the flow cell apparatus described above and titrated with 0.01 *M* NaOH. Absorbance spectra, pH, and mV values were recorded after each addition.

Solution for the Titration of DIPY with Aluminum(III)

A stock solution of 0.00333 *M* $Al(NO_3)_3$ (0.0355 g, Aldrich, 99.997%, in 50 mL H_2O) was prepared for use in this titration experiment. For the 1:1 Al(III) and DIPY titration experiment the concentrations were both 2 x 10^{-5} *M*. A solution of 300 µl 0.00333 *M* $Al(NO_3)_3$ was added to a 50.0 ± 0.05 mL aliquot of the 2 x 10^{-5} *M* DIPY in 0.01 *M* $HClO_4$ and 0.09 *M* $NaClO_4$ solution. This solution was placed in the flow cell apparatus described above and titrated with 0.01 *M* NaOH recording absorbance spectra, pH, and mV after each addition.

Solution for Titrations of DIPY with Cadmium(II)

A stock solution of 0.0333 *M* $Cd(ClO_4)_2 \cdot 6H_2O$ (0.6981 g, Aldrich, in 50 mL H_2O) was prepared for use in these titration experiments. For the 500:1 Cd(II) and DIPY titration experiment the concentrations were 0.01 *M* and 2 x 10^{-5} *M* respectively. A solution of 16 mL 0.0333 *M* $Cd(ClO_4)_2$ was added to 41 ± 0.05 mL aliquot of the 2 x 10^{-5} *M* DIPY in 0.01 *M* $HClO_4$ and 0.09 *M* $NaClO_4$ solution. This solution was placed in the flow cell apparatus described above and titrated with 0.01 *M* NaOH recording

absorbance spectra, pH, and mV after each addition. For the 250:1 Cd(II) and DIPY titration experiment the concentrations were 5 x 10^{-3} *M* and 2 x 10^{-5} *M* respectively. A solution of 8.8 mL 0.0333 *M* $Cd(ClO_4)_2$ was added to 50 ± 0.05 mL aliquot of the 2 x 10^{-5} *M* DIPY in 0.01 *M* $HClO_4$ and 0.09 *M* $NaClO_4$ solution. This solution was placed in the flow cell apparatus described above and titrated with 0.01 *M* NaOH recording absorbance spectra, pH, and mV after each addition.

Solutions for Titrations of DIPY with Cobalt(II)

Stock solutions of 0.0333 *M* $CoCl_2 \cdot 6H_2O$ (0.3959 g, Fisher Scientific, in 50 mL H_2O) and 0.999 *M* $CoCl_2 \cdot 6H_2O$ (11.878 g, Fisher Scientific, in 50 mL H_2O) were prepared for use in these titration experiments. For the first 1:1 Co(II) and DIPY titration experiment the concentrations were both 2 x 10^{-3} *M*. A 50 ± 0.05 mL aliquot of the 2 x 10^{-3} *M* DIPY in 0.01 *M* $HClO_4$ and 0.09 *M* $NaClO_4$ solution was taken and 100 µl of 0.999 *M* $CoCl_2$ added to it. This solution was placed in the flow cell apparatus described above and titrated with 0.01 *M* NaOH recording absorbance spectra, pH, and mV after each addition. For the second 1:1 Co(II) and DIPY titration experiment the concentrations were both 2 x 10^{-4} *M*. A 50 ± 0.05 mL aliquot of 2 x 10^{-4} *M* DIPY in 0.01 *M* $HClO_4$ and 0.09 *M* $NaClO_4$ solution was taken and 300 µl of 0.0333 *M* $CoCl_2$ added to it. This solution was placed in the flow cell apparatus described above and titrated with 0.01 *M* NaOH recording absorbance spectra, pH, and mV after each addition.

Solution for Titrations of DIPY with Copper(II)

A stock solution of 0.1 *M* $Cu(ClO_4)_2 \cdot 6H_2O$ (1.852 g, Aldrich, 98%, in 50 mL H_2O) was prepared for use in these titration experiments. For the first 1:1 Cu(II) and DIPY titration experiment the concentrations were both 2 x 10^{-3} *M*. A 50 ± 0.05 mL aliquot of the 2 x 10^{-3} *M* DIPY in 0.01 *M* $HClO_4$ and 0.09 *M* $NaClO_4$ solution was taken and 1 mL of 0.1 *M* $Cu(ClO_4)_2$ added to it. This solution was placed in the flow cell apparatus described above and titrated with 0.01 *M* NaOH recording absorbance spectra, pH, and mV after each addition. For the second 1:1 Cu(II) and DIPY titration experiment the concentrations were both 2 x 10^{-4} *M*. A 50 ± 0.05 mL aliquot of the 2 x 10^{-4} *M* DIPY in 0.01 *M* $HClO_4$ and 0.09 *M* $NaClO_4$ solution was taken and l00 µl of 0.1 *M* $Cu(ClO_4)_2$ added to it. This solution was placed in the flow cell apparatus described above and titrated with 0.01 *M* NaOH recording absorbance spectra, pH, and mV after each addition. For the third 1:1 Cu(II) and DIPY titration experiment the concentrations were both 2 x 10^{-5} *M*. A 50 ± 0.05 mL aliquot of the 2 x 10^{-5} *M* DIPY in 0.01 *M* $HClO_4$ and 0.09 *M* $NaClO_4$ solution was taken and l0 µl of 0.1 *M* $Cu(ClO_4)_2$ added to it. This solution was placed in the flow cell apparatus described above and titrated with 0.01 *M* NaOH recording absorbance spectra, pH, and mV after each addition.

Solution for Titrations of DIPY with Gallium(III)

A stock solution of 0.1 *M* $Ga(NO_3)_3$ (1.279 g, Aldrich, in 50 mL H_2O) was prepared for use in this titration experiment. For the 1:1 Ga(III) and DIPY titration

experiment the concentrations were both 2 x 10^{-5} *M*. A 50 ± 0.05 mL aliquot of the 2 x 10^{-5} *M* DIPY in 0.01 *M* $HClO_4$ and 0.09 *M* $NaClO_4$ solution was taken and 10 µl of 0.1 *M* $Ga(NO_3)_3$ added to it. This solution was placed in the flow cell apparatus described above and titrated with 0.01 *M* NaOH recording absorbance spectra, pH, and mV after each addition.

Solution for Titrations of DIPY with Nickel(II)

A stock solution of 0.1 *M* $Ni(ClO_4)_2 \cdot 6H_2O$ (1.828 g, Alfa Aesar, in 50 mL H_2O) was prepared for use in these titration experiments. For the fist 1:1 Ni(II) and DIPY titration experiment the concentrations were both 2 x 10^{-4} *M*. A 50 ± 0.05 mL aliquot of the 2 x 10^{-4} *M* DIPY in 0.01 *M* $HClO_4$ and 0.09 *M* $NaClO_4$ solution was taken and 100 µl of 0.1 *M* $Ni(ClO_4)_2$ added to it. This solution was placed in the flow cell apparatus described above and titrated with 0.01 *M* NaOH recording absorbance spectra, pH, and mV after each addition. For the second 1:1 Ni(II) and DIPY titration experiment the concentrations were both 2 x 10^{-5} *M*. A 50 ± 0.05 mL aliquot of the 2 x 10^{-5} *M* DIPY in 0.01 *M* $HClO_4$ and 0.09 *M* $NaClO_4$ solution was taken and 10 µl of 0.1 *M* $Ni(ClO_4)_2$ added to it. This solution was placed in the flow cell apparatus described above and titrated with 0.01 *M* NaOH recording absorbance spectra, pH, and mV after each addition.

Solution for Titrations of DIPY with Zinc(II)

A stock solution of 0.0999 *M* $Zn(ClO_4)_2 \cdot 6H_2O$ (1.86 g, Aldrich, in 50 mL H_2O) was prepared for use in these titration experiments. For the 1250:1 Zn(II) and DIPY titration experiment the concentrations were 2 x 10^{-2} *M* and 1.6 x 10^{-5} *M* respectively. A 50 ± 0.05 mL aliquot of the 2 x 10^{-5} *M* DIPY in 0.01 *M* $HClO_4$ and 0.09 *M* $NaClO_4$ solution was taken and 12.5 mL of 0.0999 *M* $Zn(ClO_4)_2$ added to it. This solution was placed in the flow cell apparatus described above and titrated with 0.01 *M* NaOH recording absorbance spectra, pH, and mV after each addition. For the 50:1 Zn(II) and DIPY titration experiment the concentrations were 1 x 10^{-3} *M* and 2 x 10^{-5} *M* respectively. A 50 ± 0.05 mL aliquot of the 2 x 10^{-5} *M* DIPY in 0.01 *M* $HClO_4$ and 0.09 *M* $NaClO_4$ solution was taken and 500 µl of 0.0999 *M* $Zn(ClO_4)_2$ added to it. This solution was placed in the flow cell apparatus described above and titrated with 0.01 *M* NaOH recording absorbance spectra, pH, and mV after each addition.

Synthesis of PDA

The synthesis of PDA was followed as described in the literature.[21] The product was characterized by FT-IR and melting point analysis. A 250 mL round bottom flask was charged with 1 g of neocuprine (4.60 mmol, Alfa Aesar, 98+%) and 2.5 g selenium dioxide (22.53 mmol, Alfa Aesar, 99.4%). A solution of 67 mL 4% deionized H_2O/p-dioxane (Alfa Aesar, 99+%) was then added to the round bottom flask. The mixture was then stirred and allowed to reflux for 2 hours at 101°C in a wax bath. The hot solution was then filtered to collect a yellow precipitate. The synthesis yielded 0.681 g of 1,10-phenanthroline-2,9-dicarboxaldehyde (2.88 mmol, 62.61%).

Then a solution of 0.681 g of 1,10-phenanthroline-2,9-dicarboxaldehyde (2.88 mmol) and 18 mL of a 4:1 HNO_3 (15.8 N, Fisher Scientific)/H_2O was added to a 250 mL round bottom flask. The solution was stirred and allowed to reflux for 2 hours. The solution was then chilled and filtered to collect 0.527 g (1.965 mmol, 68.23%) of product as a yellow powder.

Titrations Involving PDA

Acid-base titrations of aqueous metal-PDA solutions were monitored using UV/Vis spectrophotometry. A 1L stock solution of 2 x 10^{-5} *M* PDA (5.3 mg)[18] in 0.1 *M* $HClO_4$ (8.62 mL, 11.6 *M*, Alfa Aesar, 70%) was used in the titration experiments. A stock solution of 0.01 *M* $HClO_4$ in 0.09 *M* $NaClO_4$ and a 0.01 *M* NaOH (100 µl, 10 *M*, VWR, in 100 mL H_2O) solution were also prepared for use in pH-mV calibrations done prior to every titration experiment. These calibrations were done by taking a 25.0 ± 0.05 mL aliquot of the 0.01 *M* $HClO_4$ in 0.09 *M* $NaClO_4$ solution and making fifty 1 mL additions of 0.01 *M* NaOH recording pH and mV readings after every addition.

Solutions for Titration of PDA

In order to determine the protonation constants for PDA a 50.0 ± 0.05 mL aliquot of the 2 x 10^{-5} *M* PDA in 0.1 *M* $HClO_4$ solution was placed in the flow cell apparatus described above and titrated with 0.01 *M* NaOH. Absorbance spectra, pH, and mV values were recorded after each addition.

Solution for Titrations of PDA with In(III)

A stock solution of 0.01 *M* $In(NO_3)_3 \cdot H_2O$ (159 mg, Alfa Aesar, 99.99%, in 50 mL H_2O) was prepared for use in this titration experiment. For the 1:1 In(III) and PDA titration experiment the concentrations were both 2 x 10^{-5} *M*. A solution of 100 µl 0.01 *M* $In(NO_3)_3 \cdot H_2O$ was added to a 50.0 ± 0.05 mL aliquot of the 2 x 10^{-5} *M* PDA in 0.1 *M* $HClO_4$ solution. This solution was placed in the flow cell apparatus described above and titrated with NaOH recording absorbance spectra, pH, and mV after each addition.

Solutions for Titrations of PDA with Uranyl(VI)

A stock solution of 0.1 *M* $UO_2(NO_3)_2 \cdot 6H_2O$ (2.511 g, Fisher Scientific, in 50 mL H_2O) was prepared for use in these titration experiments. For the 48 hour 1:1 uranyl(VI) and PDA titration experiment the concentrations were both 2 x 10^{-5} *M*. A solution of 10 µl 0.1 *M* $UO_2(NO_3)_2 \cdot 6H_2O$ was added to a 50.0 ± 0.05 mL aliquot of the 2 x 10^{-5} *M* PDA in 0.1 *M* $HClO_4$ solution. This solution was placed in the flow cell apparatus described above and titrated with NaOH to a pH of about 3.3. The absorbance spectra, pH, and mV were recorded in 10 minute increments for the first several hours then recorded after a number of hours. For the 24 hour 1:1000:1 Uranyl(VI), Cd(II), and PDA titration experiment the concentrations were 2 x 10^{-5} *M*, 2 x 10^{-2} *M*, and 2 x 10^{-5} *M* respectively. A solution of 10 µl 0.1 *M* $UO_2(NO_3)_2 \cdot 6H_2O$ and 30 mL 0.0333 *M* $Cd(ClO_4)_2 \cdot 6H_2O$ were added to a 50.0 ± 0.05 mL aliquot of the 2 x 10^{-5} *M* PDA in 0.1 *M* $HClO_4$ solution. This solution was placed in the flow cell apparatus described above and titrated with NaOH to a pH of about 3.4. The absorbance spectra, pH, and mV were

recorded in 10 minute increments for the first several hours then recorded after a number of hours. For the 24 hour 1:1:1 uranyl(VI), gadolinium(III), and PDA titration experiment a stock solution of 0.0357 *M* $Gd(ClO_4)_3 \cdot 6H_2O$ (2.01 g, Aldrich 99%, in 50 mL H_2O) was prepared. The concentrations of all reactants were 2 x 10^{-5} *M*. A solution of 10 µl 0.1 *M* $UO_2(NO_3)_2 \cdot 6H_2O$ and 28 µl 0.0357 *M* $Gd(ClO_4)_3 \cdot 6H_2O$ were added to a 50.0 ± 0.05 mL aliquot of the 2 x 10^{-5} *M* PDA in 0.1 *M* $HClO_4$ solution. This solution was placed in the flow cell apparatus described above and titrated with NaOH to a pH of about 3.85. The absorbance spectra, pH, and mV were recorded in 10 minute increments for the first several hours then recorded after a number of hours. For the two 24 hour 1:1:1 uranyl(VI), indium(III), and PDA titration experiments the concentrations were all 2 x 10^{-5} *M*. In one experiment the uranyl(VI) was added to the PDA solution first and in the other the Indium(III) was added first. In both titrations a solution of 10 µl 0.1 *M* $UO_2(NO_3)_2 \cdot 6H_2O$ and 100 µl 0.01 *M* $In(NO_3)_3 \cdot H_2O$ were added to a 50.0 ± 0.05 mL aliquot of the 2 x 10^{-5} *M* PDA in 0.1 *M* $HClO_4$ solution. These solutions were placed in the flow cell apparatus described above and titrated with NaOH to a pH of approximately 3.9. The absorbance spectra, pH, and mV were recorded in 10 minute increments for the first several hours then recorded after a number of hours. For the 1:1 uranyl(VI) and PDA titration experiment the concentrations were both 2 x 10^{-6} *M*. A solution of 1 µl 0.1 *M* $UO_2(NO_3)_2 \cdot 6H_2O$ was added to a 5.0 ± 0.05 mL aliquot of the 2 x 10^{-5} *M* PDA in 0.1 *M* $HClO_4$ solution in 45mL of DI water. This solution was placed in the flow cell apparatus described above and titrated with NaOH recording the absorbance spectra, pH, and mV after each addition.

RESULTS AND DISCUSSION

UV-Vis Spectrophotometric Titrations Involving 8PQ

UV/Vis spectroscopy was used as an analytical tool to determine the stability constants (log K_1) of the metal-8PQ complexes. Absorbance scans were recorded from 200 to 350nm and were taken after each addition of 0.1 *M* NaOH. Absorbance data was taken at selected wavelengths of 218, 243, 265, 278, and 317nm. Absorbance spectra of the free ligand at varying pH at these wavelengths can be seen in Figure 8. Peak shifts were seen for these absorbances upon complexation of 8PQ with a metal ion.

In order to determine the protonation constants for 8PQ, a titration was performed at 25.0 ± 0.1 °C at 0.1 *M* ionic strength (0.1 *M* $NaClO_4$). Figure 9 shows absorbance versus wavelength (nm) scans at pH values of approximately 2 to 7.5. A plot of E (mV) against the calculated pH, which was used to calculate E^0, is shown in Figure 10. Absorbance data for the selected wavelengths were used to generate a plot of absorbance versus pH. This plot is shown in Figure 11. The points drawn in are the experimental values and the solid lines are theoretical curves of absorbance versus pH calculated for the constants corresponding to the observed protonation equilibria. The theoretical curves of absorbance versus pH in Figure 11 were fitted to the experimental points using the SOLVER tool of the program EXCEL [22]. The standard deviations of these protonation constants were calculated using the SOLVSTAT macro provided in reference 22. The protonation constants for 8PQ were calculated using the absorbance data and pH values from this plot. The calculated protonation constants of pK_1 and pK_2 were 5.45 and 1.83, respectively. A scheme showing the proposed protonation equilibria for 8PQ can be seen in Figure 12.

a.)

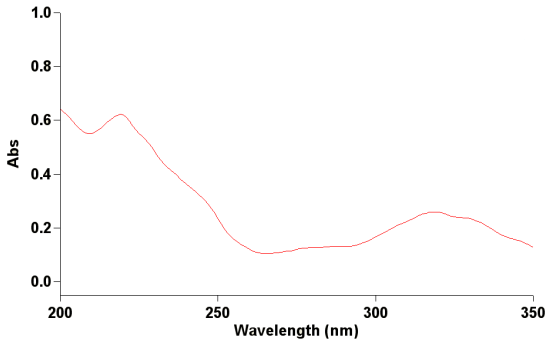

b.)

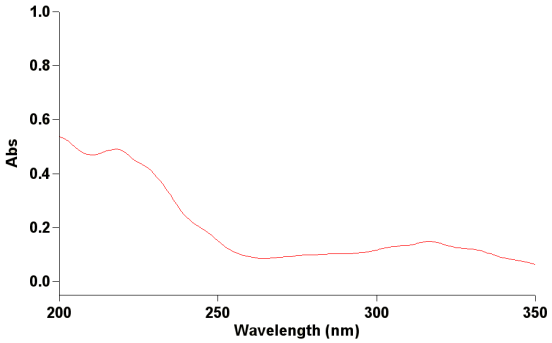

c.)

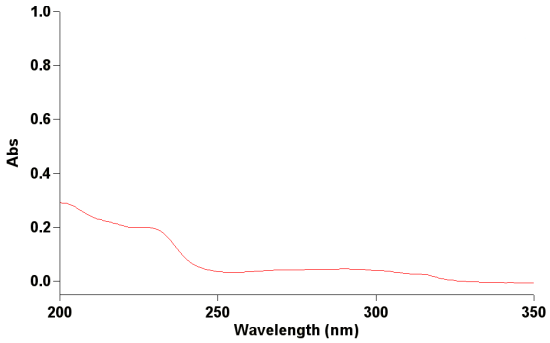

d.)

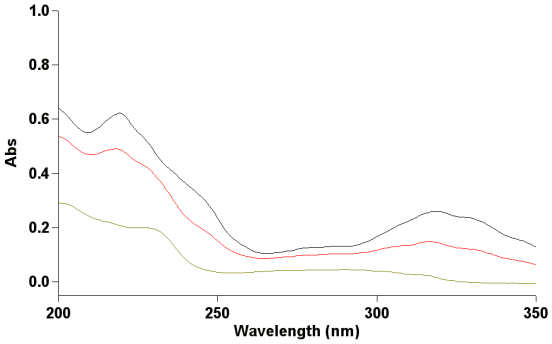

Figure 8: Plots of absorbance versus wavelength (nm) spectra at varying pH of 2 x 10^{-5} *M* 8PQ at 25.0 ± 0.1 °C with 0.1 *M* NaOH. a.) pH = 2.11, b.) pH = 5.13, c.) pH = 7.35, d.) overlay of pH 2.11, 5.13, and 7.35 spectra.

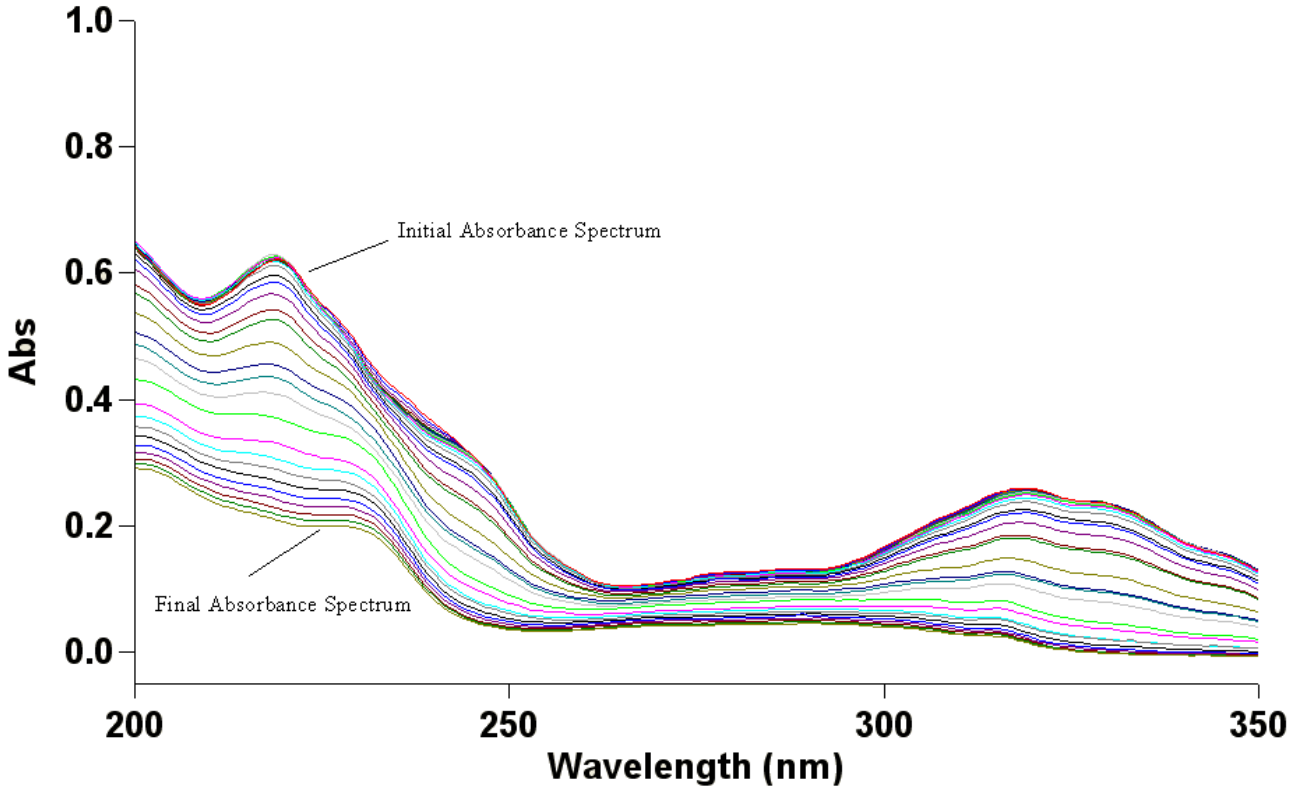

Figure 9: Absorbance versus wavelength (nm) spectra from the titration of 2 x 10^{-5} *M* 8PQ at 25.0 ± 0.1 °C with 0.1 *M* NaOH with a pH range of approximately 2.00 to 7.5.

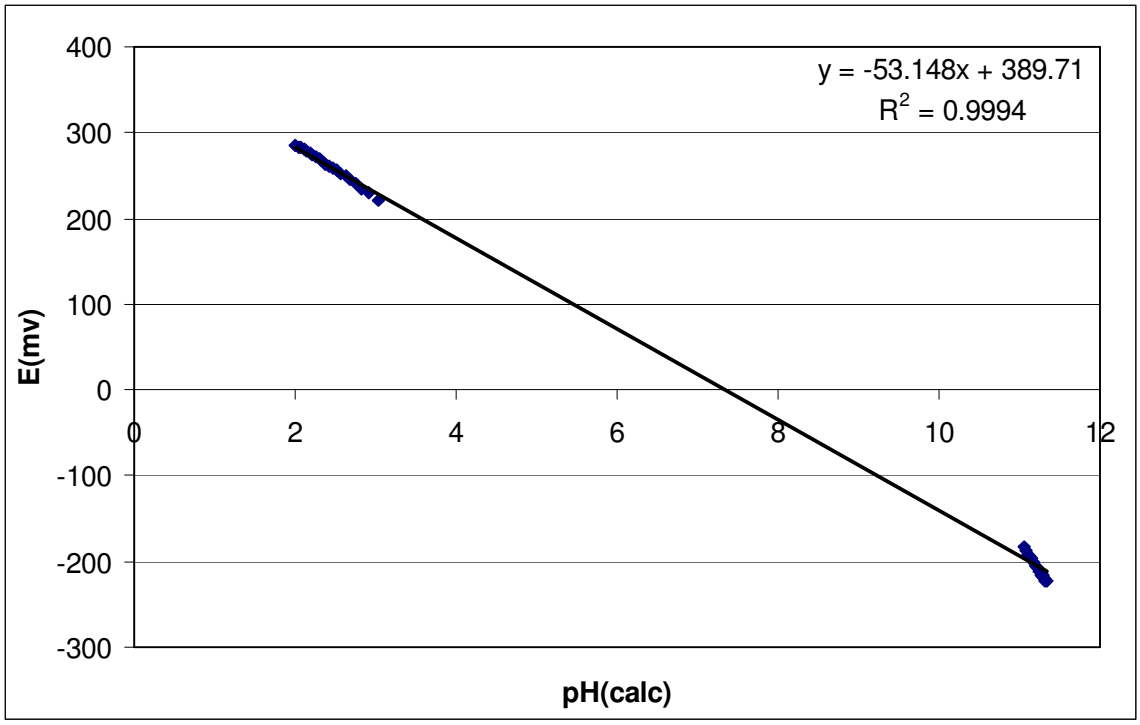

Figure 10: Plot of the correlation between E (mV) and the calculated pH used to calculate E^0 for the titration of 2 x 10^{-5} *M* 8PQ at 25.0 ± 0.1 °C with 0.1 *M* NaOH.

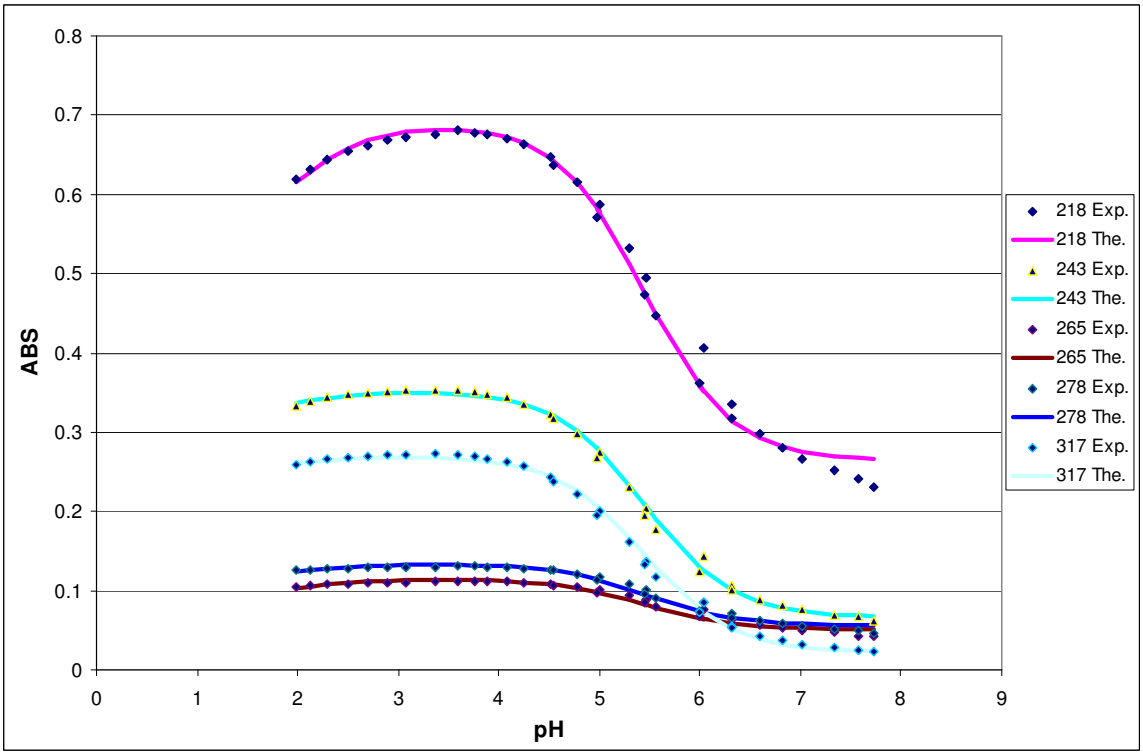

Figure 11: Experimental absorbance data (Exp.) fitted with calculated values (The.) to determine the protonation constants of 2 x 10^{-5} *M* 8PQ.

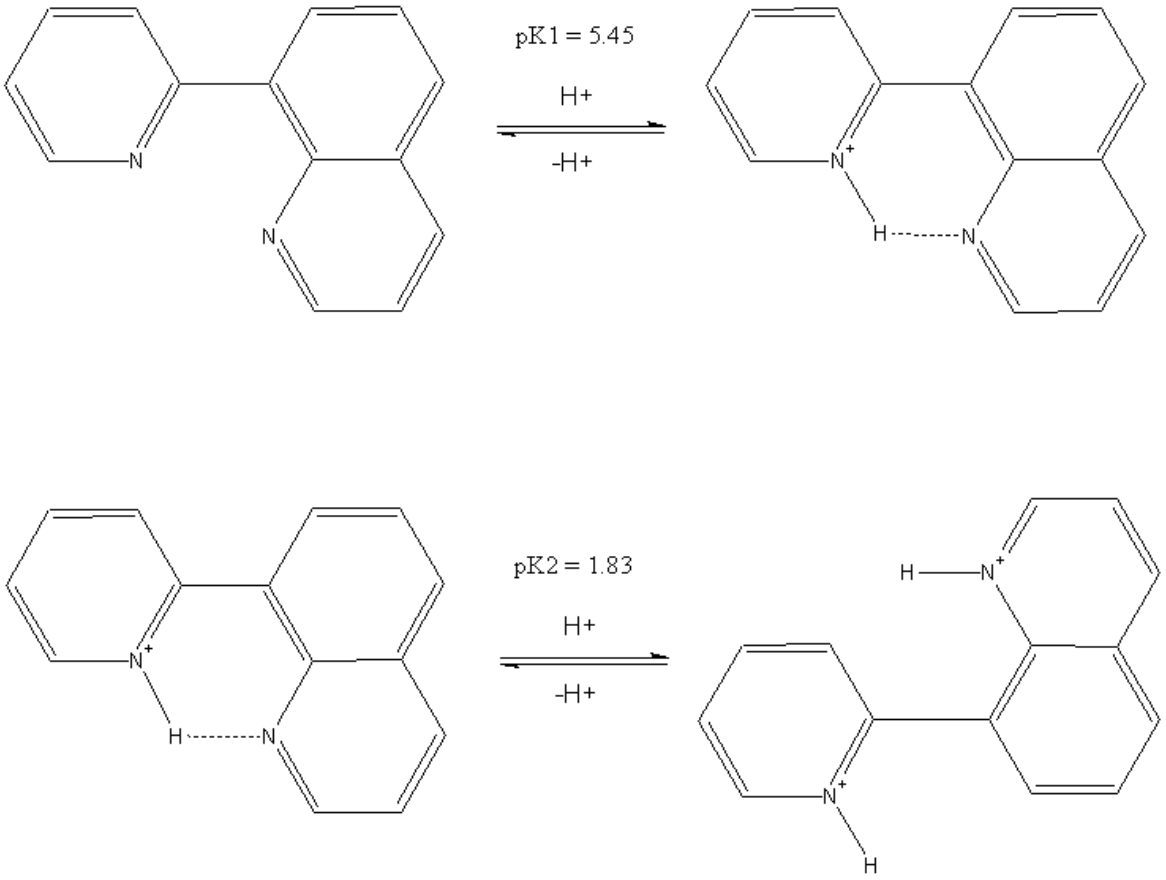

Figure 12: The proposed protonation equilibria for 8-(2-pyridyl)quinoline (8PQ).

As can be seen in Figure 12, 8PQ has two protonation constants, pK_1 and pK_2, with values of 5.45 and 1.83 respectively. The following calculations were used to determine these protonation constants for 8PQ. After obtaining the observed absorbances it was necessary to correct them for dilution using Eq(1).

$$\text{Corrected Absorbance} = \frac{\text{Abs} \cdot \text{V}_{\text{total}}}{\text{V}_{\text{initial}}} \tag{1}$$

Plots of the corrected absorbance versus pH were drawn up for each wavelength. The total ligand concentration, $[\text{L}]_{total}$, in solution can be described by Eq(2).

$$[\text{L}]_{total} = [\text{L}] + [\text{LH}] + [\text{LH}_2] \tag{2}$$

Eq(2) can be rearranged by adding the following protonation constants, each representing a different protonation event, to get Eq(5).

$$\text{K}_1 = \frac{[LH]}{[L][H]} \tag{3}$$

$$\text{K}_1\text{K}_2 = \frac{[LH_2]}{[L][H]^2} \tag{4}$$

$$[\text{L}]_{total} = [\text{L}] + \text{K}_1[\text{L}][\text{H}] + \text{K}_1\text{K}_2[\text{L}][\text{H}]^2 \tag{5}$$

By dividing out the ligand concentration, [L], Eq(5) can be simplified to Eq(6).

$$\frac{L_{total}}{[L]} = 1 + \text{K}_1[\text{H}^+] + \text{K}_1\text{K}_2[\text{H}^+]^2 \tag{6}$$

The theorectical absorbance, Eq(7), was calculated by multiplying the concentration of the species present in solution [L, LH, and LH_2] by absorbance of each of these species at 2 x 10^{-5} M concentration, as shown in Eq(6).

$$\text{Abs(theor)} = \frac{1x[Abs(L)] + K_1[H^+][Abs(LH)] + K_1K_2[H^+]^2[Abs(LH_2)]}{1 + K_1[H^+] + K_1K_2[H^+]^2} \qquad (7)$$

Abs(L) is the absorbance of the fully unprotonated ligand in solution. Abs(LH) and Abs(LH_2) describe the absorbances of the mono- and di-protonated species present in the equilibrium. Plots of pH versus corrected absorbance were then fitted with plots of pH versus the theoretical absorbance using the SOLVER tool. This resulted in the pK_a values shown in Figure 12 with a minimum standard deviation.

Titrations Involving Metal Ion Complexation with 8PQ

In these titrations, unless stated otherwise, the same procedure was performed for each metal-ligand complex at the same wavelengths as done with the free ligand. To determine the log K_1 for metal ion stability the effect the metal ion has on the protonation events must be considered. For example if the protonation of a ligand involves the displacement of the metal ion by protons:

$$ML + H^+ \leftrightarrows M + LH \qquad (8)$$

In this case one proton can be attached to the ligand and the log K_1 for the complex can be calculated as follows. In the case of no metal ion present, a protonation is evidenced by an inflection of absorbance versus pH. The midpoint on this inflection results in the pK_a. In the presence of a metal ion, if a complex is formed, an inflection in the absorbance versus pH curve is observed but now at a lower pH. This protonation event corresponds to that shown in equation 8. From the midpoint of the inflection that corresponds to equation 8, one can calculate the reaction constant below.

$$K_{reaction} = \frac{[LH][M]}{[ML][H^+]} \tag{9}$$

In equation 9, [H] is the proton concentration at pH_{50}, which is the pH where [LH] = [ML]. To calculate $K_{reaction}$ it is also important to include the free metal ion concentration, [M]. Therefore, $K_{reaction}$ is equal to the free metal ion concentration, which at pH_{50} will be 50% of the total metal ion concentration ([ML] = [M]), divided by [H] at pH_{50}. K_1 for the metal ion complex can now be found by combining the $K_{reaction}$ from equation 9 with the protonation constant K_a.

$$K_1 = \frac{1}{K_a K_{reaction}} \tag{10}$$

$$= \frac{[LH]}{[L][H^+]} \text{ x } \frac{[ML][H^+]}{[LH][M]}$$

$$= \frac{[ML]}{[L][M]} \tag{11}$$

For multiprotic ligands such as 8PQ the calculations are done in the same fashion except that two protonation constants are included.

$$ML + 2H^+ \rightarrow M + LH_2 \tag{12}$$

$$K_{reaction} = \frac{[LH_2][M]}{[ML][H^+]^2} \tag{13}$$

$$K_1 = \frac{1}{K_{a1} K_{a2} K_{reaction}} \tag{14}$$

$$= \frac{[LH_2]}{[L][H^+]^2} \text{ x } \frac{[ML][H^+]^2}{[LH_2][M]}$$

$$= \frac{[ML]}{[L][M]} \quad (15)$$

Other possible sources of protonation events for metal-ligand complexes are events involving hydroxides on the complex or protonation of the complex itself. These events can be seen in equations 16 and 17 respectively.

$$MLOH + H^+ \leftrightarrows ML \quad (16)$$

$$ML + H^+ \leftrightarrows MLH^+ \quad (17)$$

The protonation constants for these events can be determined but are not needed to calculate the stability constants of the ligand with metal ions. Equations 1-15 were used to calculate the formation constants for each metal ion with 8PQ. By finding the protonation constants of the given metal-8PQ complex the $\log K_1$ can be obtained. The $\log K_1$ of a metal-8PQ complex can be found by taking the difference of the pK_a values relative to the free ligand and adding the negative log of the concentration of the free metal. The stability constants determined with the metal ions with 8PQ from UV-Vis spectroscopy titration experiments can be seen in Table 3. The stability constants are compared to that of bipyridine. A graph comparing the difference in $\log K_1$ values of 8PQ and bipyridine can be seen in Figure 13. It shows that bipyridine has a proportionally greater preference for smaller metal ions than that of 8PQ. The $\log K_1$ values for 8PQ are also consistently lower then those of bipyridine. This could be due to that fact that 8PQ is stericly hindered when in the conformation needed to form complexes and therefore prefers to be in its *trans* conformation, lowering its binding strengths.

Metal	Ionic Radius (Å)	log *K*1 with 8PQ	log *K*1 with BIPY	Δ log *K*1
Cd(II)	0.97	2.19	4.24	-2.05
Ca(II)	0.99	≈ 0	≈ 0	0
Cu(I)	0.77	4.66	7.5	-2.84
Cu(II)	0.57	4.37	8.12	-3.75
Ni(II)	0.69	3.3	7.04	-3.74
Pd(II)	0.64	(16.4)	19.8	
Zn(II)	0.74	3.48	5.12	-1.64

Table 3: Comparison of log K_1 data for metal ions with 8PQ and BIPY.

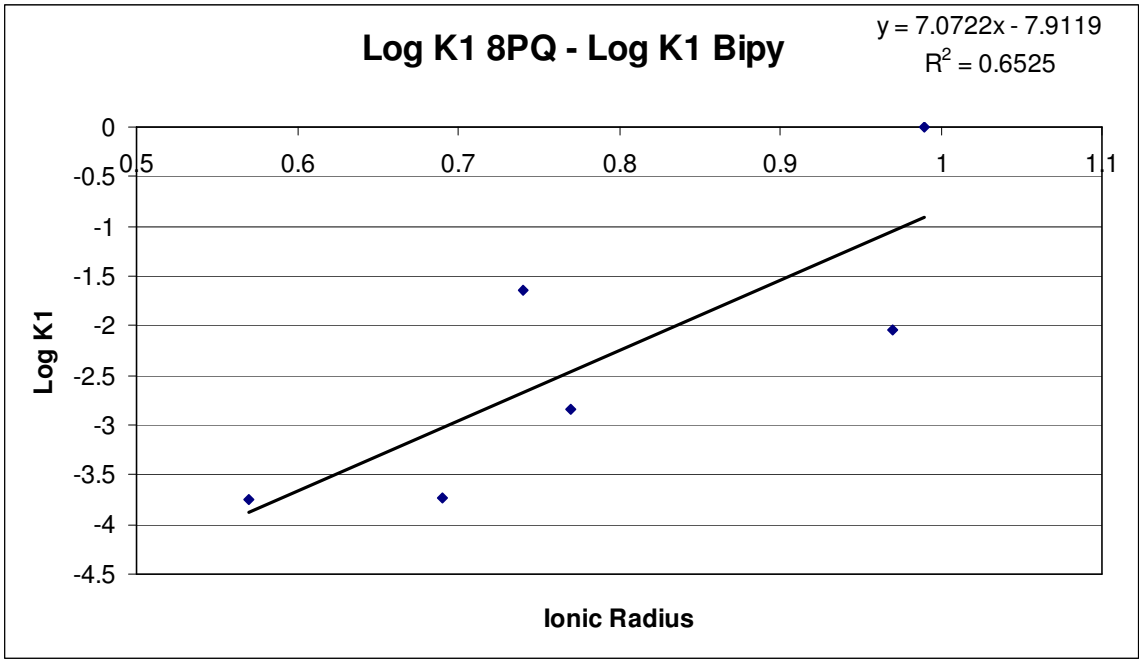

Figure 13: A graph comparing the difference in log K_1 values of 8PQ and Bipyridine.

Cadmium(II)-8PQ Results

Cadmium(II) has an ionic radius of 0.97Å which is much larger then the ideal radius of 0.45Å. The UV absorbance spectrum for the 500:1 cadmium(II) and 8PQ titration experiment is shown in Figure 14. A graph with the experimental absorbance data fitted with calculated values to determine the protonation constant for the

cadmium(II) and 8PQ solution is shown in Figure 15. The equilibrium observed is described below at the pH it occurred.

$$Cd(8PQ)^{2+} + H^{+} \leftrightarrows Cd^{2+} + (8PQ)H^{+} \qquad (pH = 5.26)$$

By using equations 1-15 the log K_1 for the cadmium(II)-8PQ complex was found to be 2.19 and calculated as follows,

$$\text{Log } K_1 = 5.45 - 5.26 - \log(0.01)$$

where 5.45 is the pK_a of the free ligand, 5.26 is the pK_1 equilibrium of complex formation and 0.01 represents the amount of free metal ion at the midpoint of the equilibrium where Cd(II) is displaced from 8PQ.

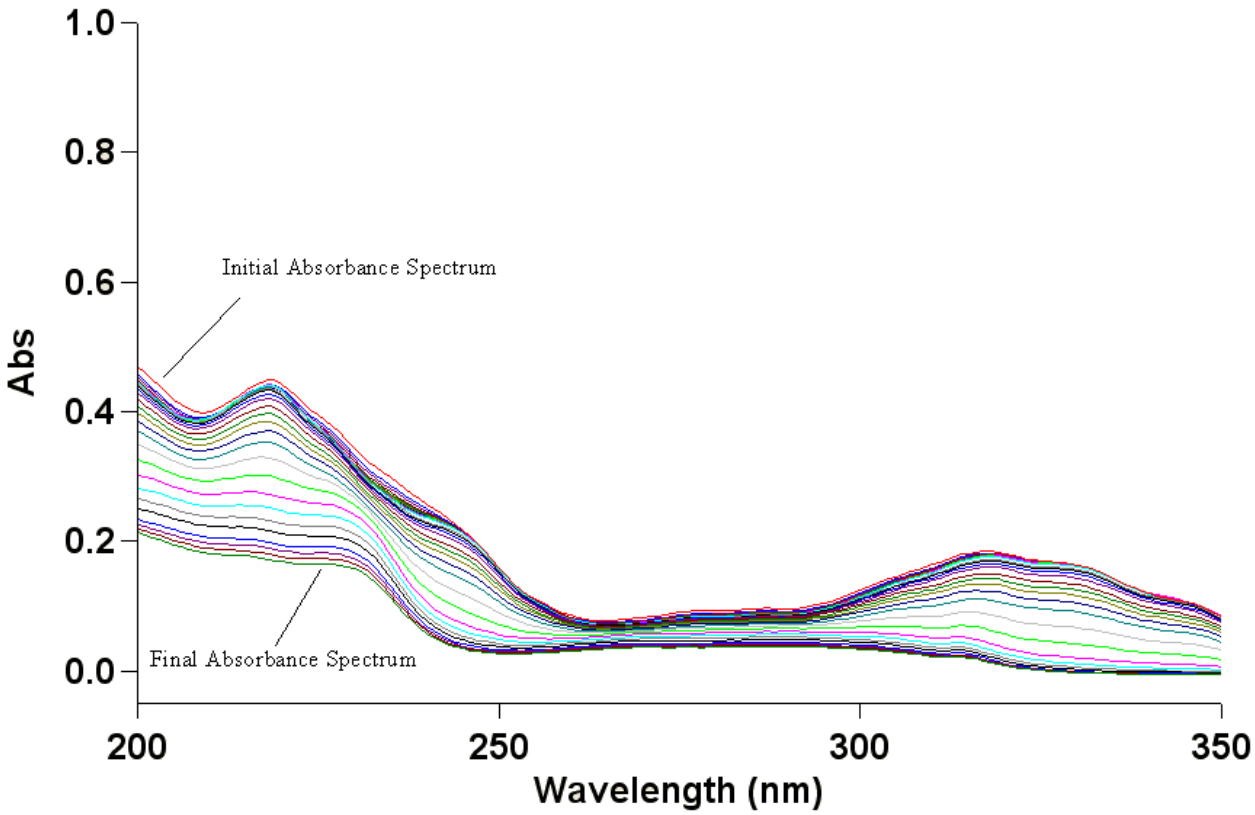

Figure 14: Absorbance versus wavelength (nm) spectra from the titration of the cadmium(II) and 8PQ solution that was 1 x 10^{-2} M and 2 x 10^{-5} M respectively at 25.0 ± 0.1 °C with 0.1 M NaOH with a pH range of approximately 2 to 8.

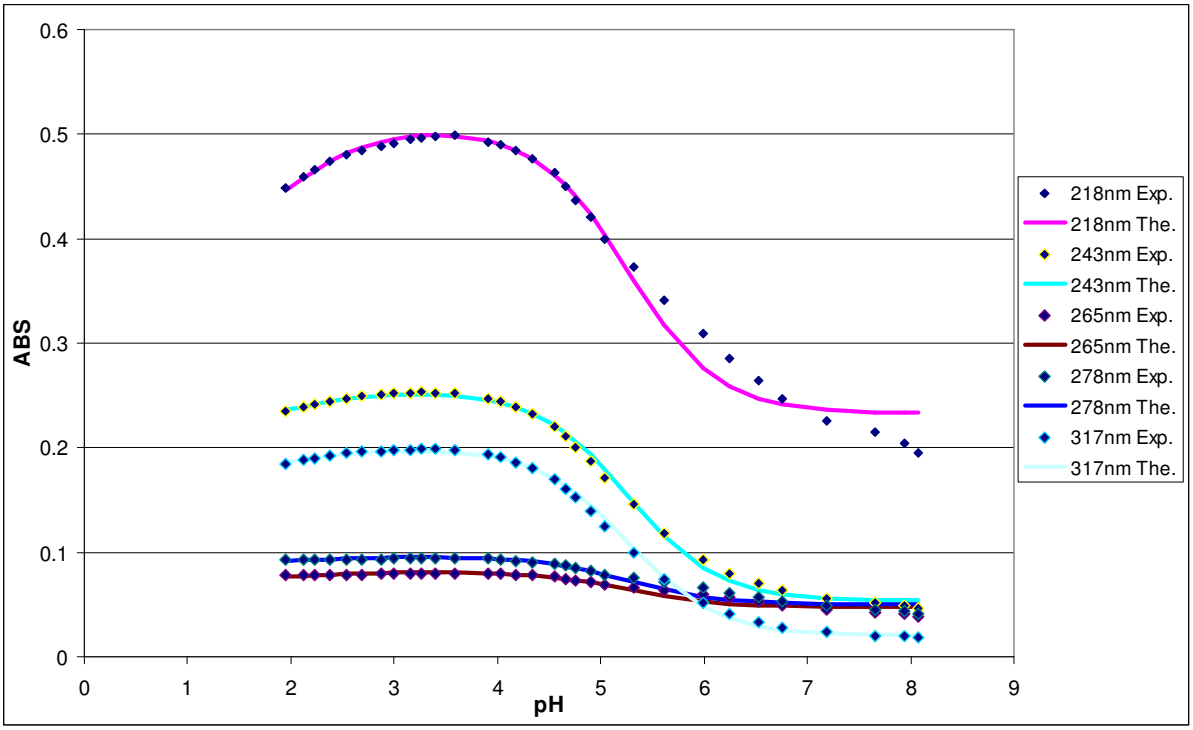

Figure 15: Experimental absorbance data (Exp.) fitted with calculated values (The.) to determine the protonation constants for the cadmium(II) and 8PQ solution that was 1 x $10^{-2}\,M$ and 2 x $10^{-5}\,M$ respectively.

Calcium(II)-8PQ Results:

Calcium(II) has an ionic radius of 0.99Å which is much larger then the ideal radius of 0.45Å and therefore should have a very low log K_1 for the 8PQ complex. In this experiment a solution of 8PQ at pH 6 was titrated with 0.0333 M $Ca(ClO_4)_2$. Absorbance values were recorded at each of the selected wavelength and the UV absorbance spectrum for calcium(II) and 8PQ can be seen in Figure 16. A graph of $\bar{n}$ vs. Log[Ca^{2+}] for this titration was produced and a theoretical curve for $\bar{n}$ fitted to it using the SOLVER tool. This was done for all five selected wavelengths and the graph of this data for 218 nm is shown in Figure 17. Only this wavelength was shown since this graph at each wavelength is virtually identical. The value of $\bar{n}$ can be expressed by equation (18) seen below.

$$\bar{n} = \frac{Abs - Abs_{ini}}{Abs_{\inf} - Abs_{ini}} \tag{18}$$

Here Abs_{ini} is the corrected absorbance for $8PQH^+$ and $Abs_{\inf}$ is the corrected absorbance of 8PQ. The initial ligand concentration must be corrected due to the dilution from the titration additions. Equation (19) shows how, $[L]_{total}$, the total ligand concentration was calculated.

$$[L]_{total} = \frac{[L]_{ini}\, xV_{ini}}{V_{total}} \tag{19}$$

After obtaining the values of $\bar{n}$ and total ligand concentration, the distribution between the complexed ligand, [ML] and the free ligand, [L], were calculated using equations (20) and (21).

$$[ML] = \bar{n} \cdot [L]_{total} \quad (20)$$

$$[L] = [L]_{total} - [ML] \quad (21)$$

The stability constant, log K_1, was then calculated for Ca(II) with 8PQ using equation (22) where $p[metal]_{50}$ is the negative log of the concentration of free metal in solution after half of the ligand in solution is complexed.

$$\text{Log } K \text{ (8PQ-M)} = \Delta \text{ pK}_a + p[metal]_{50} \quad (22)$$

The value for log K_1 of the calcium(II)-8PQ complex was then calculated for each of the five selected wavelengths. Taking the average of these values for each of the five wavelengths produces a value for log K_1 of the calcium(II)-8PQ complex of 4.37. This result was counterintuitive since 8PQ tends to prefer metal ions of small size (about 0.45Å) and yet the large metal ion of calcium(II) (ionic radius of 1.00Å) was calculated to have a relatively strong log K_1 of 4.37. After having double checked the calculations and finding them to be correct it was decided to double check the method of this titration. To check this method the same titration would be repeated with the only change being instead of titrating with 0.0333 *M* $Ca(ClO_4)_2$, 0.1 *M* $NaClO_4$ would be used. Absorbance values were recorded at each of the selected wavelength and the UV absorbance spectrum for sodium and 8PQ can be seen in Figure 18. A graph of nbar vs. Log[Na] for this titration was produced and a theoretical curve fitted to it. This was done for all five selected wavelengths and the graph of this data for 218 nm is shown in Figure

19. Again only this wavelength was shown since the graphs of the other wavelengths were virtually identical. By using equations 16-22 the log K_1 for the Sodium-8PQ complex was found to be 4.06. This value signifies that the log K_1 of 4.37 found for calcium(II)-8PQ complex is not a legitimate value as titrating with $NaClO_4$ should show only dilution and yet it does not. It is speculated that what is being observed is the free ligand plating out slowly due to the solution being held at a higher pH for an extended period of time. It can be concluded that this is not an accurate method to use in this instance. It is also evident from these results that the calcium(II)-8PQ complex has a negligible log K_1 as one would expect due to its relatively large ionic radius of 0.99Å.

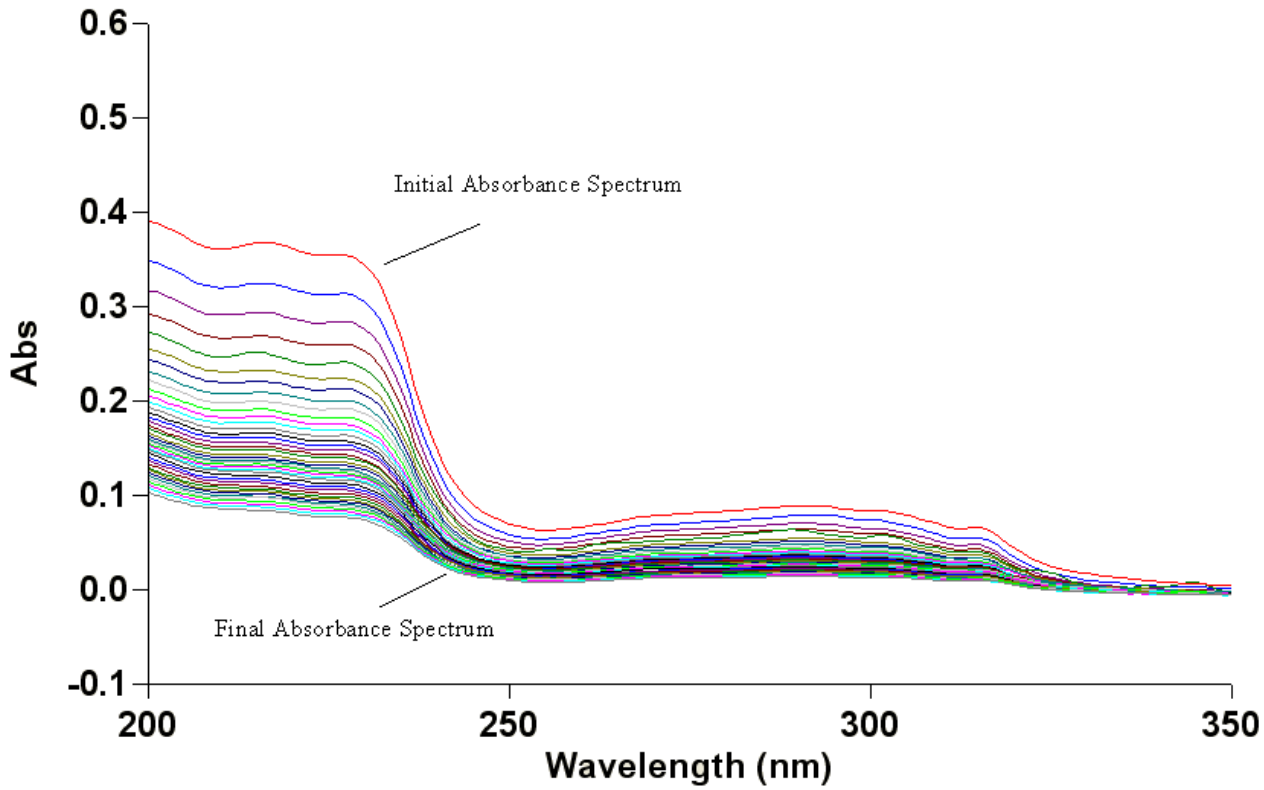

Figure 16: Absorbance versus wavelength (nm) spectra from the titration of a 2 x 10^{-5} *M* 8PQ solution with 0.0333 *M* $Ca(ClO_4)_2$ at 25.0 ± 0.1 °C and pH ≈ 6.

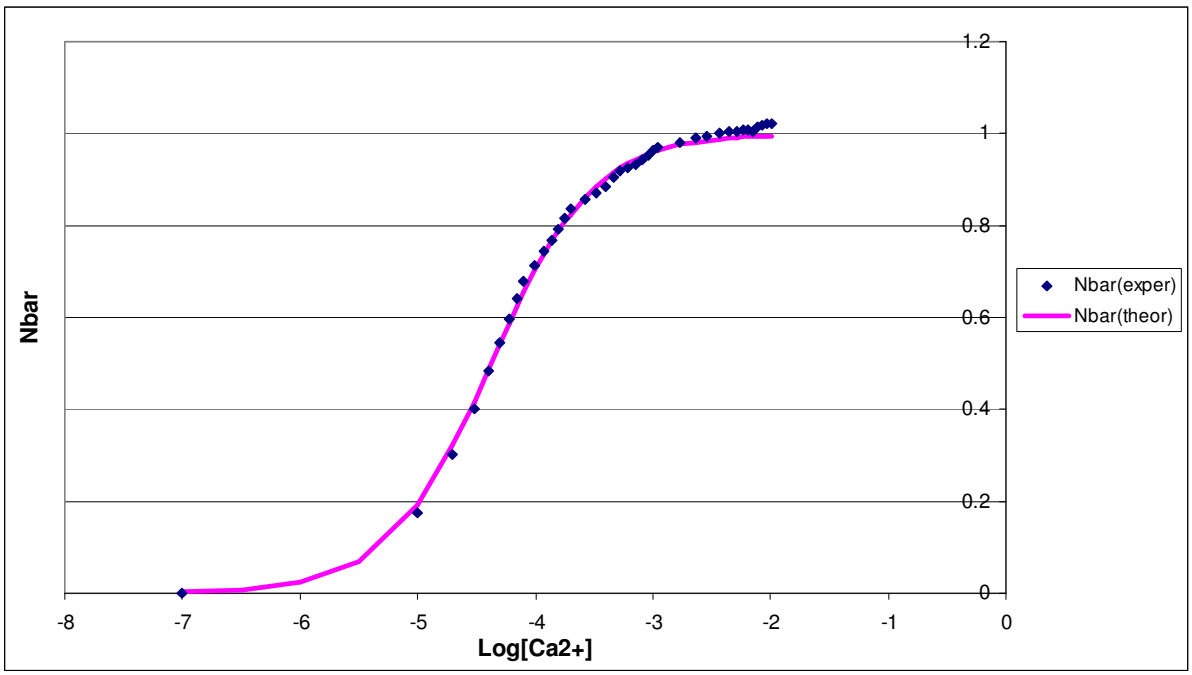

Figure 17: Experimental Nbar(exper) fitted with the calculated values of Nbar(theor) from the titration of a 2 x 10^{-5} *M* 8PQ solution with 0.0333 *M* $Ca(ClO_4)_2$ at 25.0 ± 0.1 °C and pH ≈ 6 for the wavelength 218nm.

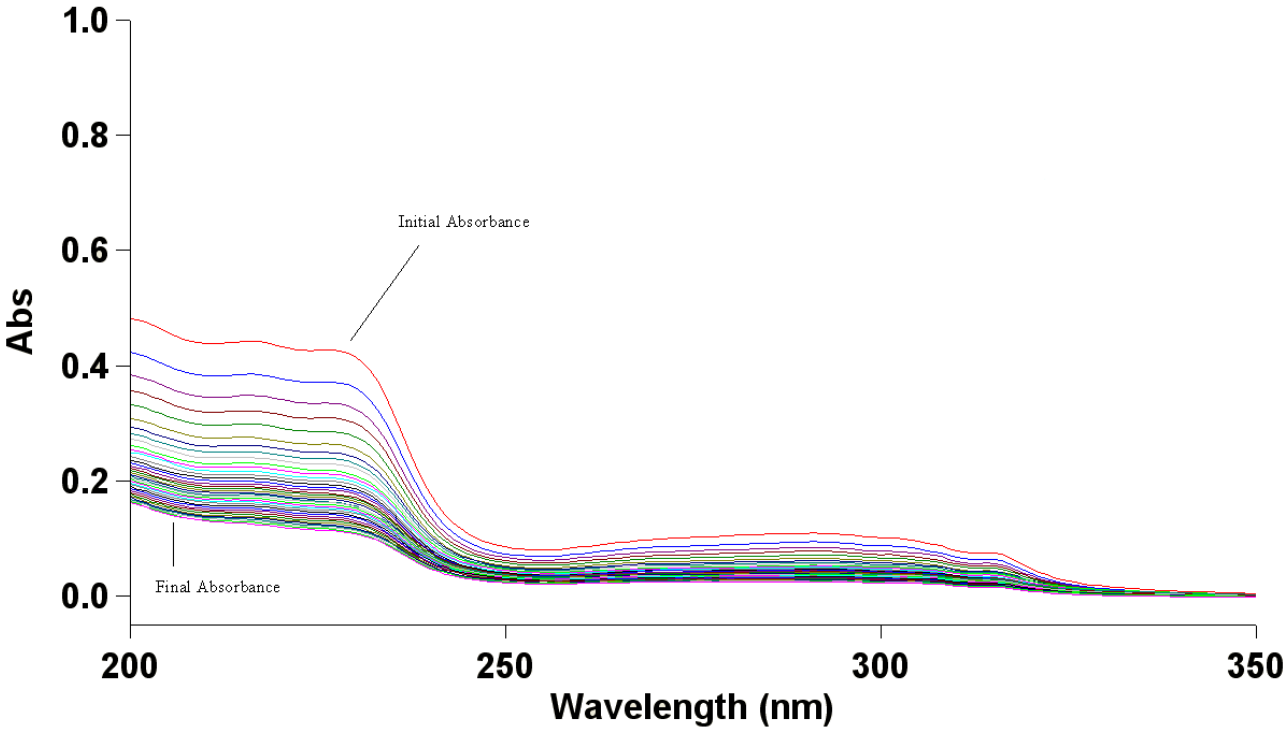

Figure 18: Absorbance versus wavelength (nm) spectra from the titration of a 2 x 10^{-5} *M* 8PQ solution with 0.1 *M* $NaClO_4$ at 25.0 ± 0.1 °C and pH ≈ 6.

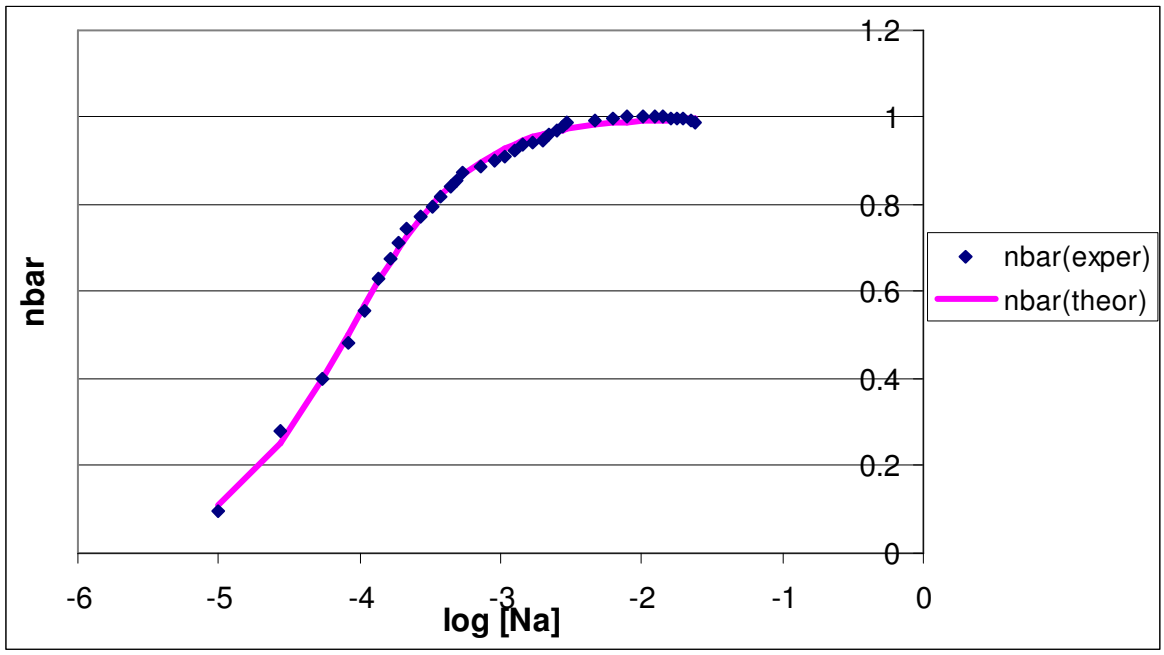

Figure 19: Experimental Nbar(exper) fitted with the calculated values of Nbar(theor) from the titration of a 2 x 10^{-5} *M* 8PQ solution with 0.1 *M* $NaClO_4$ at 25.0 ± 0.1 °C and pH ≈ 6 for the wavelength 218nm.

Copper(I)-8PQ Results:

Copper(I) has an ionic radius of 0.77Å which would classify it as medium sized metal ion. The UV absorbance spectrum for the 1:1 copper(I) and 8PQ titration experiment where both were of the concentration 2 x $10^{-5} M$ is shown in Figure 20. A graph with the experimental absorbance data fitted with calculated values to determine the protonation constant for the copper(I) and 8PQ solution is shown in Figure 21. By using equations 1-15 the log K_1 for the copper(I)-8PQ complex was found to be 5.13. Another titration experiment was done except this time at higher concentrations. A 1:1 copper(I) and 8PQ titration were both were at concentrations of 1 x $10^{-4} M$ was completed and the UV absorbance spectrum can be seen in Figure 22. The graph fitting calculated values to the experimental absorbance data to again determine the protonation constant for the copper(I) and 8PQ solution is shown in Figure 23. By again using equations 1-15 the log K_1 for the copper(I)-8PQ complex was this time found to be 4.66. This value for log K_1 is in close agreement with the value obtained from the first 1:1 titration. The equilibrium observed from these titrations is described below at the pH it occurred.

$$Cu(8PQ)^+ + H^+ \leftrightarrows Cu^+ + (8PQ)H^+ \qquad (pH = 5.09)$$

The absorbance data for both titrations were globally fitted with one another to produce a collective value for the log K_1 for the copper(I)-8PQ complex of 4.66 and was calculated as follows,

$$\text{Log } K_1 = 5.45 - 5.09 - \log(0.00005)$$

where 5.45 is the pK_a of the free ligand, 5.09 is the pK_1 equilibrium of complex formation and 0.00005 represents the amount of free metal ion at the midpoint of the equilibrium where Cu(I) is displaced from 8PQ.

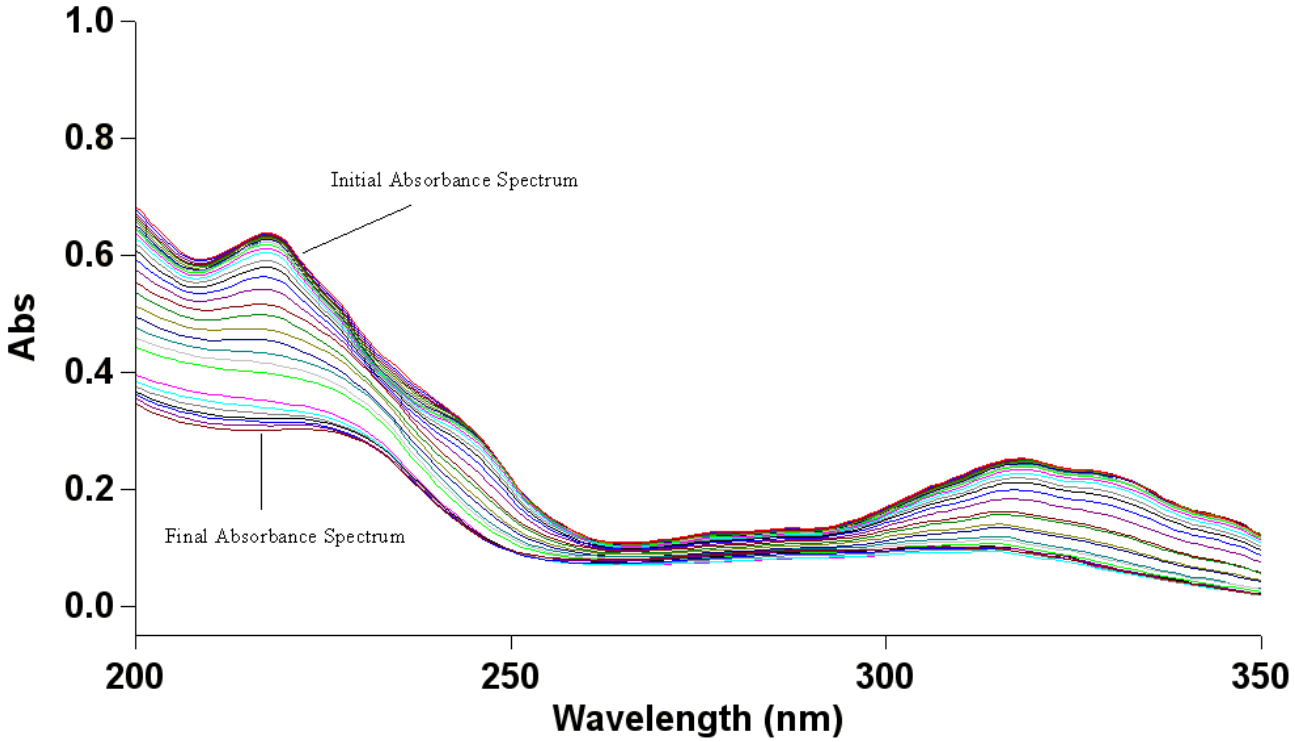

Figure 20: Absorbance versus wavelength (nm) spectra from the titration of the 1:1 copper(I) and 8PQ solution at concentrations of 2 x 10^{-5} *M* at 25.0 ± 0.1 °C with 0.1 *M* NaOH with a pH range of approximately 2 to 8.

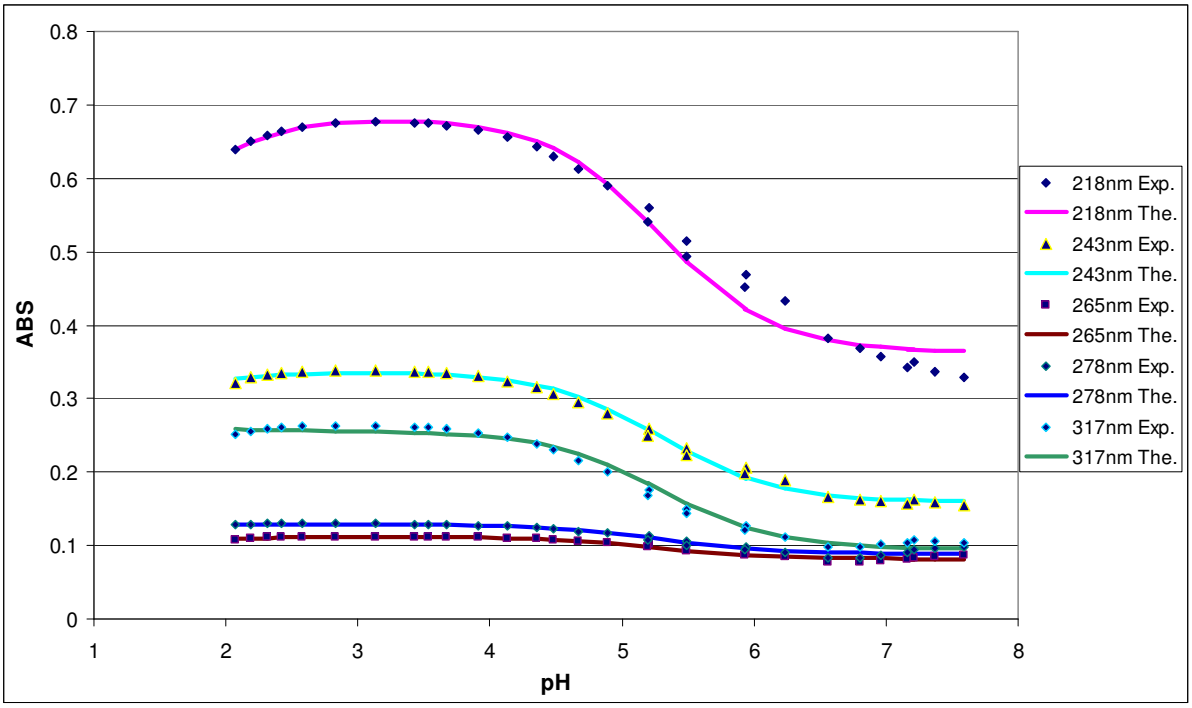

Figure 21: Experimental absorbance data (Exp.) fitted with calculated values (The.) to determine the protonation constants for the 1:1 copper(I) and 8PQ solution at concentrations of 2 x 10^{-5} *M*.

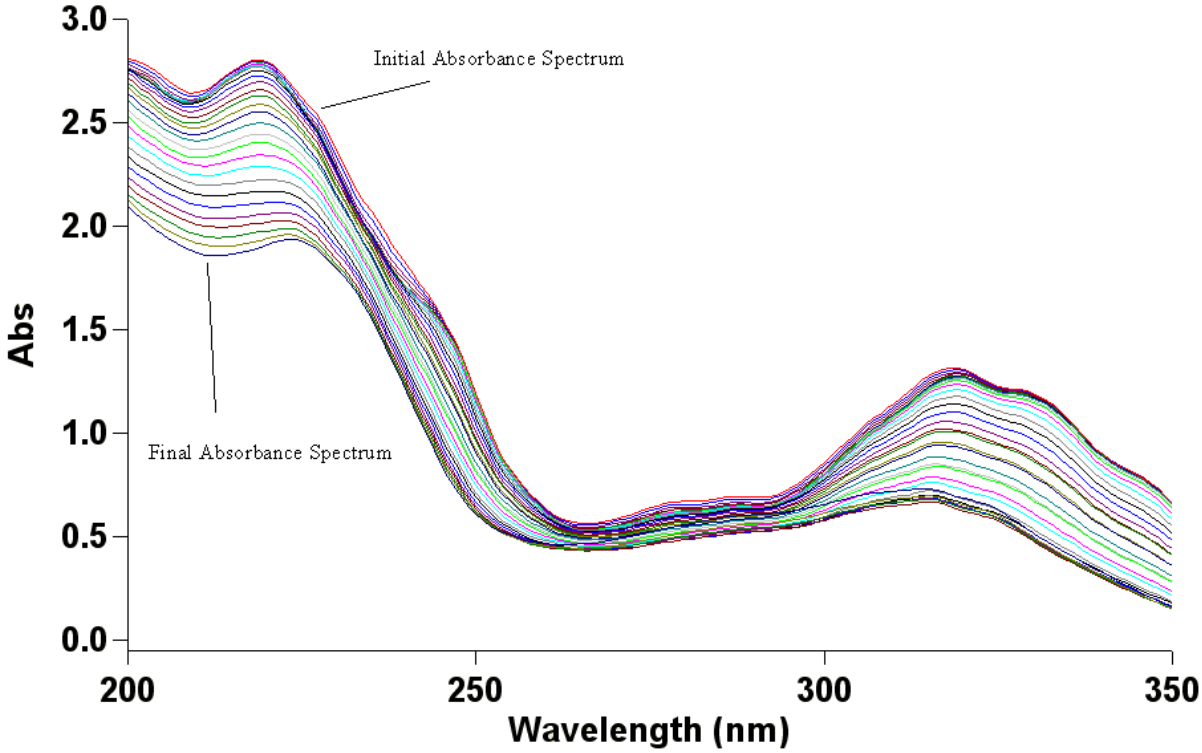

Figure 22: Absorbance versus wavelength (nm) spectra from the titration of a 1:1 copper(I) and 8PQ solution at concentrations of 1 x 10^{-4} *M* at 25.0 ± 0.1 °C with 0.1 *M* NaOH with a pH range of approximately 2 to 7.

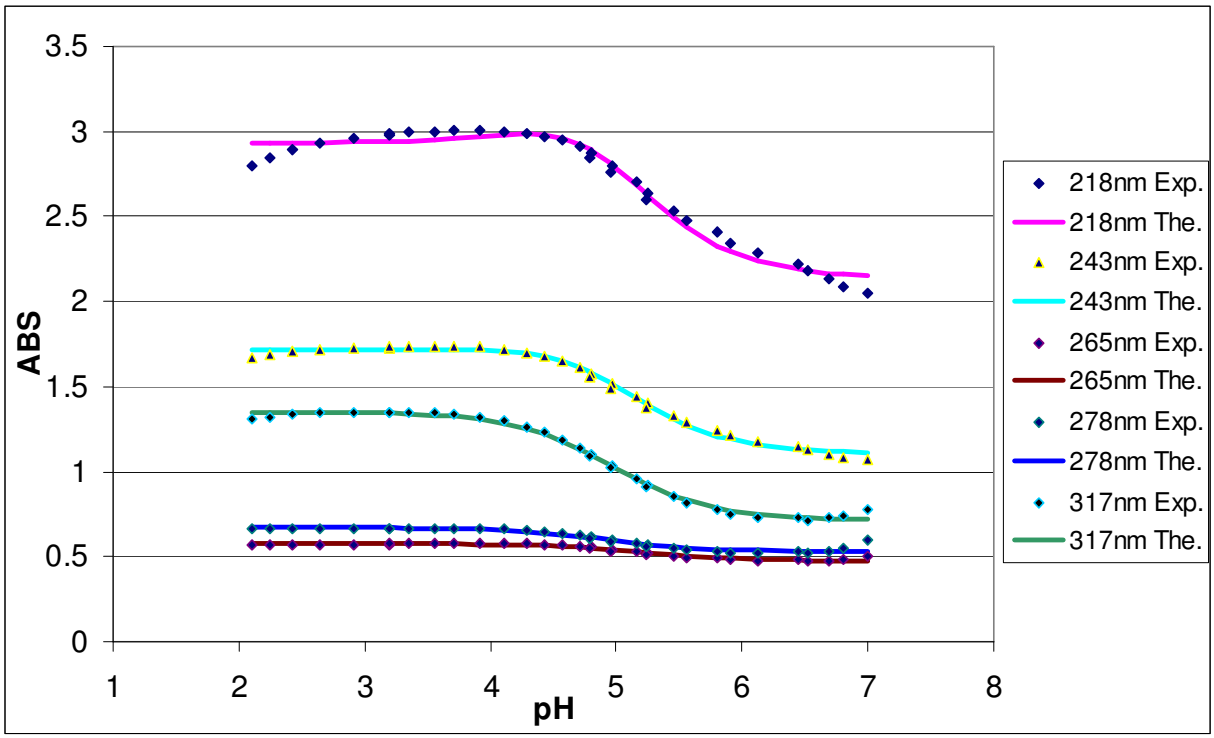

Figure 23: Experimental absorbance data (Exp.) fitted with calculated values (The.) for the titration of 1:1 copper(I) and 8PQ at concentrations of 1 x 10^{-4} *M*.

Copper(II)-8PQ Results:

Copper(II) has an ionic radius of 0.57Å which makes it a fairly small metal ion, smaller then the copper(I) ion. The UV absorbance spectrum for the 100:1 copper(II) and 8PQ titration experiment where the concentrations were 2 x $10^{-3} M$ and 2 x $10^{-5} M$ respectively is shown in Figure 24. A plot of correlation between E (mV) and the calculated pH, which was used to calculate E^0, is shown in Figure 25. A graph with the experimental absorbance data fitted with calculated values to determine the protonation constant for the copper(II) and 8PQ solution is shown in Figure 26. By using equations 1-15 the log K_1 for the copper(II)-8PQ complex was found to be 4.68. Another titration experiment was performed to better confirm these results. The UV absorbance spectrum for the 10:1 copper(II) and 8PQ titration experiment where the concentrations were 2 x $10^{-4} M$ and 2 x $10^{-5} M$ respectively is shown in Figure 27. A plot of correlation between E (mV) and the calculated pH, which was used to calculate E^0, is shown in Figure 28. A graph with the experimental absorbance data fitted with calculated values to determine the protonation constant for the copper(II) and 8PQ solution is shown in Figure 29. Again by using equations 1-15 the log K_1 for the copper(II)-8PQ complex was this time found to be 4.3. This value for log K_1 is not far off the first value obtained from the 100:1 titration experiment. The equilibrium observed from these titrations is described below at the pH it occurred.

$$Cu(8PQ)^{2+} + H^+ \leftrightarrows Cu^{2+} + (8PQ)H^+ \qquad (pH = 3.78)$$

The absorbance data for both titrations were globally fitted with one another to produce a collective value for the log K_1 for the copper(II)-8PQ complex of 4.37 and was calculated as follows,

$$\text{Log } K_1 = 5.45 - 3.78 - \log(0.002)$$

where 5.45 is the pK_a of the free ligand, 3.78 is the pK_1 equilibrium of complex formation and 0.002 represents the amount of free metal ion at the midpoint of the equilibrium where Cu(II) is displaced from 8PQ. It is found that the log K_1 for the copper(II) complex is lower then that of the copper(I) complex (4.66). This can be explained by the fact that even though the copper(II) ion has a smaller ionic radius, it is unwilling to form a tetrahedral complex where as copper(I) can.

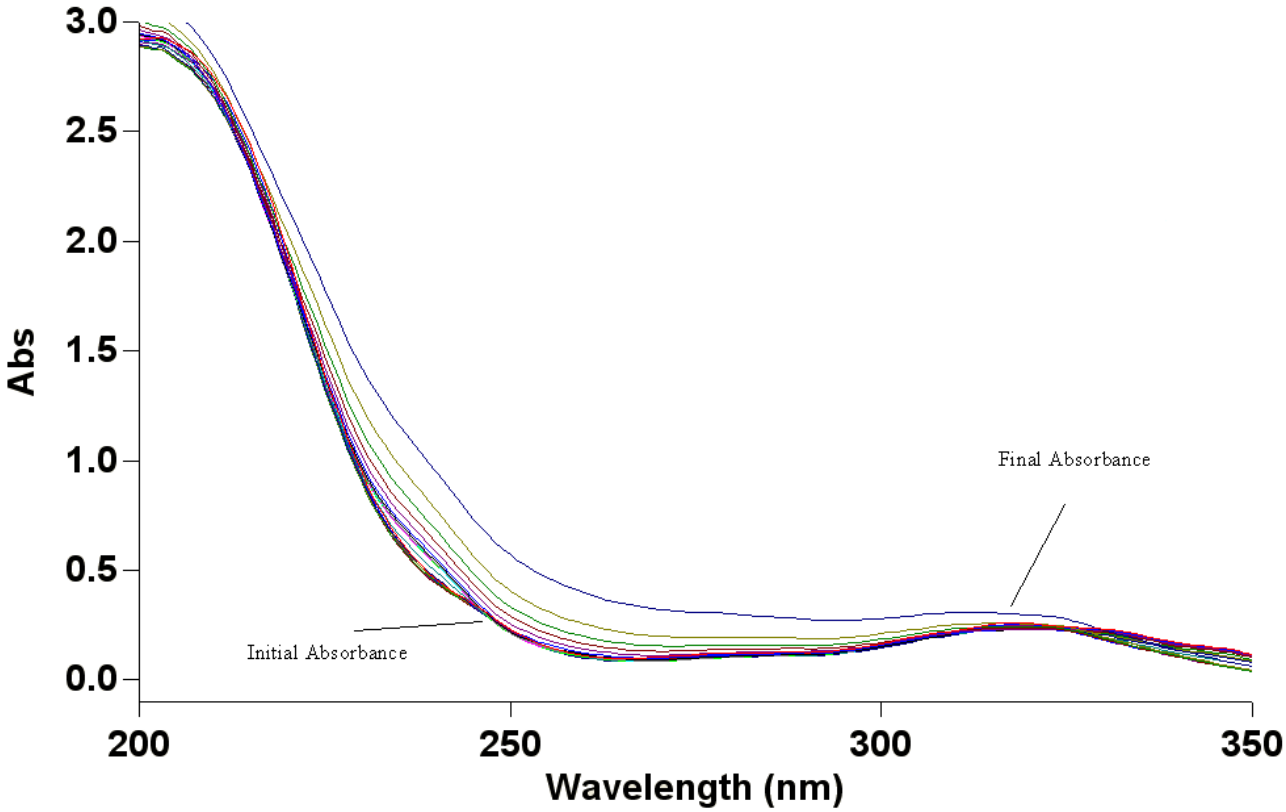

Figure 24: Absorbance versus wavelength (nm) spectra from the titration of the 100:1 copper(II) and 8PQ solution at concentrations of 2 x 10^{-3} M and 2 x 10^{-5} M respectively at 25.0 ± 0.1 °C with 0.1 M NaOH with a pH range of approximately 2 to 6.5.

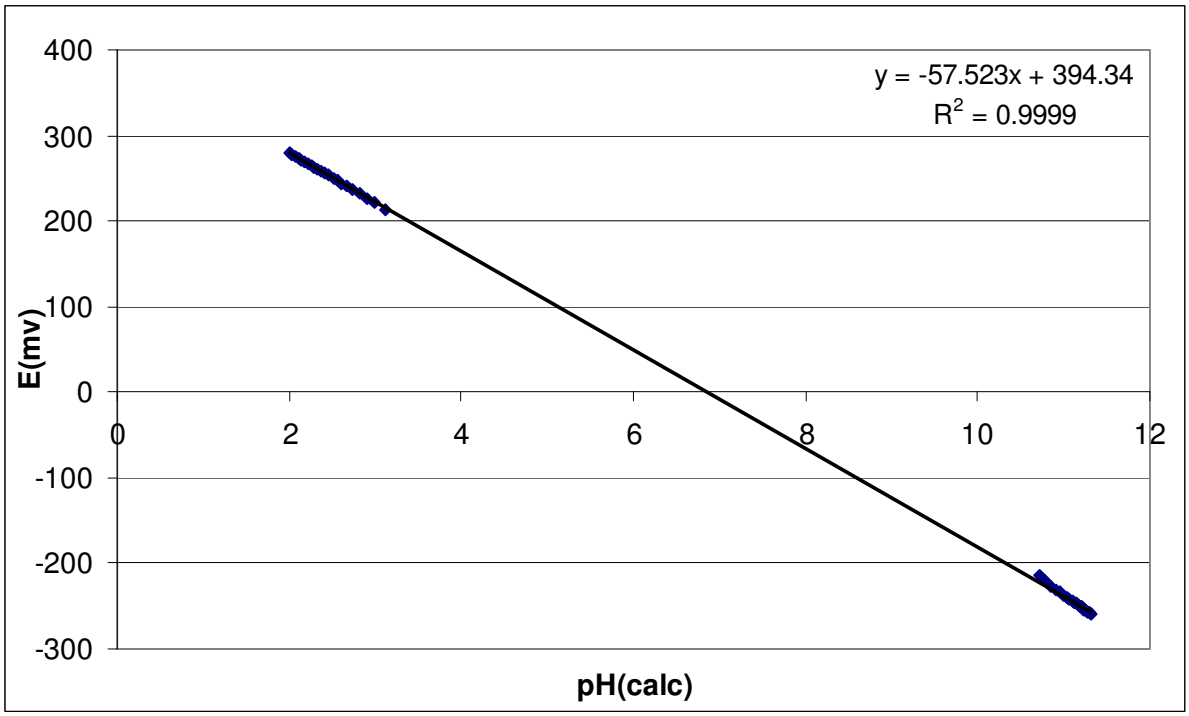

Figure 25: Plot of the correlation between E (mV) and the calculated pH used to calculate E^0 for the titration of the 100:1 copper(II) and 8PQ solution at concentrations of 2 x 10^{-3} *M* and 2 x 10^{-5} *M* respectively at 25.0 ± 0.1 °C with 0.1 *M* NaOH.

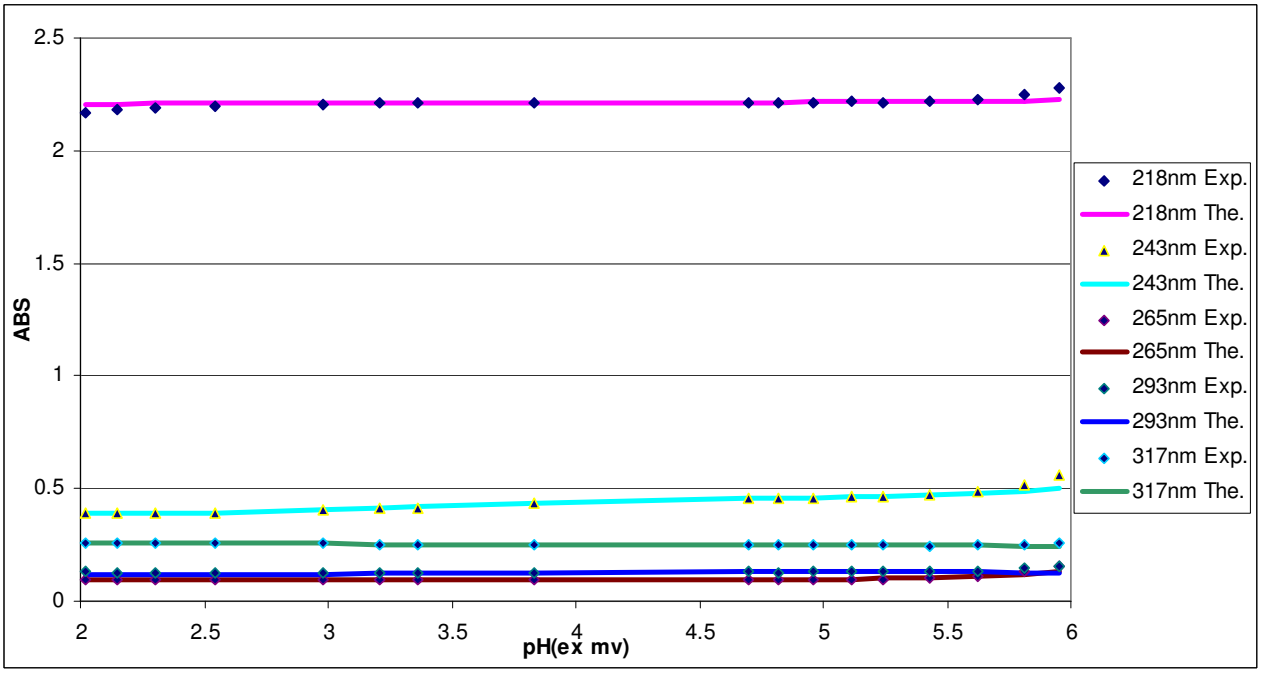

Figure 26: Experimental absorbance data (Exp.) fitted with calculated values (The.) for the titration of 100:1 copper(II) and 8PQ solution at concentrations of 2 x 10^{-3} *M* and 2 x 10^{-5} *M* respectively.

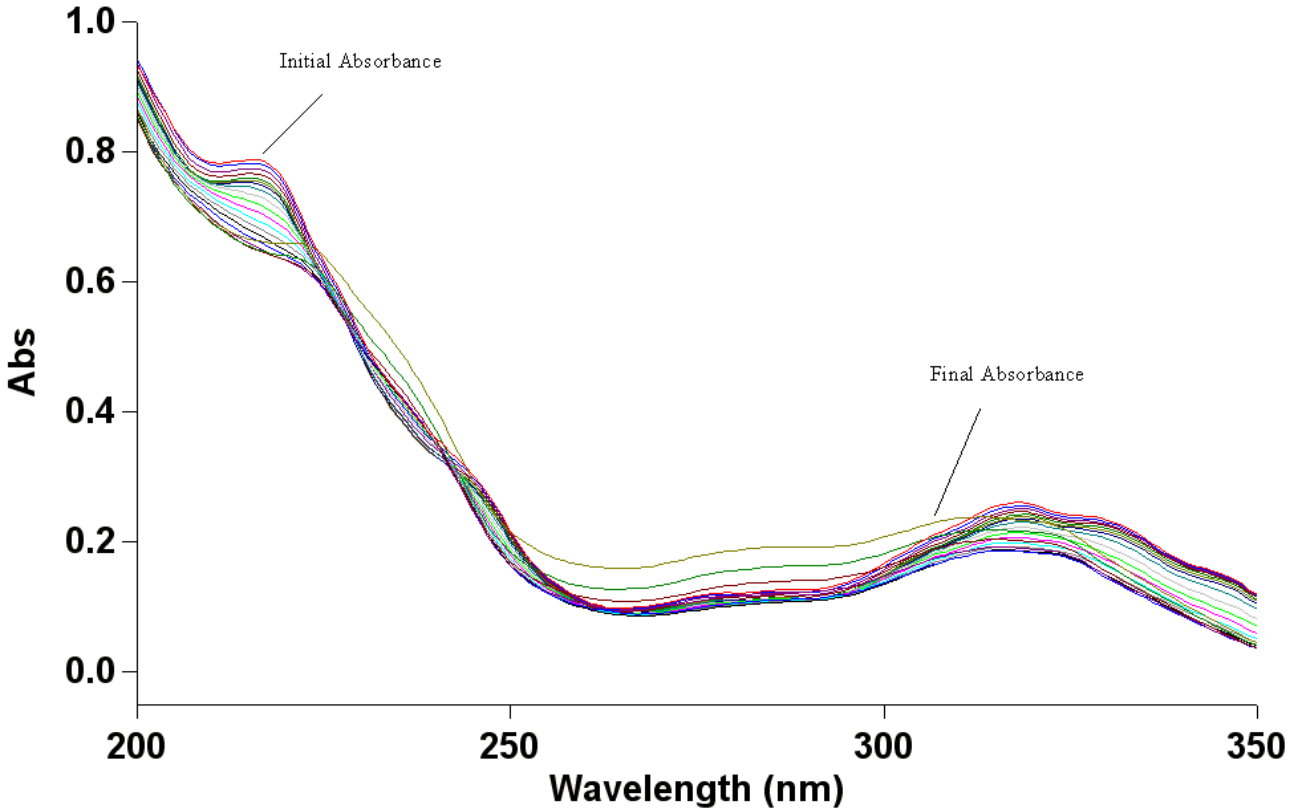

Figure 27: Absorbance versus wavelength (nm) spectra from the titration of the 10:1 copper(II) and 8PQ solution at concentrations of 2 x 10^{-4} *M* and 2 x 10^{-5} *M* respectively at 25.0 ± 0.1 °C with 0.1 *M* NaOH with a pH range of approximately 2 to 6.5.

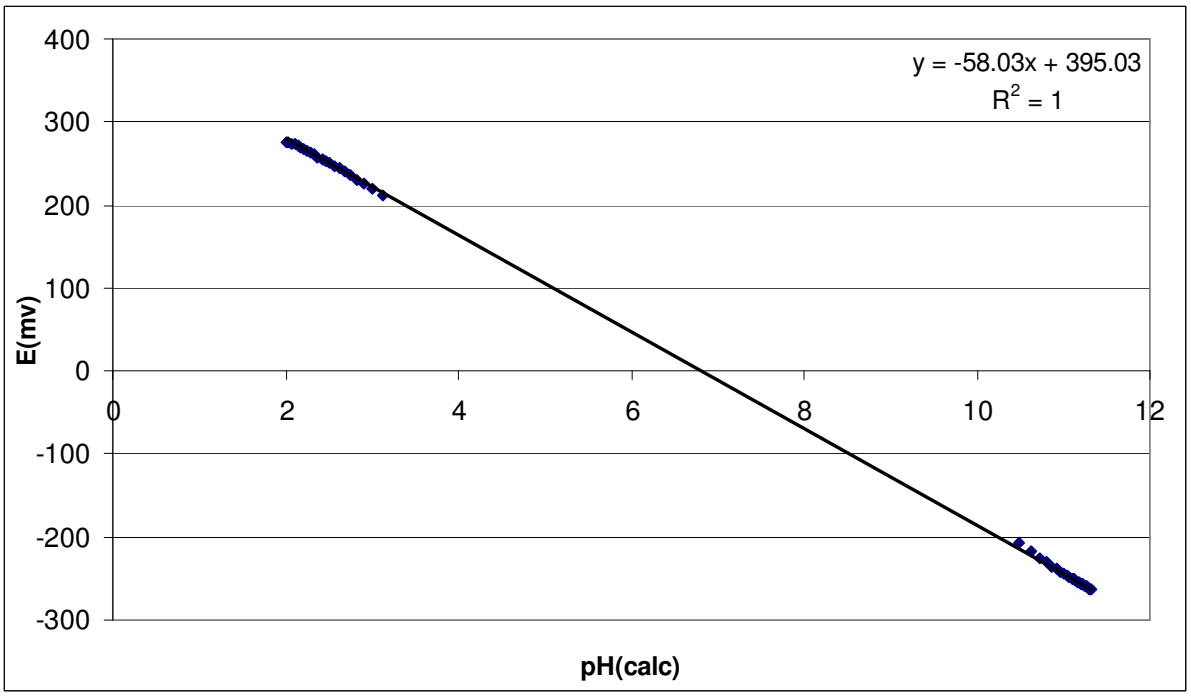

Figure 28: Plot of the correlation between E (mV) and the calculated pH used to calculate E^0 for the titration of the 10:1 copper(II) and 8PQ solution at concentrations of 2 x 10^{-4} *M* and 2 x 10^{-5} *M* respectively at 25.0 ± 0.1 °C with 0.1 *M* NaOH.

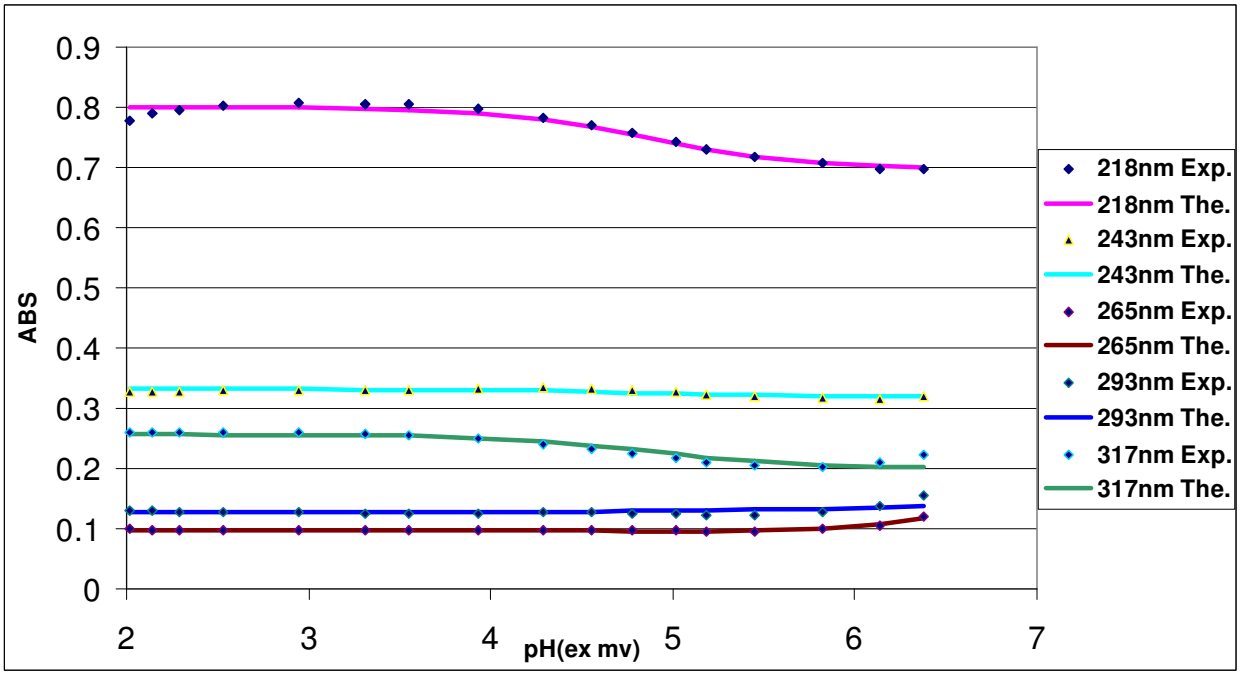

Figure 29: Experimental absorbance data (Exp.) fitted with calculated values (The.) for the titration of 10:1 copper(II) and 8PQ solution at concentrations of 2 x 10^{-4} *M* and 2 x 10^{-5} *M* respectively.

Nickel(II)-8PQ Results

Nickel(II) has an ionic radius of 0.69Å which classifies it as a medium sized metal ion. Three different titration experiments were run with nickel(II) and 8PQ resulting in three different log K_1 values. The absorbance data from all titrations were fitted together to result in a collective log K_1 for the nickel(II)-8PQ complex. The UV absorbance spectrum for the 1665:1 nickel(II) and 8PQ titration experiment is shown in Figure 30. In addition to the five selected wavelengths (218, 243, 265, 278, and 317nm), absorbance values were recorded at wavelengths 231 and 345nm. These wavelengths were included as they exhibited at a large variance in absorbance due to complexation. The graph showing the experimental absorbance data fitted with the calculated values used to determine the protonation constants for the nickel(II) and 8PQ solution is shown in Figure 31. By using equations 1-15 the log K_1 for the nickel(II)-8PQ complex was found to be 3.23. The second titration experiment was a 500:1 nickel(II) and 8PQ titration and its UV absorbance spectrum is shown in Figure 32. As with the first titration absorbance values were recorded at wavelengths 231 and 345nm along with the five standard wavelengths as they were greatly influenced by complexation. The graph showing this experimental absorbance data and the fitted theoretical absorbance curves can be seen in Figure 33. Again by using equations 1-15 the log K_1 for the nickel(II)-8PQ complex was this time found to be 3.32. The last titration experiment was a 50:1 nickel(II) and 8PQ titration and its UV absorbance spectrum is shown in Figure 34. Only the absorbance at the five standard wavelengths was recorded this time as this was adequate in displaying the effect of complexation. The graph showing this experimental absorbance data and the fitted theoretical absorbance curves can be seen in Figure 35.

Lastly by again using equations 1-15 the log K_1 for the nickel(II)-8PQ complex was found to be 3.31. The equilibrium observed from these titrations are described below at the pH they occurred.

$Ni(8PQ)^{2+} + H^+ \leftrightarrows Ni^{2+} + (8PQ)H^+$ (pH = 5.15)

The absorbance data for these three titrations were globally fitted with one another to produce a collective value for the log K_1 for the nickel(II)-8PQ complex of 3.30. This value was calculated as follows,

$$\text{Log } K_1 = 5.45 - 5.15 - \log(0.001)$$

where 5.45 is the pK_a of the free ligand, 5.15 is the pK_1 equilibrium of complex formation and 0.001 represents the amount of free metal ion at the midpoint of the equilibrium where Ni(II) is displaced from 8PQ.

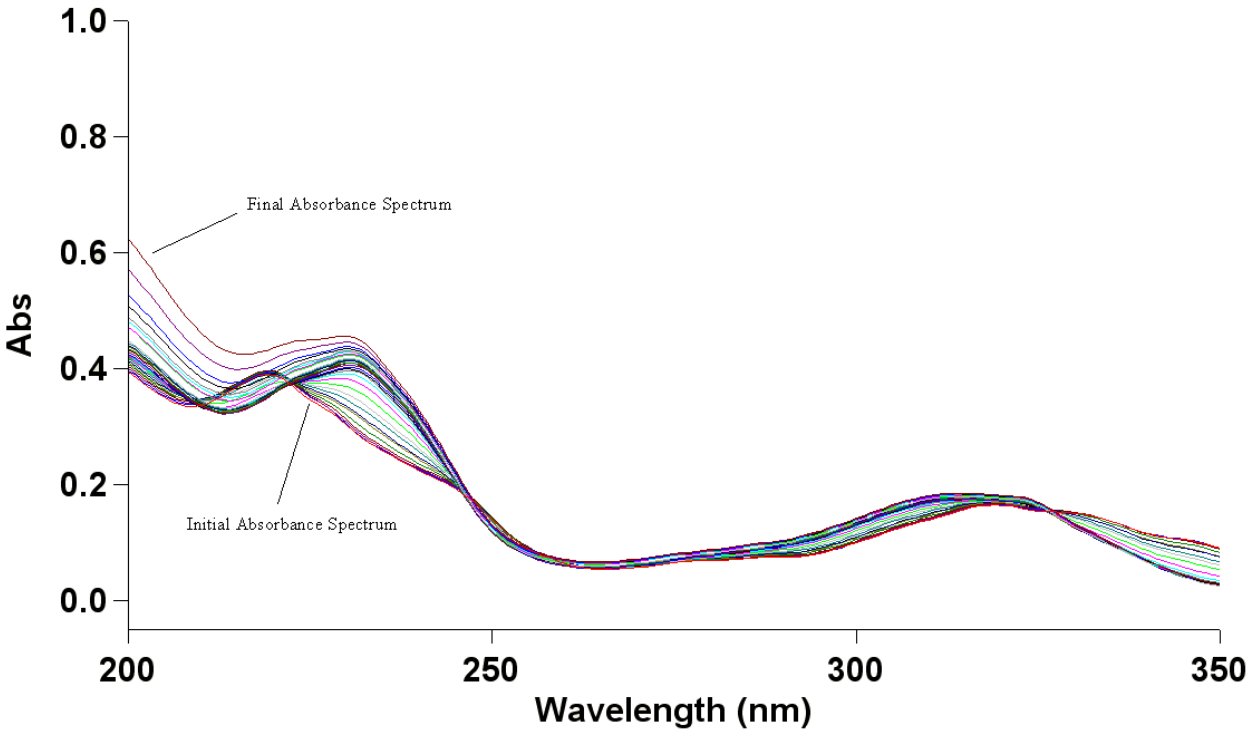

Figure 30: Absorbance versus wavelength (nm) spectra from the titration of a 1665:1 nickel(II) and 8PQ solution at concentrations of 0.0333 *M* and 2 x 10^{-5} *M* respectively at 25.0 ± 0.1 °C with 0.1 *M* NaOH with a pH range of approximately 2 to 7.5.

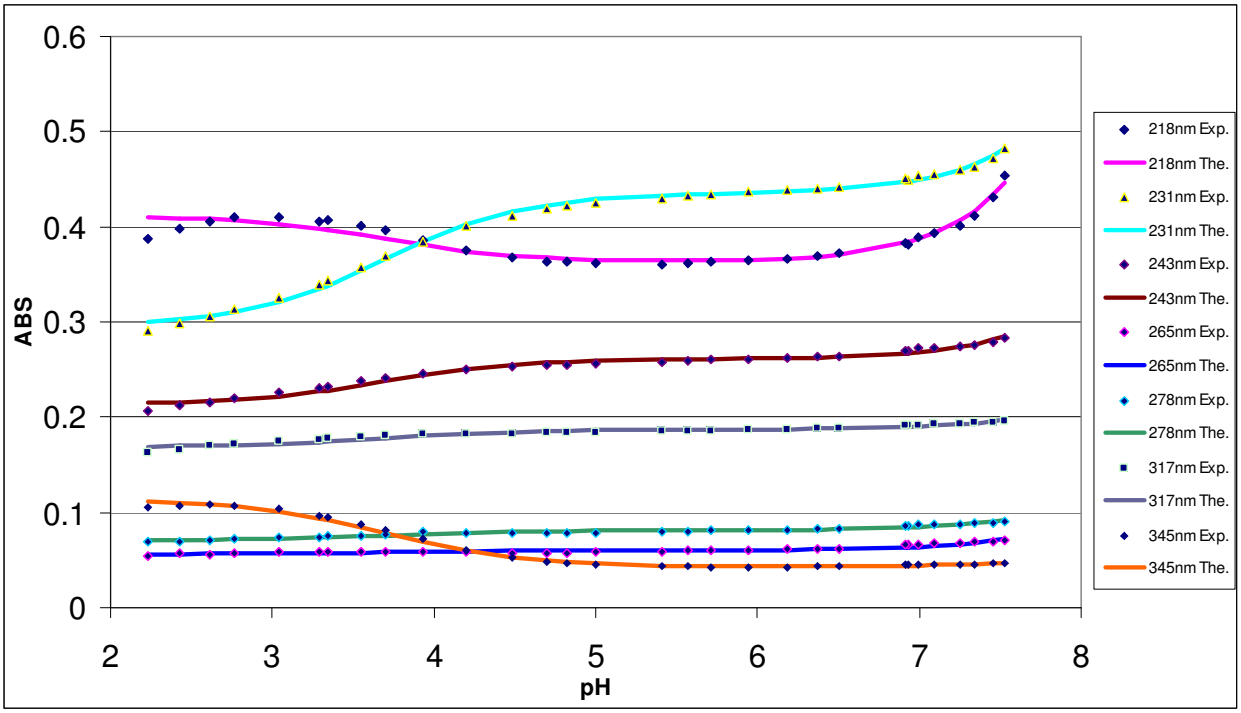

Figure 31: Experimental absorbance data (Exp.) fitted with calculated values (The.) for the titration of 1665:1 nickel(II) and 8PQ solution at concentrations of 0.0333 M and 2 x 10^{-5} M respectively.

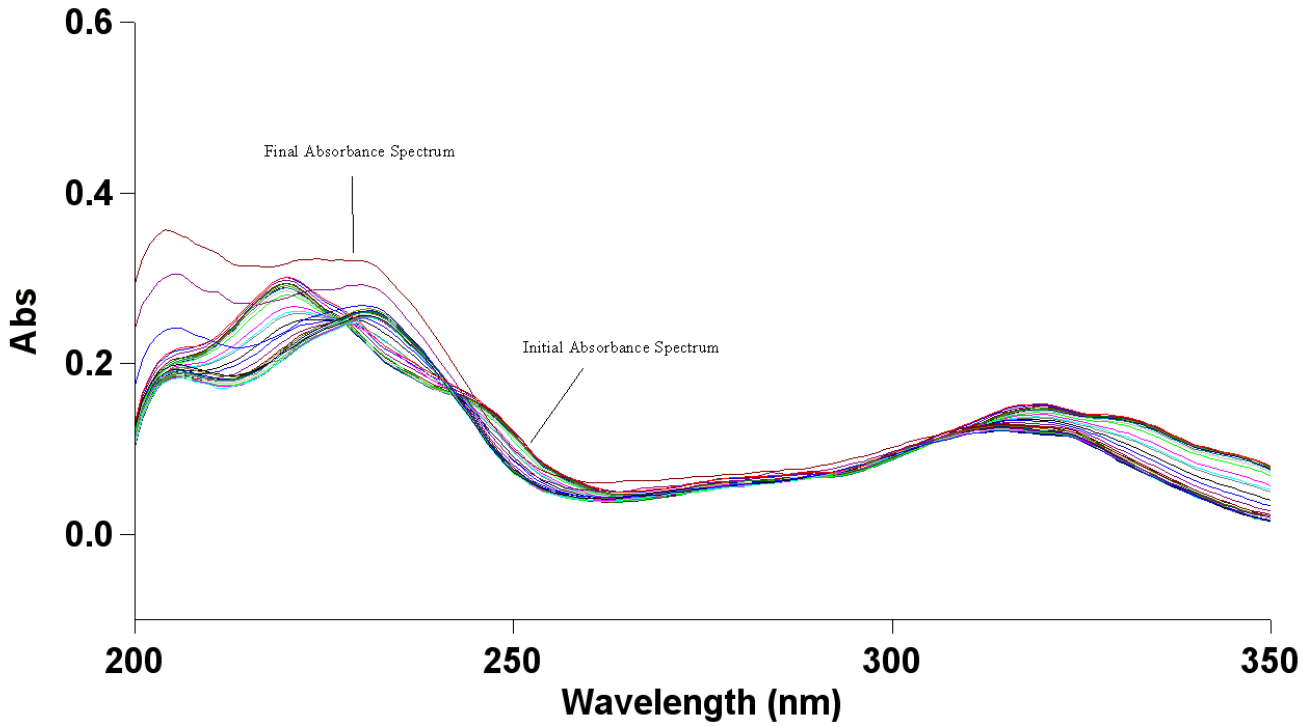

Figure 32: Absorbance versus wavelength (nm) spectra from the titration of a 500:1 nickel(II) and 8PQ solution at concentrations of 0.01 *M* and 2 x 10^{-5} *M* respectively at 25.0 ± 0.1 °C with 0.1 *M* NaOH with a pH range of approximately 2 to 8.

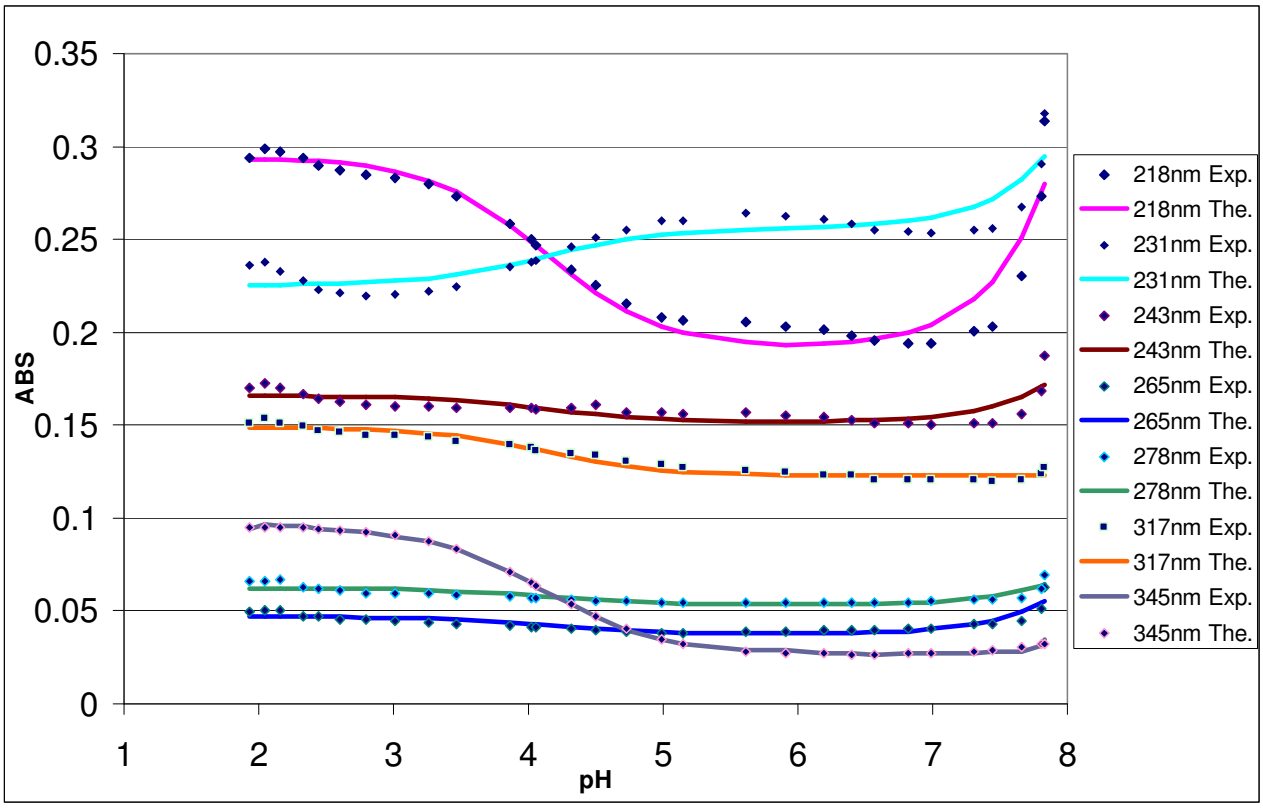

Figure 33: Experimental absorbance data (Exp.) fitted with calculated values (The.) for the titration of 500:1 nickel(II) and 8PQ solution at concentrations of 0.01 M and 2 x 10^{-5} M respectively.

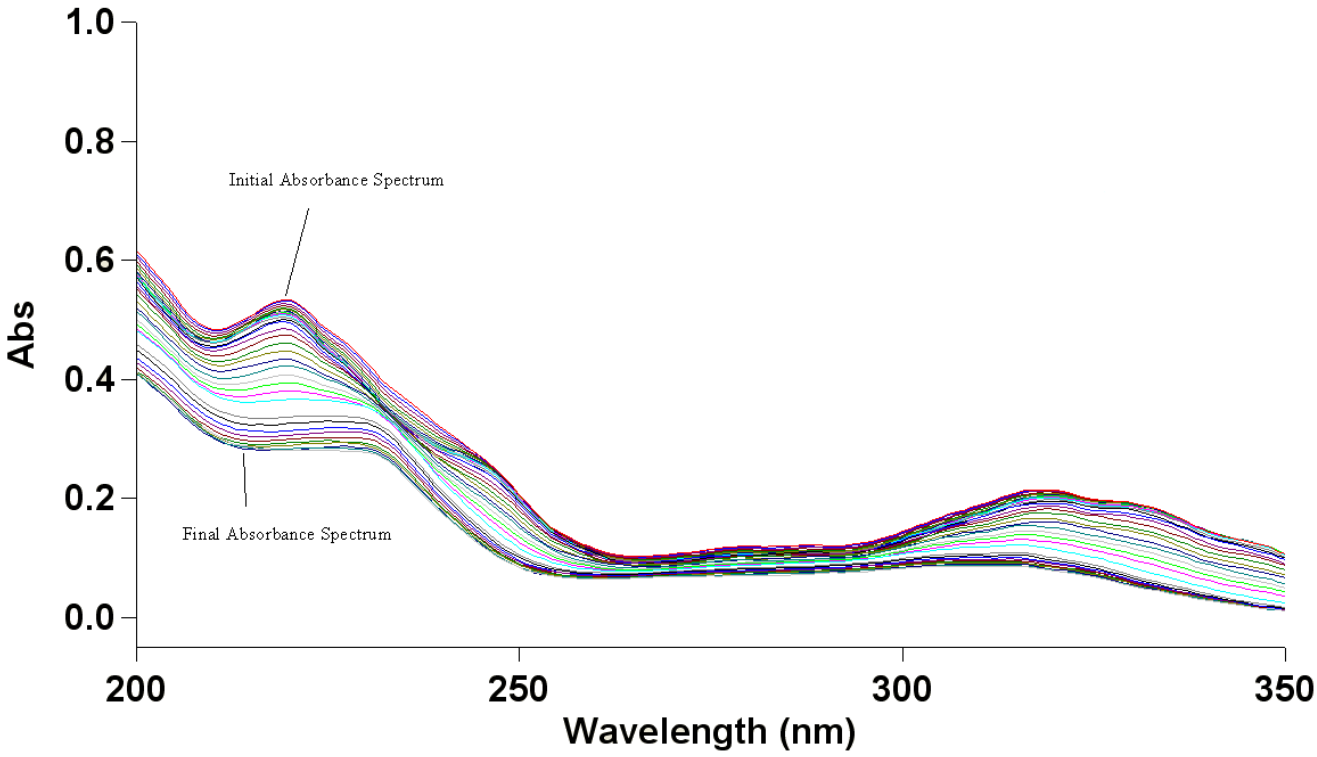

Figure 34: Absorbance versus wavelength (nm) spectra from the titration of a 50:1 nickel(II) and 8PQ solution at concentrations of 1 x 10^{-3} *M* and 2 x 10^{-5} *M* respectively at 25.0 ± 0.1 °C with 0.1 *M* NaOH with a pH range of approximately 2 to 8.

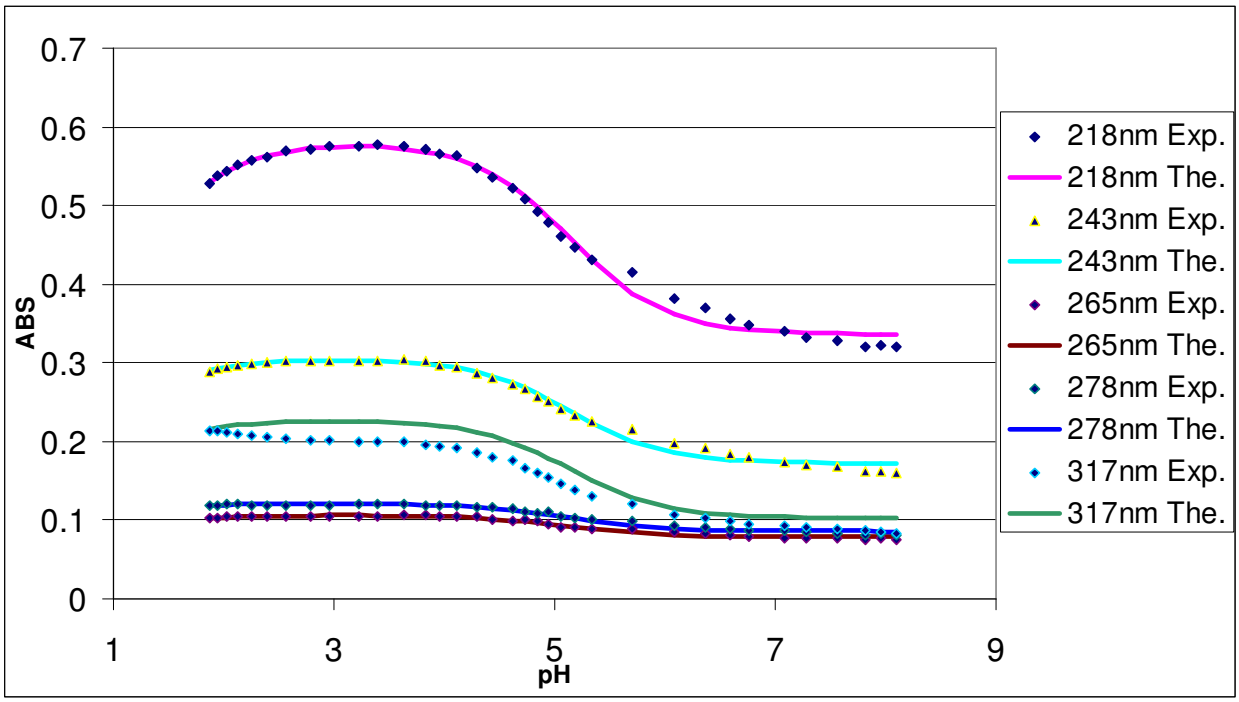

Figure 35: Experimental absorbance data (Exp.) fitted with calculated values (The.) for the titration of 50:1 nickel(II) and 8PQ solution at concentrations of 1 x 10^{-3} *M* and 2 x 10^{-5} *M* respectively.

Palladium(II)-8PQ Results

Palladium(II) has an ionic radius of 0.64Å which classifies it as a fairly small metal ion. This titration experiment involved a solution of 1:1 palladium(II) and 8PQ solution where concentrations were both at 2 x 10^{-5} M. Knowing that palladium(II) has slow kinetics extra time was given between additions of 0.1 M NaOH to allow it to equilibrate. The UV absorbance spectrum for this 1:1 palladium(II) and 8PQ titration experiment is shown in Figure 36. It can be seen in the absorbance spectrum that the palladium(II)-8PQ complex is formed even before the titration starts and does not dissociate at any point of the titration. Due to this complex being kinetically inert it is not possible to fit this data set in such a way to determine a value for the log K_1 of this complex. However, using Figure 13, a graph comparing the difference in log K_1 values of 8PQ and bipyridine, it is possible to predict the log K_1 value for Pd(II) with 8PQ. The trends shown in the graph predict that the log K_1 value for Pd(II) with 8PQ is 16.4.

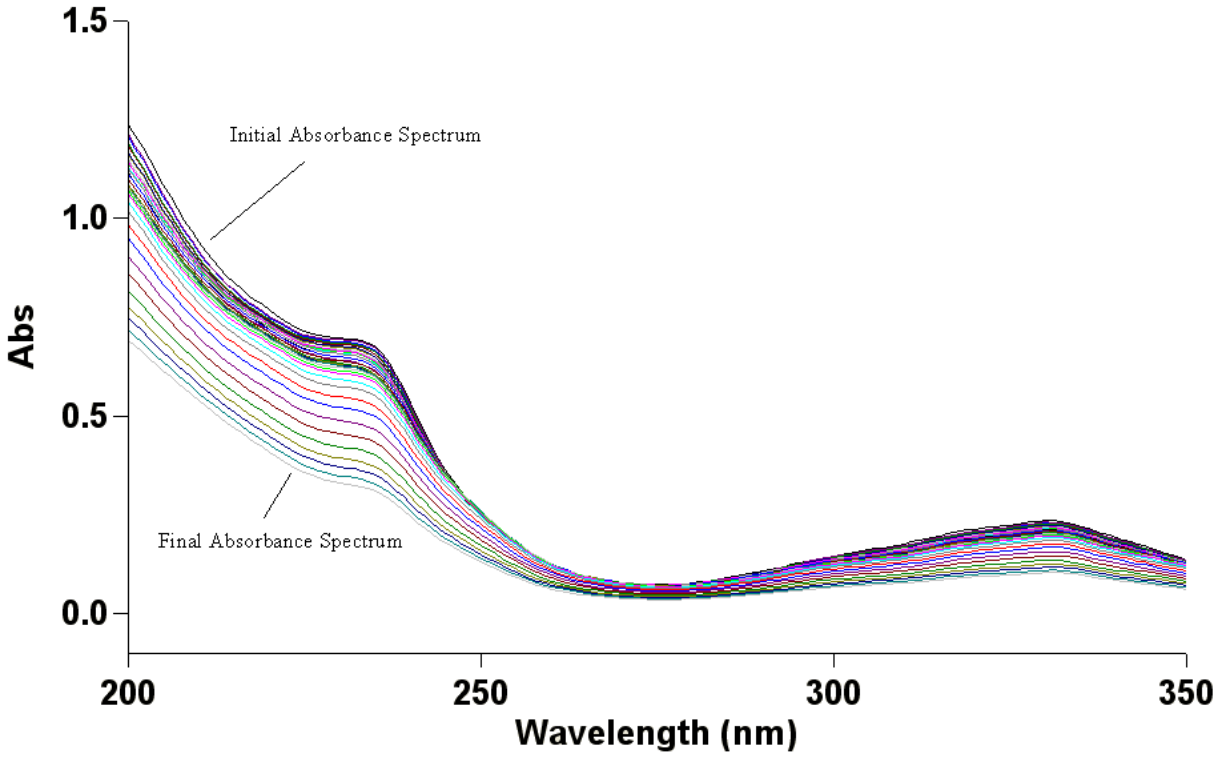

Figure 36: Absorbance versus wavelength (nm) spectra from the titration of a 1:1 palladium(II) and 8PQ solution at concentrations of 2 x 10^{-5} *M* at 25.0 ± 0.1 °C with 0.1 *M* NaOH with a pH range of approximately 2 to 7.

Zinc(II)-8PQ Results

Zinc(II) has an ionic radius of 0.74Å which classifies it as a medium sized metal ion. Two different titration experiments were run with zinc(II) and 8PQ resulting in two different log K_1 values. The absorbance data from all titrations were fitted together to result in a collective log K_1 for the zinc(II)-8PQ complex. The UV absorbance spectrum for the 1665:1 zinc(II) and 8PQ titration experiment is shown in Figure 37. The graph showing the experimental absorbance data fitted with the calculated values used to determine the protonation constants for the zinc(II) and 8PQ solution is shown in Figure 38. By using equations 1-15 the log K_1 for the zinc(II)-8PQ complex was found to be 1.82. The second titration experiment was a 100:1 zinc(II) and 8PQ titration and its UV absorbance spectrum is shown in Figure 39. The graph showing this experimental absorbance data and the fitted theoretical absorbance curves can be seen in Figure 40. Again by using equations 1-15 the log K_1 for the zinc(II)-8PQ complex was this time found to be 1.17. The equilibria observed from these titrations are described below at the pH they occurred.

$$Zn(8PQ)^{2+} + H^{+} \leftrightarrows Zn^{2+} + (8PQ)H^{+} \qquad (pH = 4.66)$$

$$Zn(8PQ) + OH^{-} \leftrightarrows Zn(8PQ)OH^{-} \qquad (pH = 6.33)$$

The absorbance data for these two titrations were globally fitted with one another to produce a collective value for the log K_1 for the zinc(II)-8PQ complex of 3.48. This value was calculated as follows,

$$\text{Log } K_1 = 5.45 - 4.66 - \log(0.002)$$

where 5.45 is the pK_a of the free ligand, 4.66 is the pK_1 equilibrium of complex formation and 0.002 represents the amount of free metal ion at the midpoint of the equilibrium where Zn(II) is displaced from 8PQ.

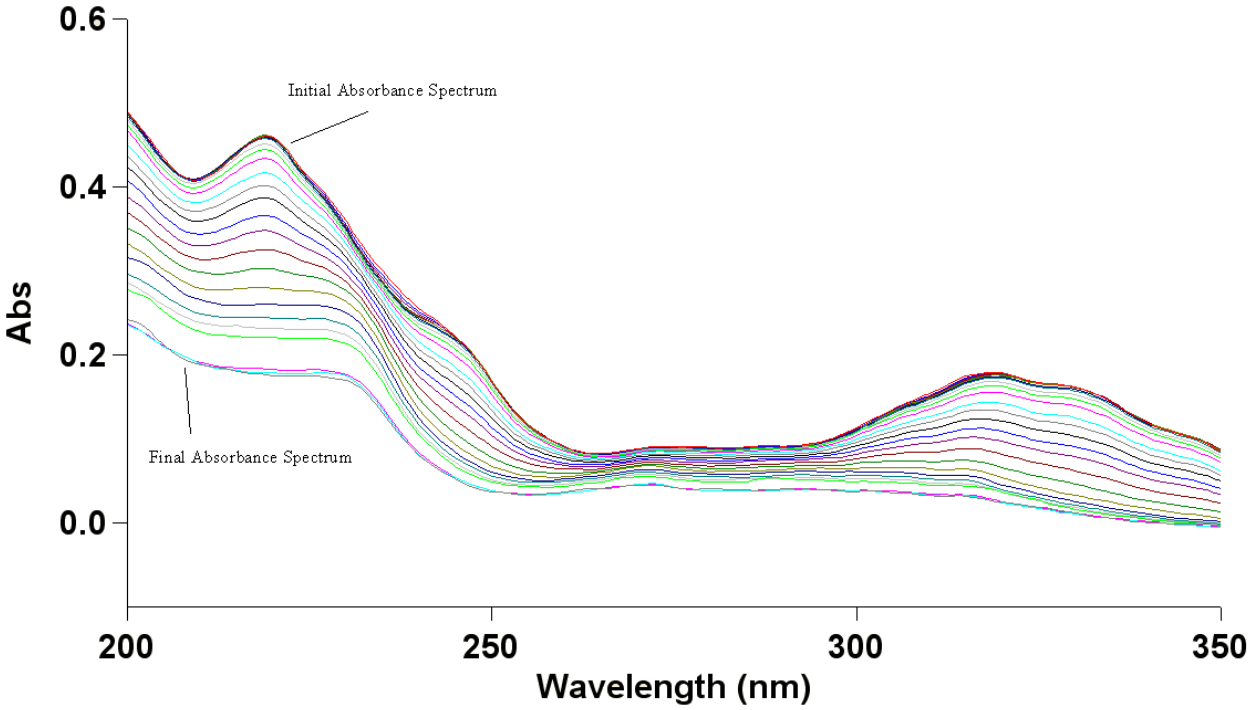

Figure 37: Absorbance versus wavelength (nm) spectra from the titration of a 1665:1 zinc(II) and 8PQ solution at concentrations of 0.0333 *M* and 2 x 10^{-5} *M* respectively at 25.0 ± 0.1 °C with 0.1 *M* NaOH with a pH range of approximately 2 to 6.5.

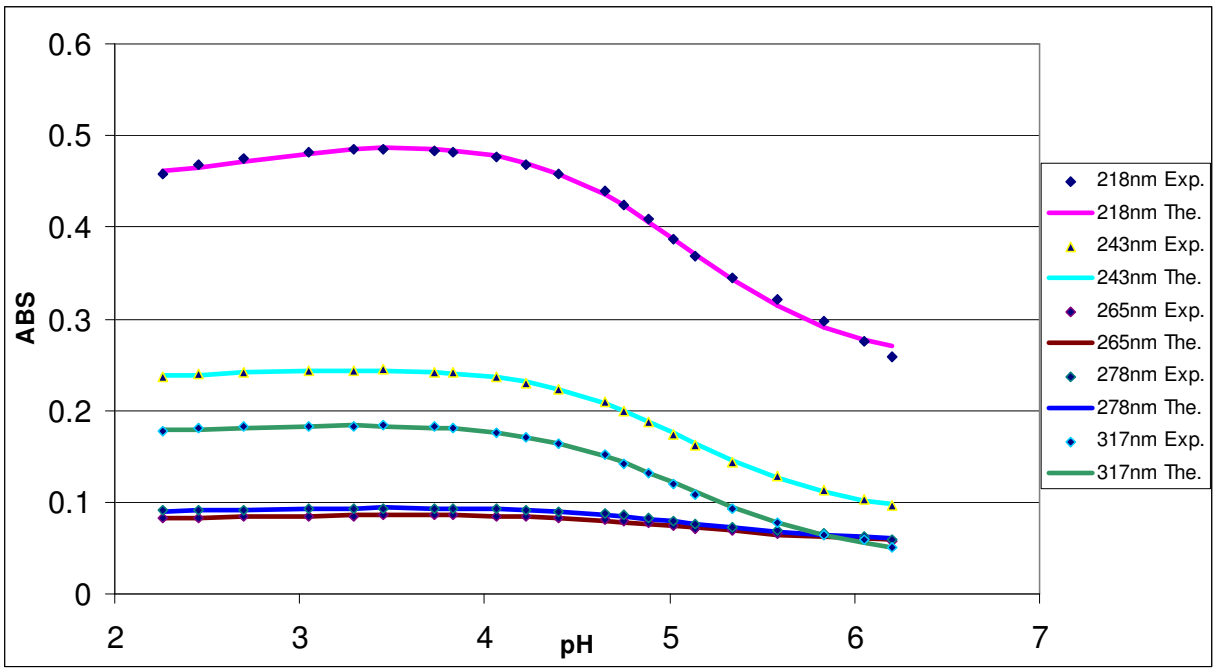

Figure 38: Experimental absorbance data (Exp.) fitted with calculated values (The.) for the titration of 1665:1 zinc(II) and 8PQ solution at concentrations of 0.0333 M and 2 x 10^{-5} M respectively.

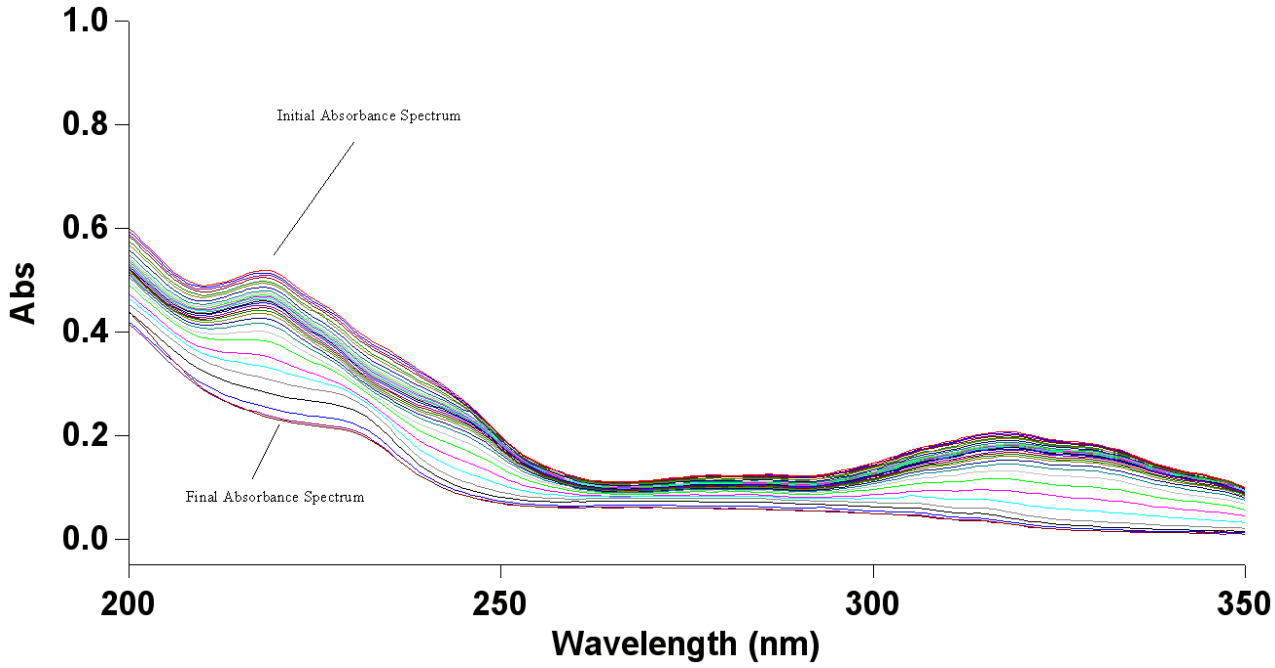

Figure 39: Absorbance versus wavelength (nm) spectra from the titration of a 100:1 zinc(II) and 8PQ solution at concentrations of 2×10^{-3} *M* and 2×10^{-5} *M* respectively at 25.0 ± 0.1 °C with 0.1 *M* NaOH with a pH range of approximately 2 to 7.

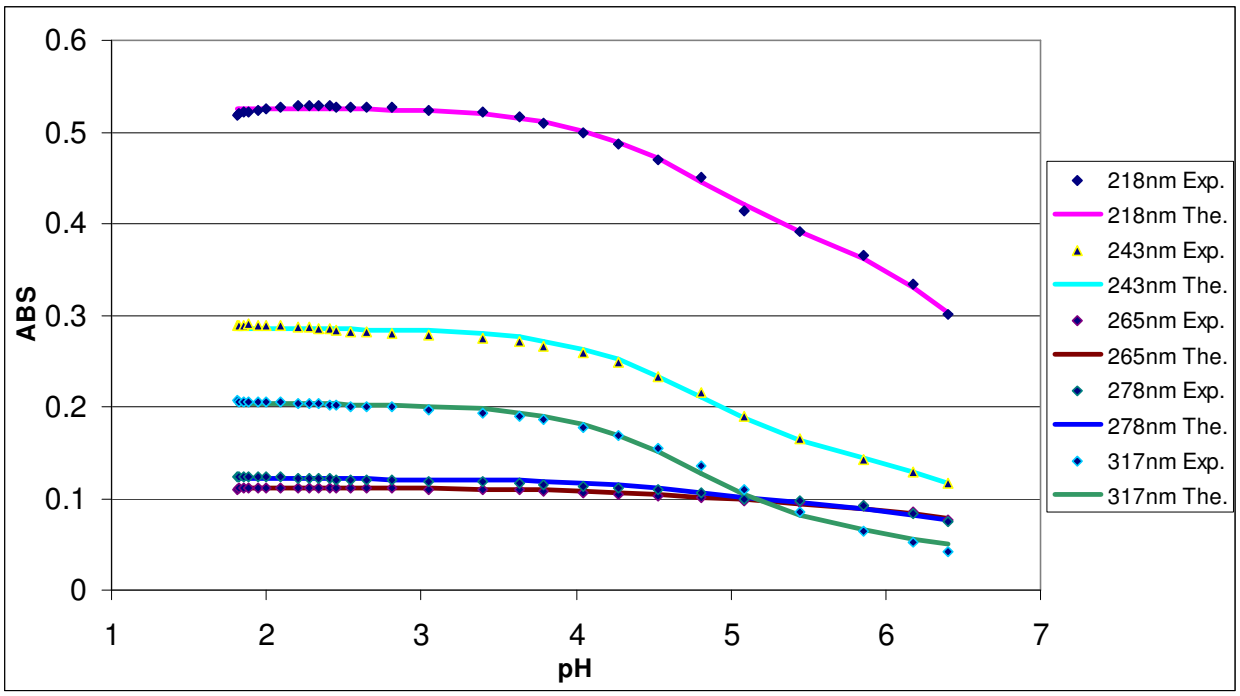

Figure 40: Experimental absorbance data (Exp.) fitted with calculated values (The.) for the titration of 100:1 zinc(II) and 8PQ solution at concentrations of 2 x 10^{-3} M and 2 x 10^{-5} M respectively.

UV-Vis Spectrophotometric Titrations Involving DIPY

UV/Vis spectroscopy was used as an analytical tool to determine the stability constants ($\log K_1$) of the metal-DIPY complexes. Absorbance scans were recorded from 200 to 350nm and were taken after each titrant addition of 0.1 *M* NaOH. Absorbance data was taken at selected wavelengths of 218, 250, 265, 293, and 322nm. Absorbance spectra of the free ligand at varying pH at these wavelengths can be seen in Figure 41. Peak shifts were seen for these absorbances upon complexation of DIPY with a metal ion.

In order to determine the protonation constants for this ligand, DIPY, a titration experiment was performed at 25.0 ± 0.1 °C at 0.1 *M* ionic strength (0.1 *M* $NaClO_4$). Figure 42 shows absorbance versus wavelength (nm) scans at pH values of approximately 2 to 10.5. A plot of correlation between E (mV) and the calculated pH, which was used to calculate E^0, is shown in Figure 43. Absorbance data for the selected wavelengths were used to generate a plot of absorbance versus pH(ex mv). This plot is shown in Figure 44. The points drawn in are the experimental values and the solid lines are theoretical curves of absorbance versus pH calculated for the constants corresponding to the observed protonation equilibria. The theoretical curves of absorbance versus pH in Figure 44 were fitted to the experimental points using the SOLVER tool of the program EXCEL[22]. The standard deviations of these protonation constants were calculated using the SOLVSTAT macro provided in reference 22. The protonation constants for DIPY were calculated using the absorbance data and pH values from this plot. DIPY, much like 8PQ, has two protonation events pK_1 and pK_2. The calculated protonation constants of pK_1 and pK_2 were 6.87 and 2.50 respectively. An illustration of the proposed

protonation equilibria for DIPY can be seen in Figure 45. These protonation constants were determined by using equations 1-7.

a.)

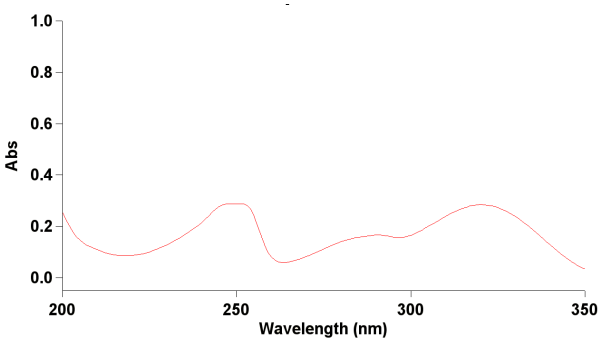

b.)

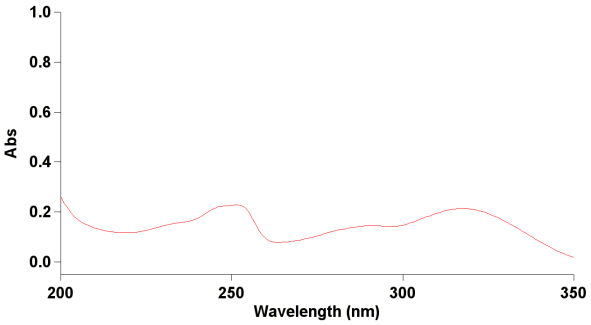

c.)

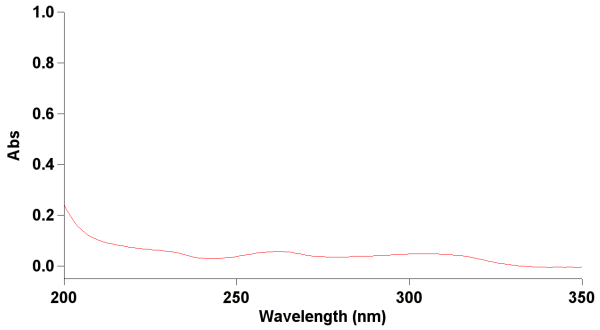

d.)

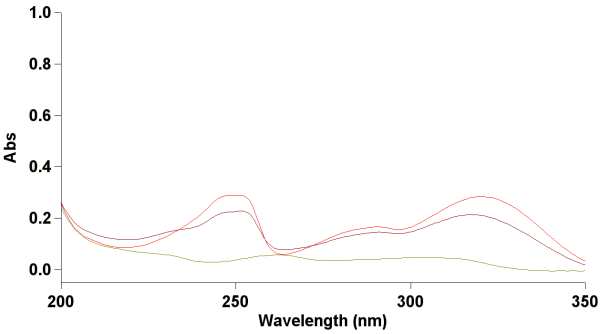

Figure 41: Plots of absorbance versus wavelength (nm) spectra at varying pH of 2 x 10^{-5} *M* DIPY at 25.0 ± 0.1 °C with 0.1 *M* NaOH. a.) pH = 2.07, b.) pH = 6.23, c.) pH = 9.81, d.) overlay of pH 2.07, 6.23, and 9.81 spectra.

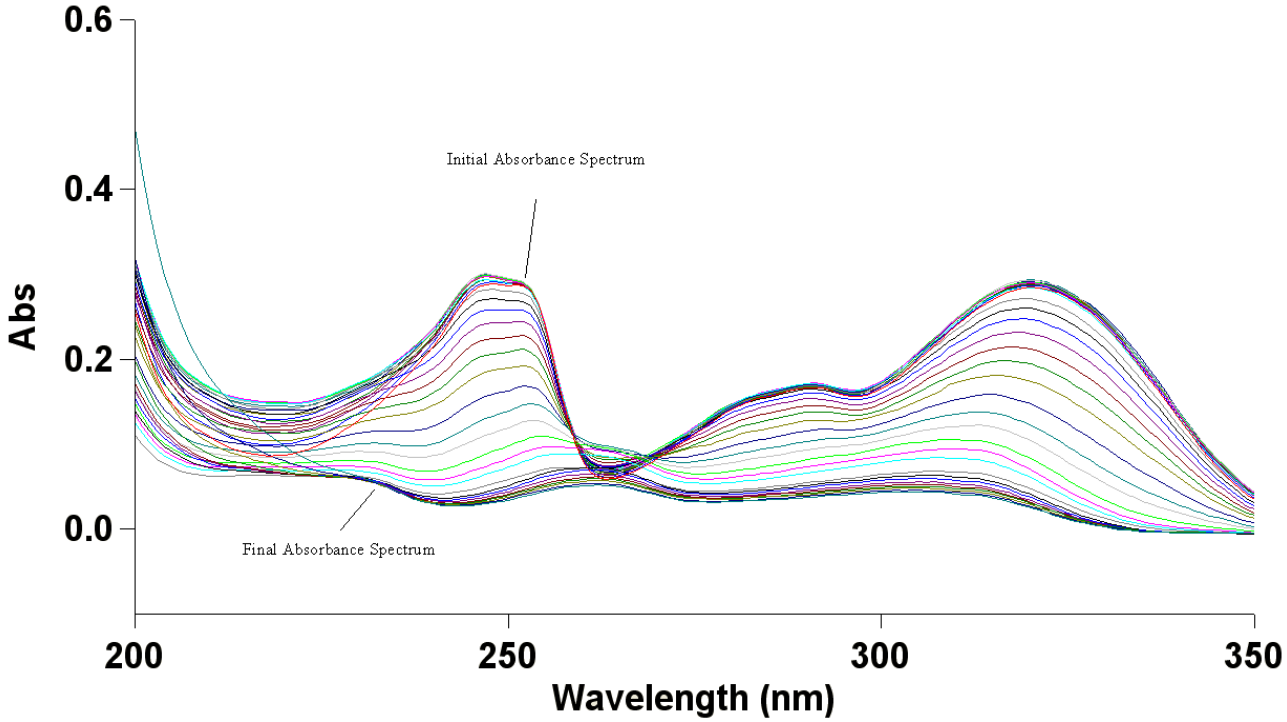

Figure 42: Absorbance versus wavelength (nm) spectra from the titration of 2 x 10^{-5} *M* DIPY at 25.0 ± 0.1 °C with 0.1 *M* NaOH with a pH range of approximately 2.00 to 10.5.

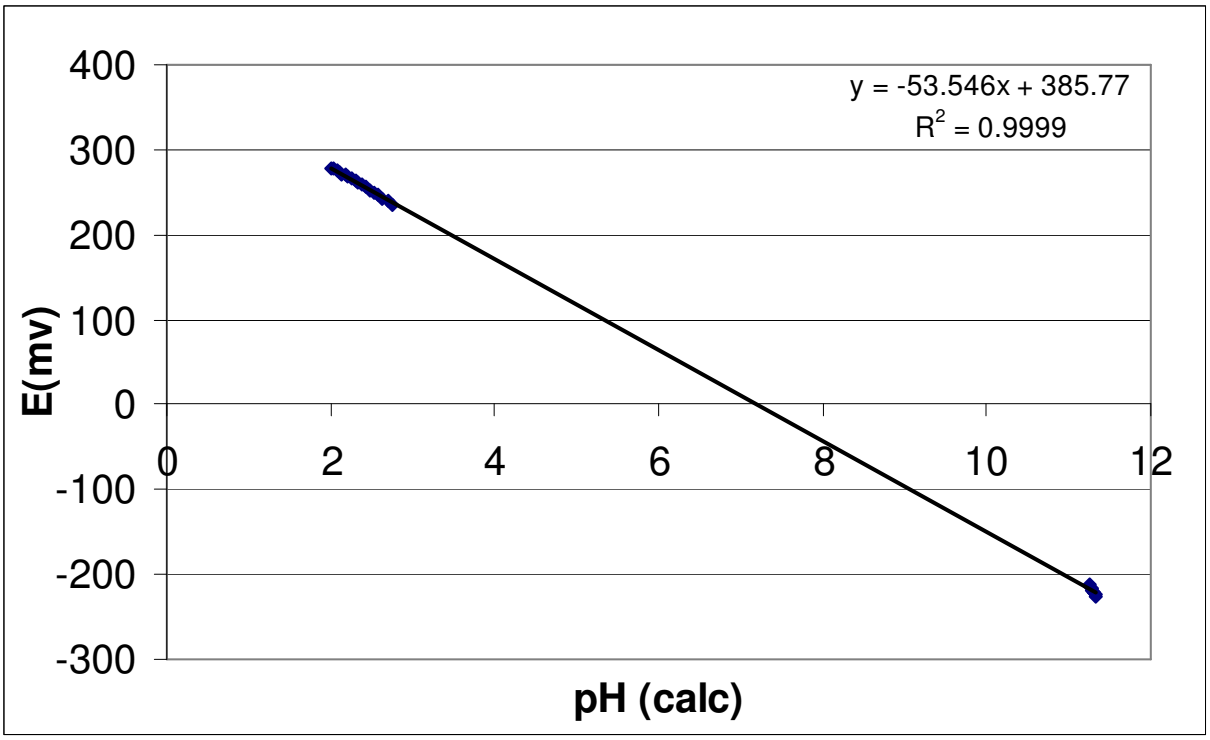

Figure 43: Plot of the correlation between E (mV) and the calculated pH used to calculate E^0 for the titration of 2 x 10^{-5} *M* DIPY at 25.0 ± 0.1 °C with 0.1 *M* NaOH.

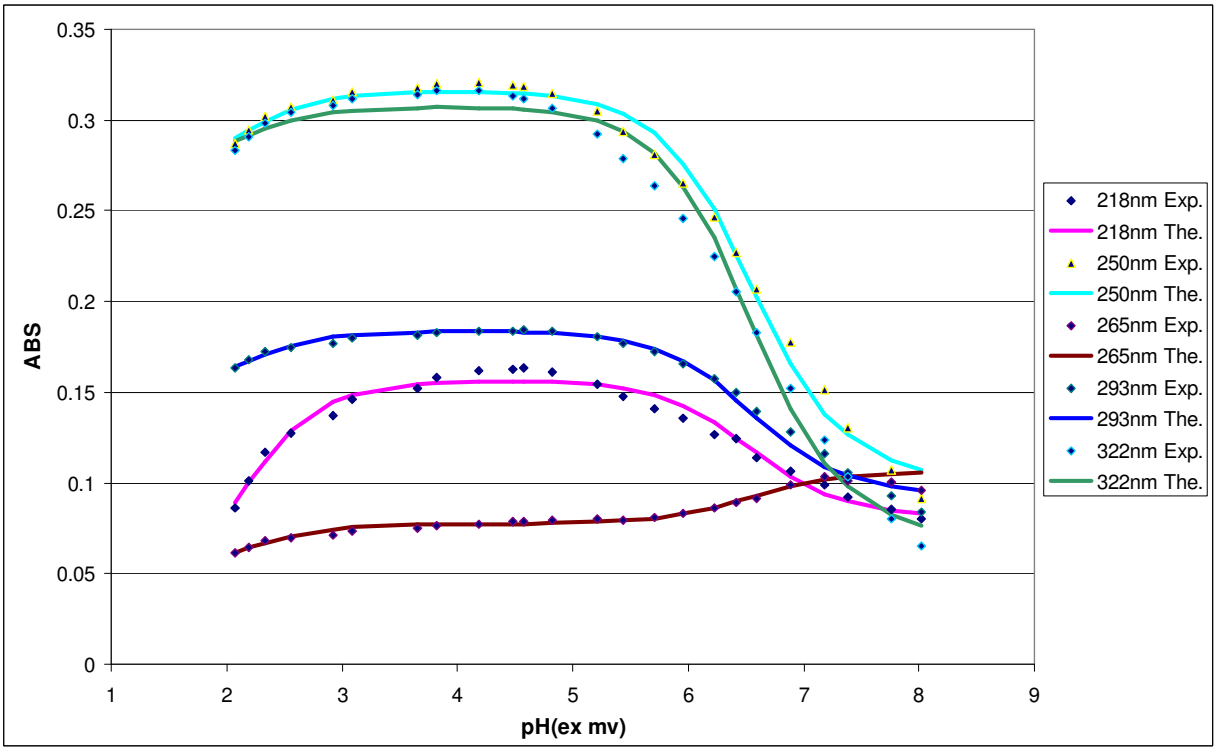

Figure 44: Experimental absorbance data (Exp.) fitted with calculated values (The.) to determine the protonation constants of 2 x 10^{-5} *M* DIPY.

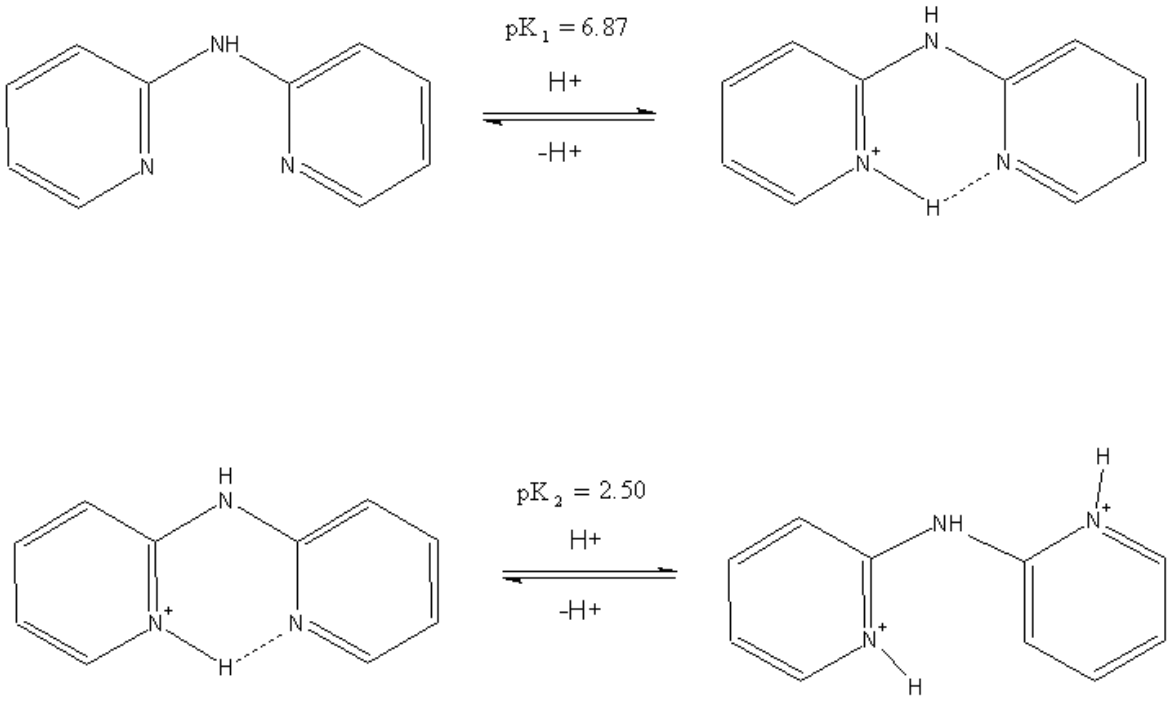

Figure 45: The proposed protonation equilibria for 2,2'-dipyridal Amine (DIPY).

Titrations Involving Metal Ion Complexation with DIPY

In these titrations, unless stated otherwise, the same procedure was performed for each metal-ligand complex at the same wavelengths as done with the free ligand. The equations 1-15 can again be used here to determine log K_1 for metal ion stability since DIPY has the same number of protonation events as 8PQ.

The stability constants determined with metal ions with DIPY from UV-Vis spectroscopy titration experiments can be seen in Table 4. The stability constants are compared to those previously recorded (NIST) and to bipyridine. The vales obtained in this study vary from the previously recorded values. This is because in the previous studies glass electrodes were used which are inaccurate at the low concentrations that these titrations need to be done at. A graph comparing the difference in log K_1 values of DIPY and bipyridine can be seen in Figure 46. It shows that DIPY shows a shift in preference for small metal ions over that of bipyridine. This can be explained by that fact that DIPY forms a 6-membered chelate ring where as bipyridine forms 5-membered chelate rings.

Metal	Ionic Radius (Å)	log *K*1 with DIPY	NIST Values	log *K*1 with BIPY	Δ log *K*1
Al(III)	0.535	NA	NA	NA	
Cd(II)	0.97	2.67	2.62	4.24	-1.57
Co(II)	0.745	4.36	4.72	5.8	-1.44
Cu(II)	0.57	7.34	8.05	8.12	-0.78
Ga(III)	0.62	NA	NA	4.52	
Ni(II)	0.69	6.15	6.25	7.04	-0.89
Zn(II)	0.74	3.52	3.75	5.12	-1.6

Table 4: Comparison of log K_1 data for metal ions with DIPY and BIPY.

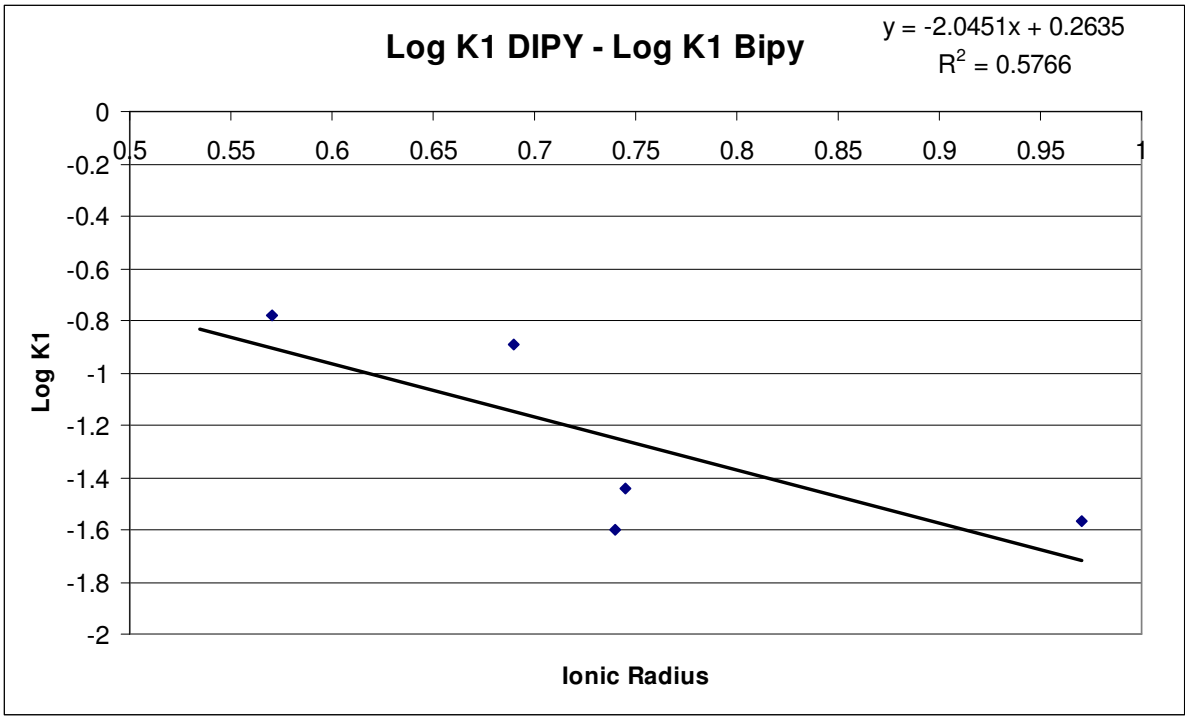

Figure 46: A graph comparing the difference in log K_1 values of DIPY and bipyridine.

Aluminum(III)-DIPY Results:

Aluminum(III) has an ionic radius of 0.535Å which would classify it as a small metal ion and it is fairly close to the ideal radius of 0.45Å for this ligand. The UV absorbance spectrum for the 1:1 aluminum(III) and DIPY titration experiment where the concentration was 2 x 10^{-5} M for both is shown in Figure 47. A plot of correlation between E (mV) and the calculated pH, which was used to calculate E^0, is shown in Figure 48. A graph with the experimental absorbance data fitted with calculated values to determine the protonation constants for the aluminum(III) and DIPY solution is shown in Figure 49. By using equations 1-15 the pK_1 for this titration was calculated to be 6.85 which was almost identical to the pK_1 of the free ligand (6.87). This means that the log K_1 for the aluminum(III)-DIPY complex is virtually zero. This may seem incorrect as

the size of the aluminum(III) metal ion is some what close to what the 6-membered chelate ring of DIPY would prefer. However, this can be explained by the fact that Al(III) has an extremely low affinity for N donors.

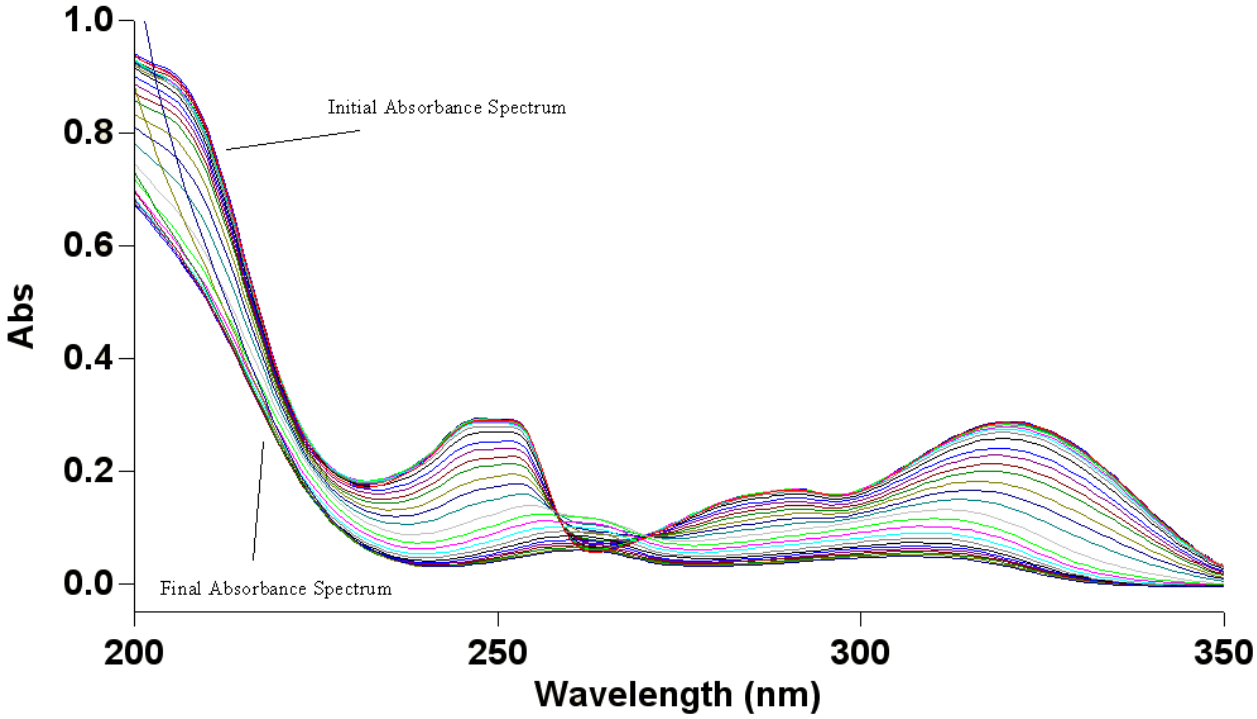

Figure 47: Absorbance versus wavelength (nm) spectra from the titration of the 1:1 solution of aluminum(III) and DIPY at concentrations of 2 x 10^{-5} *M* at 25.0 ± 0.1 °C with 0.1 *M* NaOH with a pH range of approximately 2.00 to 11.

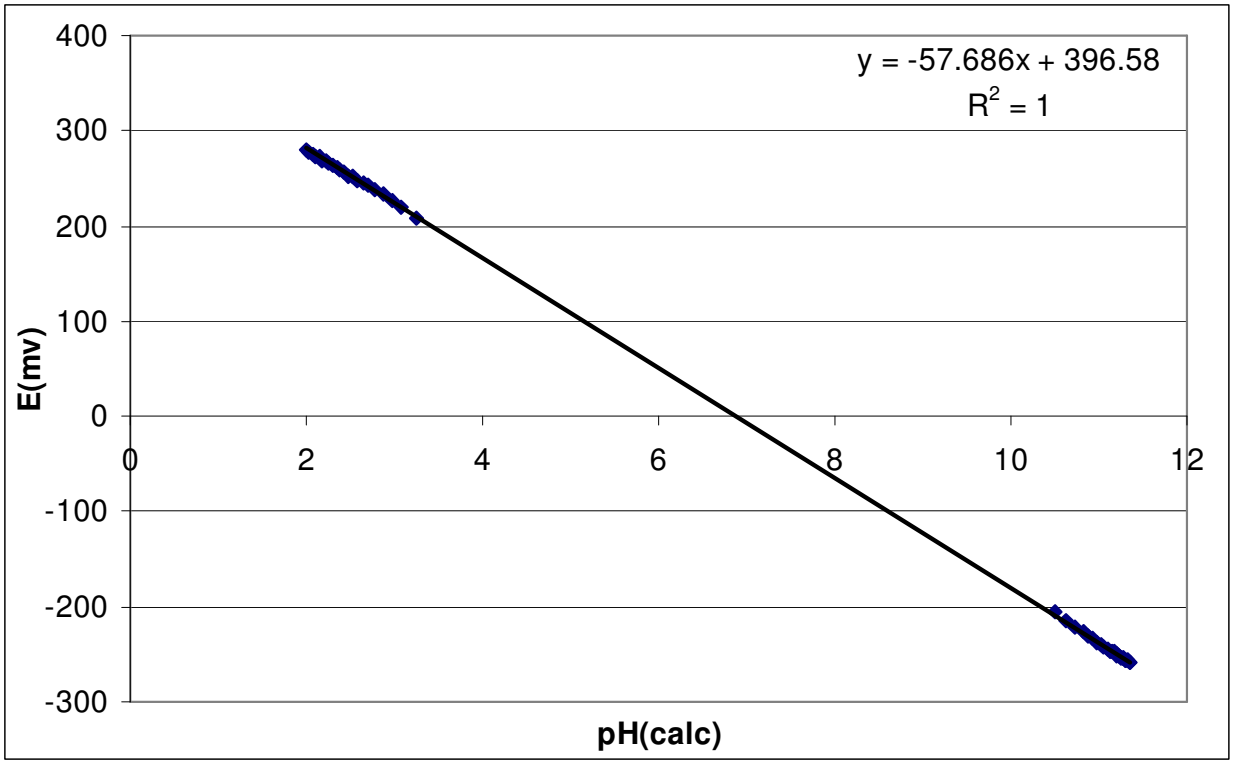

Figure 48: Plot of the correlation between E (mV) and the calculated pH used to calculate E^0 for the titration of the 1:1 aluminum(III) and DIPY solution at concentrations of $2 \times 10^{-5} M$ at 25.0 ± 0.1 °C with 0.1 M NaOH.

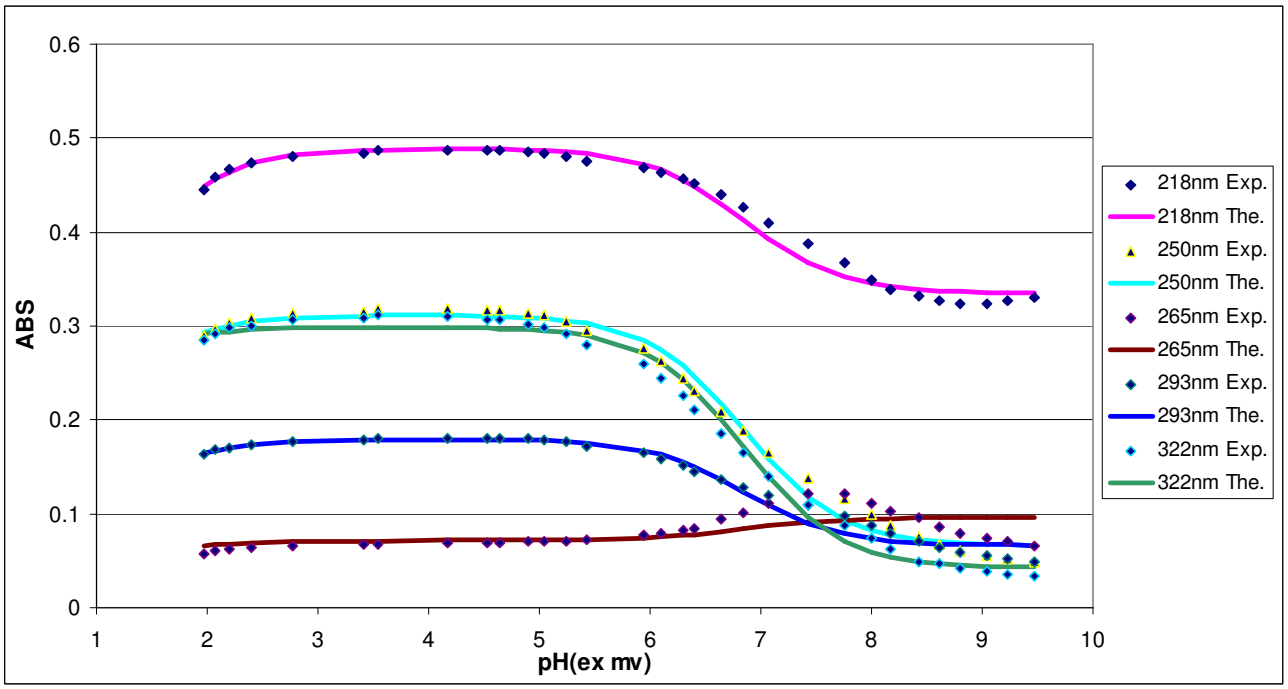

Figure 49: Experimental absorbance data (Exp.) fitted with calculated values (The.) for the titration of 1:1 aluminum(III) and DIPY solution at concentrations of $2 \times 10^{-5} M$.

Cadmium(II)-DIPY Results:

Cadmium(II) has an ionic radius of 0.97Å which makes it a large metal ion. Two different titration experiments were run with cadmium(II) and DIPY resulting in two different log K_1 values. The absorbance data from these titrations were fitted together to result in a collective log K_1 for the cadmium(II)-DIPY complex. The UV absorbance spectrum for the 500:1 cadmium(II) and DIPY titration experiment in which the concentrations were 0.01 M and 2 x 10^{-5} M respectively is shown in Figure 50. A plot of correlation between E (mV) and the calculated pH, which was used to calculate E^0, is shown in Figure 51. A graph with the experimental absorbance data fitted with calculated values to determine the protonation constants for the 500:1 cadmium(II) and DIPY solution is shown in Figure 52. By using equations 1-15 the log K_1 for the cadmium(II)-DIPY complex was found to be 3.12. The second titration experiment was of 250:1 cadmium(II) and DIPY solution in which the concentrations were 5 x 10^{-3} M and 2 x 10^{-5} M respectively. The UV absorbance spectrum of this titration can be seen in Figure 53. The plot of the correlation between E (mV) and the calculated pH used for this titration can be seen in Figure 54. The graph fitting calculated values with the experimental absorbance data to determine the protonation constants for this 250:1 cadmium(II) and DIPY solution is shown in Figure 55. Again using equations 1-15 the log K_1 for the cadmium(II)-DIPY complex was this time found to be 2.63. The equilibria observed from these titrations are described below at the pH they occurred.

$$(DIPY)H^+ + H^+ \leftrightarrows (DIPY)H_2^{2+} \qquad (pH = 2.31)$$

$$Cd(DIPY)^{2+} + H^+ \leftrightarrows Cd^{2+} + (DIPY)H^+ \qquad (pH = 6.50)$$

The absorbance data for these two titrations were globally fitted with one another to produce a collective value for the log K_1 for the cadmium(II)-DIPY complex of 2.67. This value was calculated as follows,

$$\text{Log } K_1 = 6.87 - 6.50 - \log(0.005)$$

where 6.87 is the pK_a of the free ligand, 6.50 is the pK_1 equilibrium of complex formation and 0.005 represents the amount of free metal ion at the midpoint of the equilibrium where Cd(II) is displaced from DIPY.

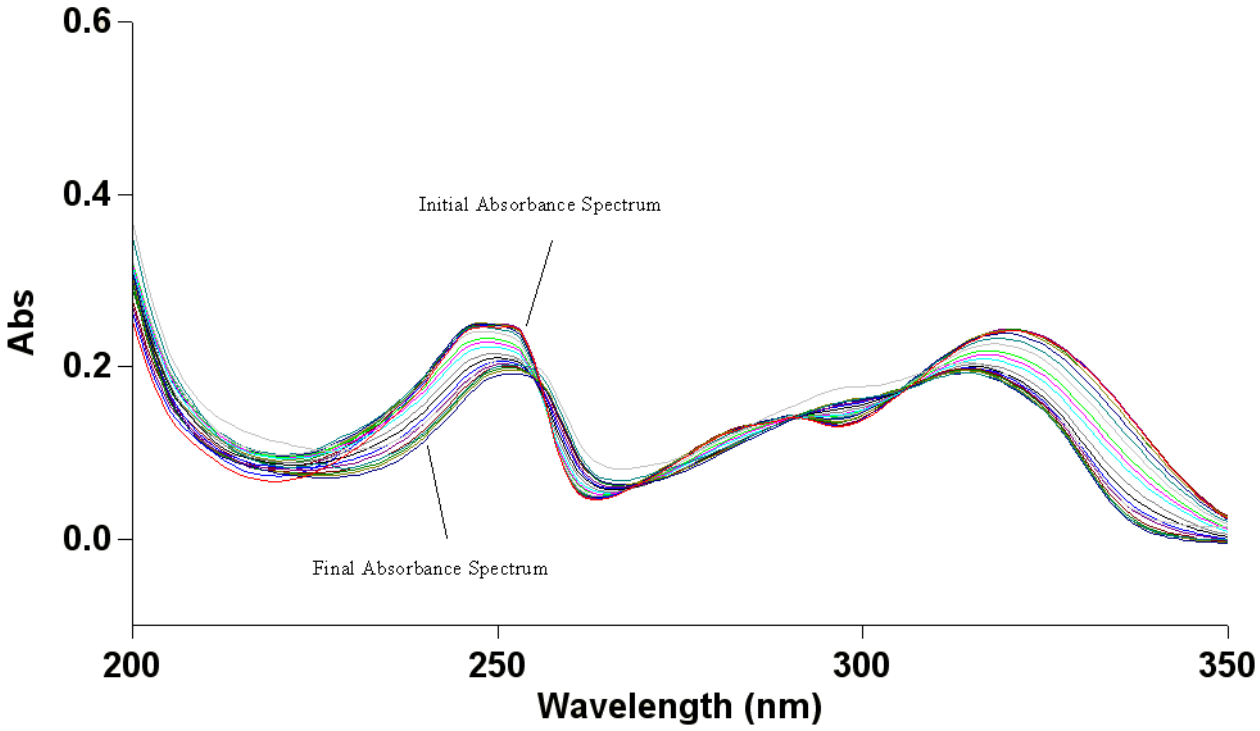

Figure 50: Absorbance versus wavelength (nm) spectra from the titration of the 500:1 solution of cadmium(II) and DIPY at concentrations 0.01 *M* and 2 x 10^{-5} *M* respectively at 25.0 ± 0.1 °C with 0.1 *M* NaOH with a pH range of approximately 2 to 8.

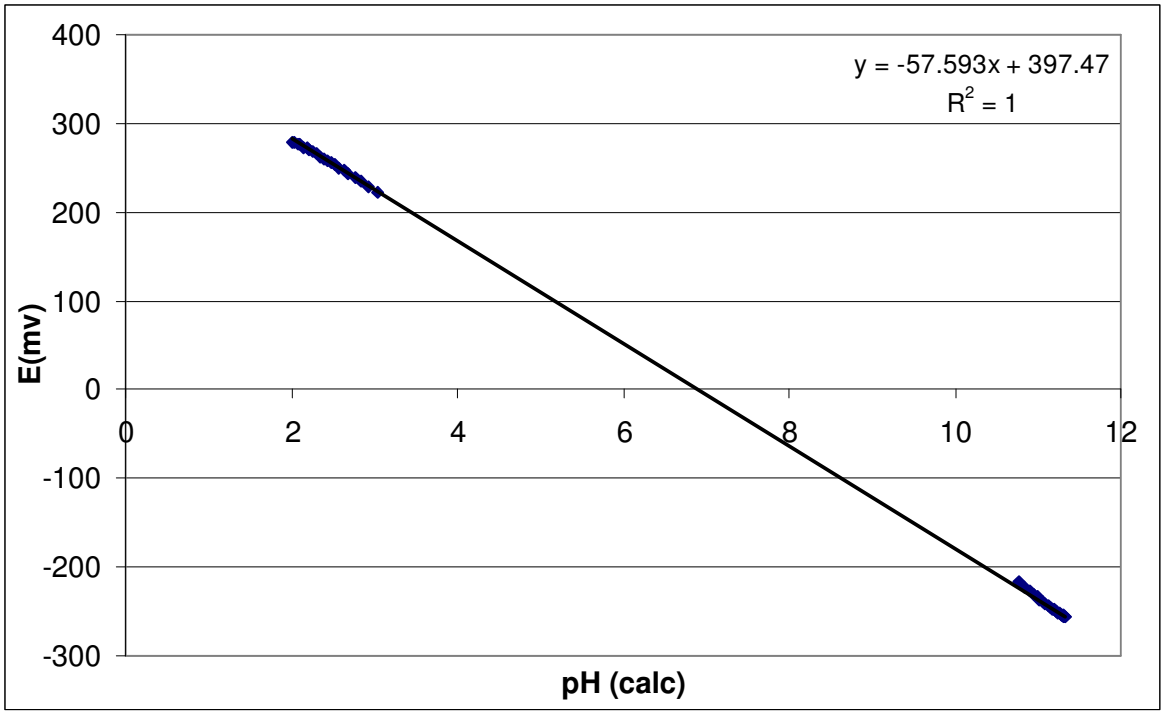

Figure 51: Plot of the correlation between E (mV) and the calculated pH used to calculate E^0 for the titration of the 500:1 cadmium(II) and DIPY solution at concentrations 0.01 *M* and 2 x 10^{-5} *M* respectively at 25.0 ± 0.1 °C with 0.1 *M* NaOH.

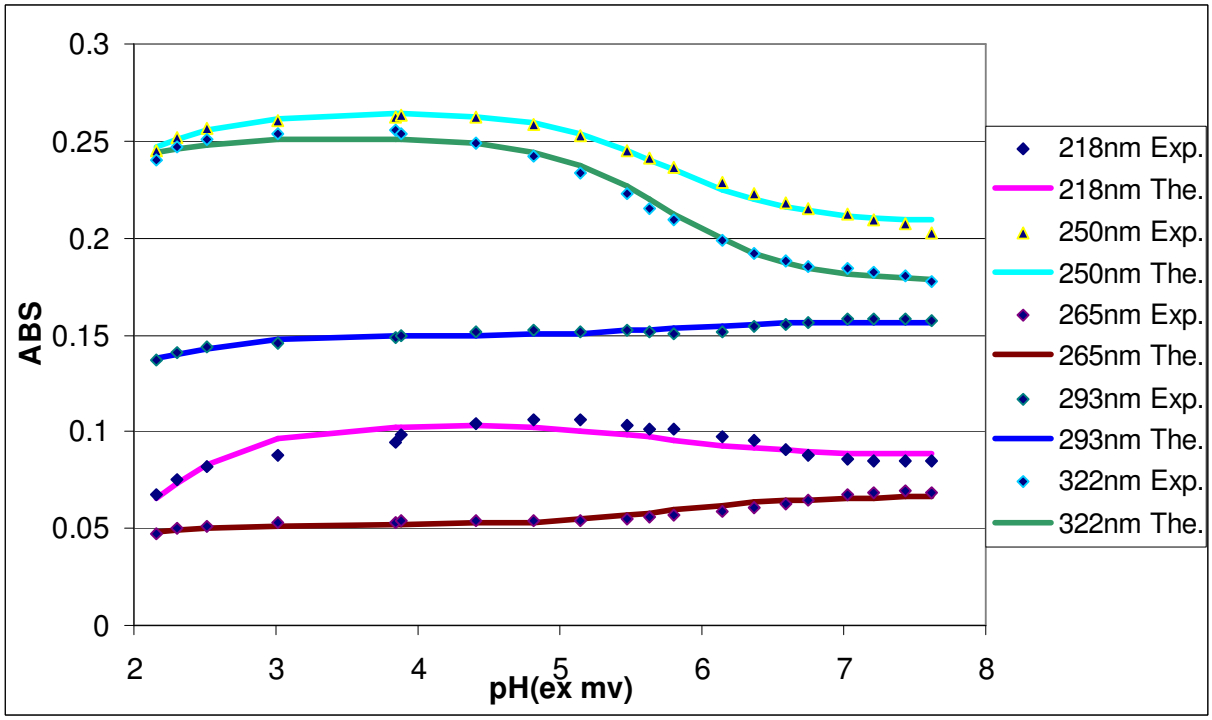

Figure 52: Experimental absorbance data (Exp.) fitted with calculated values (The.) for the titration of 500:1 cadmium(II) and DIPY solution at concentrations of 0.01 *M* and 2 x 10^{-5} *M* respectively.

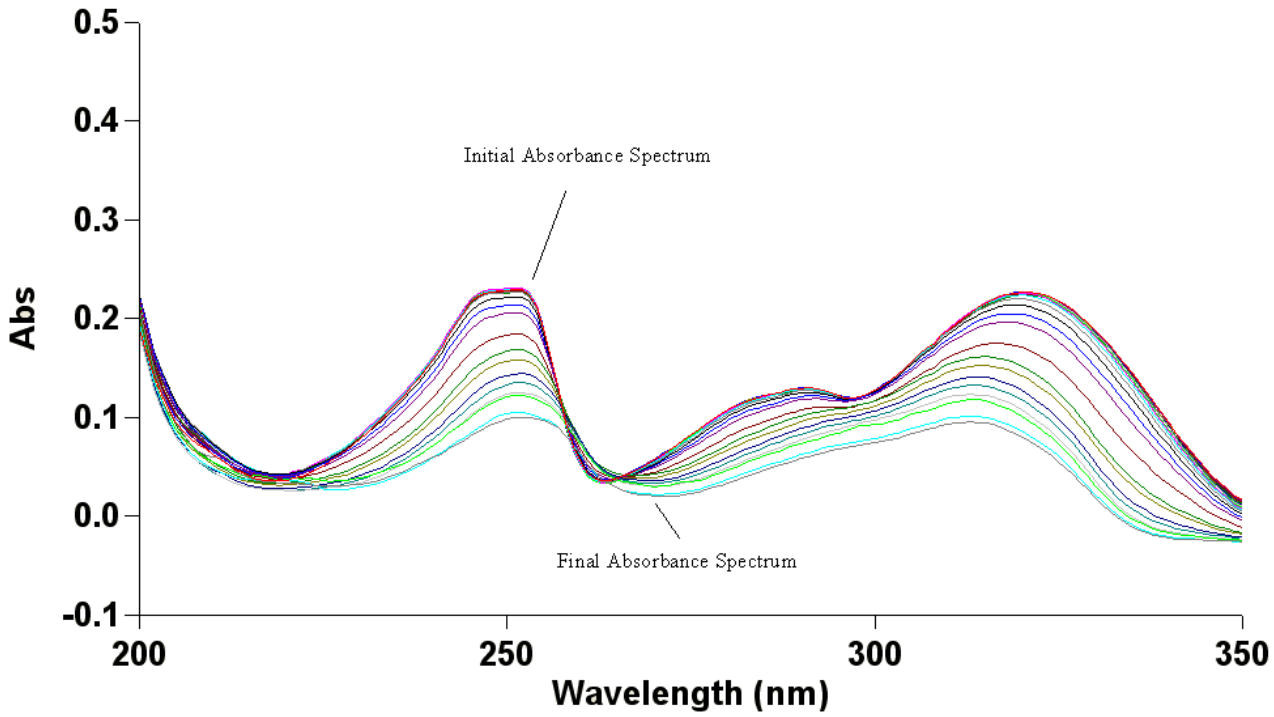

Figure 53: Absorbance versus wavelength (nm) spectra from the titration of the 250:1 solution of cadmium(II) and DIPY at concentrations 5 x 10^{-3} *M* and 2 x 10^{-5} *M* respectively at 25.0 ± 0.1 °C with 0.1 *M* NaOH with a pH range of approximately 2 to 8.

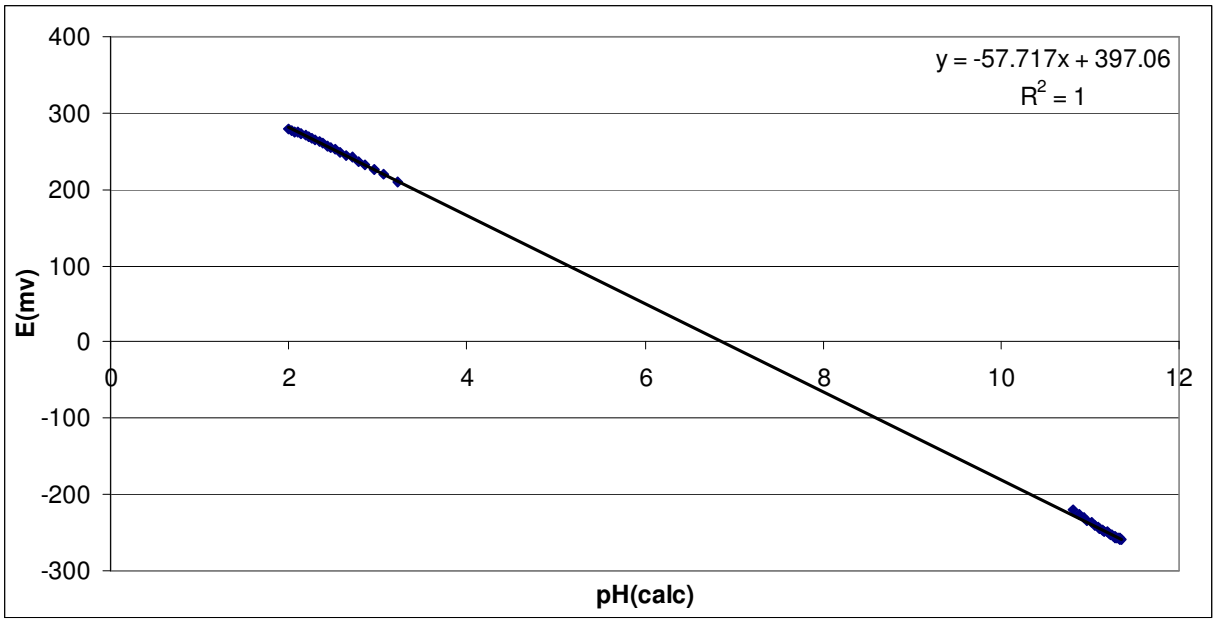

Figure 54: Plot of the correlation between E (mV) and the calculated pH used to calculate E^0 for the titration of the 250:1 cadmium(II) and DIPY solution at concentrations 5 x 10^{-3} *M* and 2 x 10^{-5} *M* respectively at 25.0 ± 0.1 °C with 0.1 *M* NaOH.

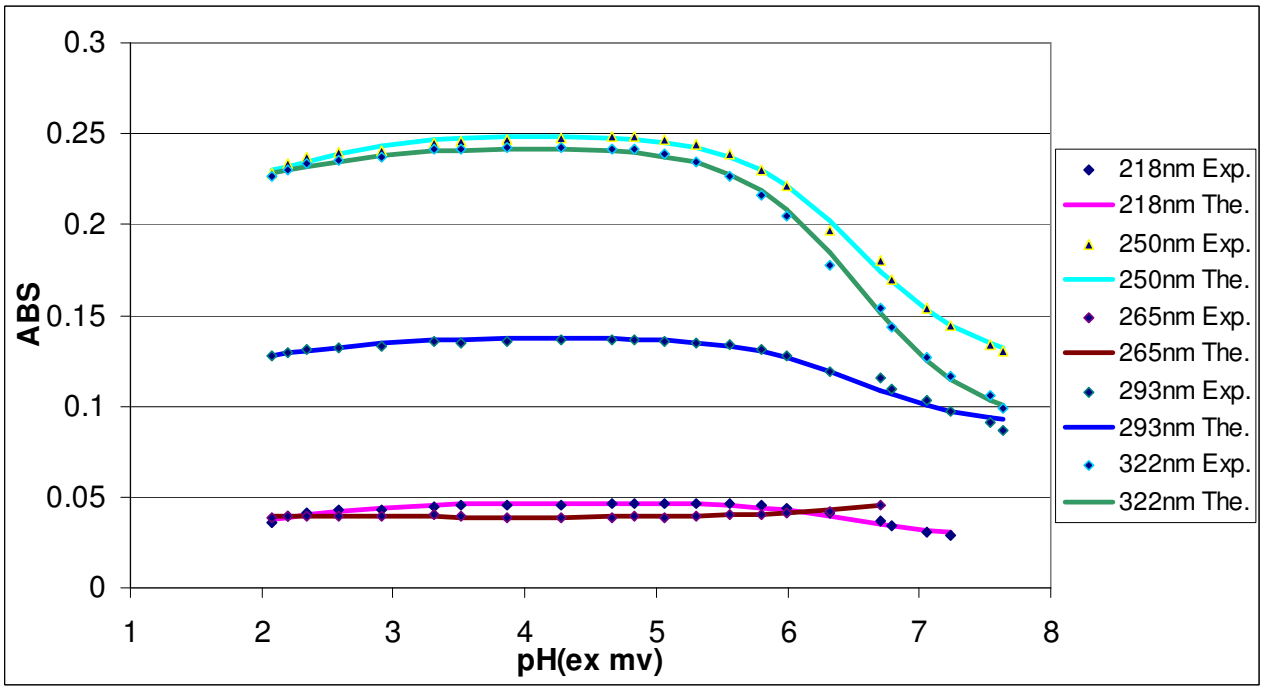

Figure 55: Experimental absorbance data (Exp.) fitted with calculated values (The.) for the titration of 250:1 cadmium(II) and DIPY solution at concentrations of 5 x 10^{-3} *M* and 2 x 10^{-5} *M* respectively.

Cobalt(II)-DIPY Results:

Cobalt(II) has an ionic radius of 0.745Å which classifies it as a medium sized metal ion. Two different titration experiments were run with cobalt(II) and DIPY resulting in two different log K_1 values. The absorbance data from these titrations were fitted together to result in a collective log K_1 for the cobalt(II)-DIPY complex. The UV absorbance spectrum for the 1:1 cobalt(II) and DIPY titration experiment in which the concentrations were both at 2 x 10^{-3} M is shown in Figure 56. This spectrum was run from wavelengths 350 to 800nm as the absorbance of such a concentrated solution would be to high to accurately measure at the standard range of 200 to 350nm. Absorbance values were recorded for the wavelengths 365, 405, 520, 600, and 700nm. A plot of correlation between E (mV) and the calculated pH, which was used to calculate E^0, is shown in Figure 57. A graph with the experimental absorbance data fitted with calculated values to determine the protonation constants for the 1:1 cobalt(II) and DIPY solution is shown in Figure 58. By using equations 1-15 the log K_1 for the cobalt(II)-DIPY complex was found to be 4.23. The second titration experiment was of a 1:1 cobalt(II) and DIPY at concentrations of 2 x 10^{-4} M and its UV absorbance spectrum can be seen in Figure 59. This spectrum was recorded in the standard wavelength range and the standard pre selected wavelengths. The plot of correlation between E (mV) and the calculated pH used to calculate E^0 is shown in Figure 60. The graph with the experimental absorbance data fitted with calculated values to determine the protonation constants for this 1:1 cobalt(II) and DIPY solution is shown in Figure 61. Again by using the equations 1-15 the log K_1 for this cobalt(II)-DIPY complex was found to be 4.37. The equilibria observed from these titrations are described below at the pH they occurred.

$Co(DIPY)^{2+} + H^{+} \leftrightarrows Co^{2+} + (DIPY)H^{+}$ (pH = 5.51)

$Co(DIPY)^{2+} + OH^{-} \leftrightarrows Co(DIPY)OH$ (pH = 10.10)

The absorbance data for these two titrations were globally fitted with one another to produce a collective value for the log K_1 for the cobalt(II)-DIPY complex of 4.36. This value was calculated as follows,

$$\text{Log } K_1 = 6.87 - 5.51 - \log(0.001)$$

where 6.87 is the pK_a of the free ligand, 5.51 is the pK_1 equilibrium of complex formation and 0.001 represents the amount of free metal ion at the midpoint of the equilibrium where Co(II) is displaced from DIPY.

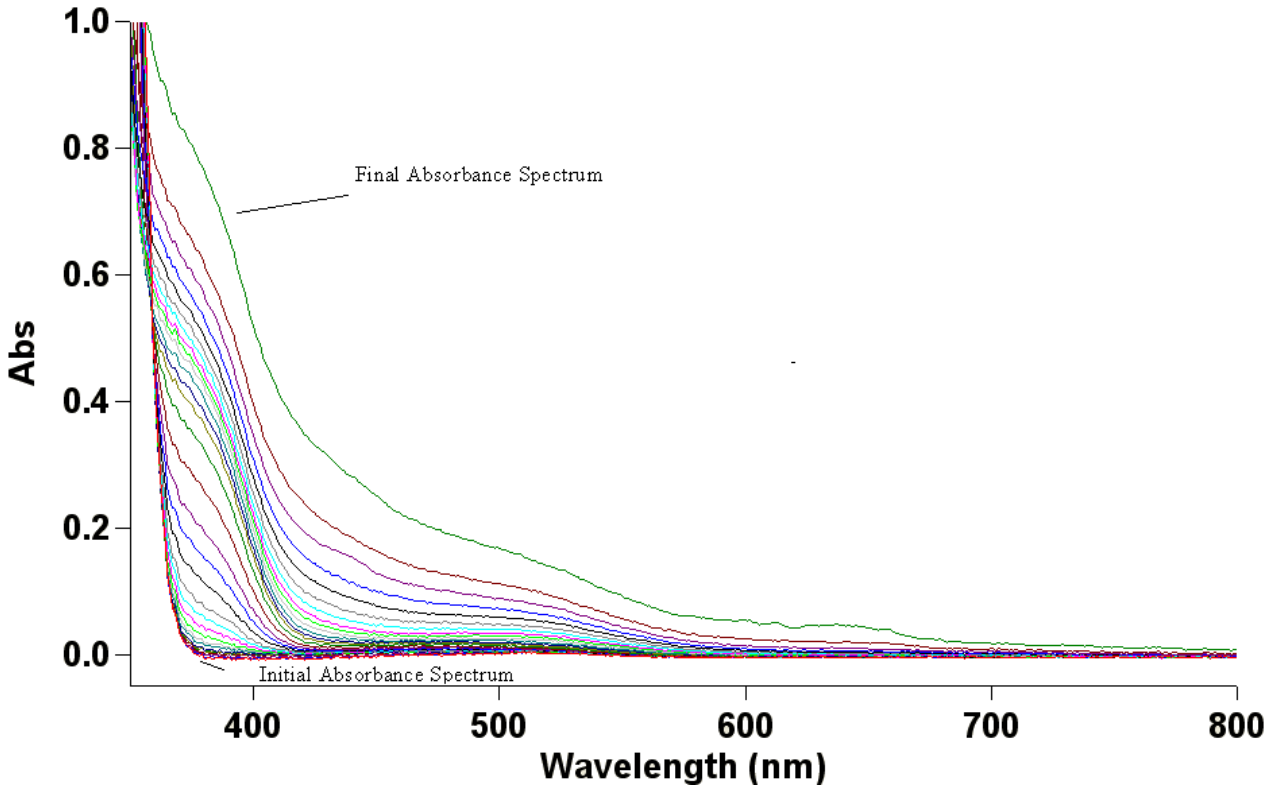

Figure 56: Absorbance versus wavelength (nm) spectra from the titration of the 1:1 solution of cobalt(II) and DIPY at concentrations of 2×10^{-3} *M* at 25.0 ± 0.1 °C with 0.1 *M* NaOH with a pH range of approximately 2 to 9.

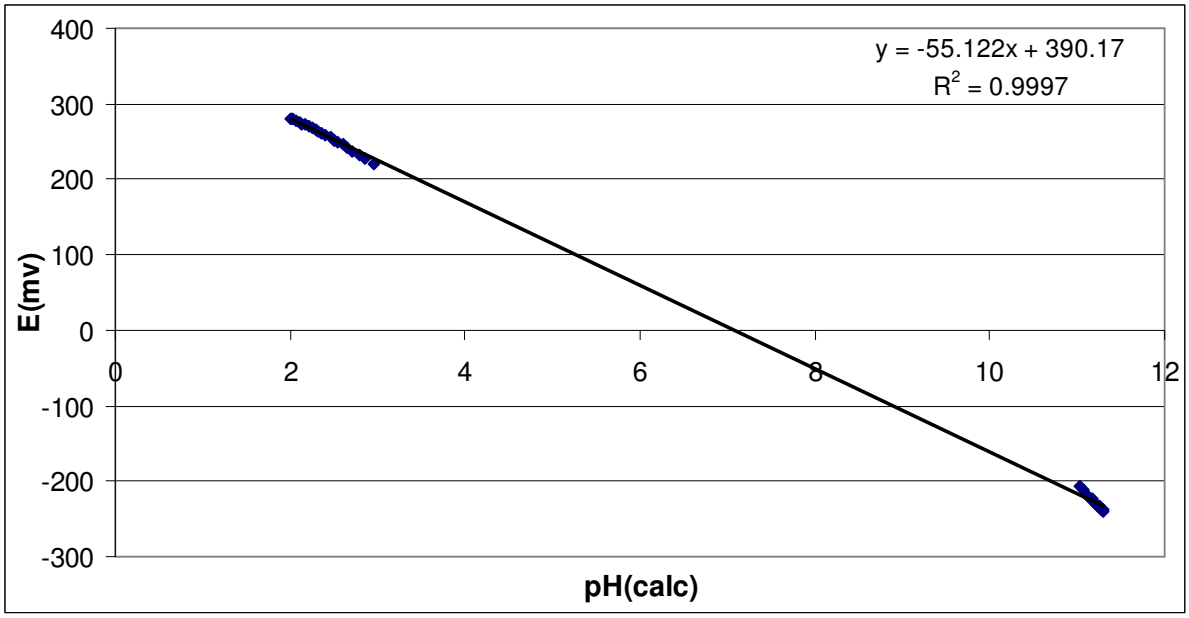

Figure 57: Plot of the correlation between E (mV) and the calculated pH used to calculate E^0 for the titration of the 1:1 cobalt(II) and DIPY solution at concentrations 2 x 10^{-3} *M* at 25.0 ± 0.1 °C with 0.1 *M* NaOH.

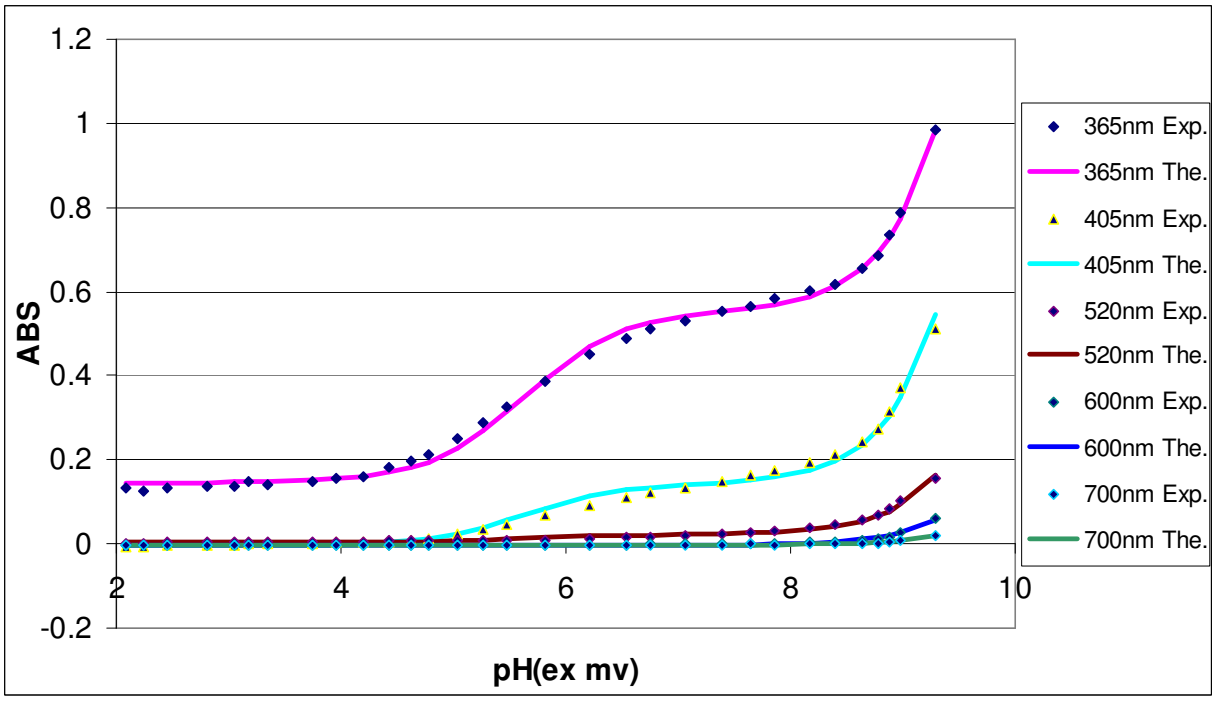

Figure 58: Experimental absorbance data (Exp.) fitted with calculated values (The.) for the titration of 1:1 cobalt(II) and DIPY solution at concentrations of 2 x 10^{-3} *M*.

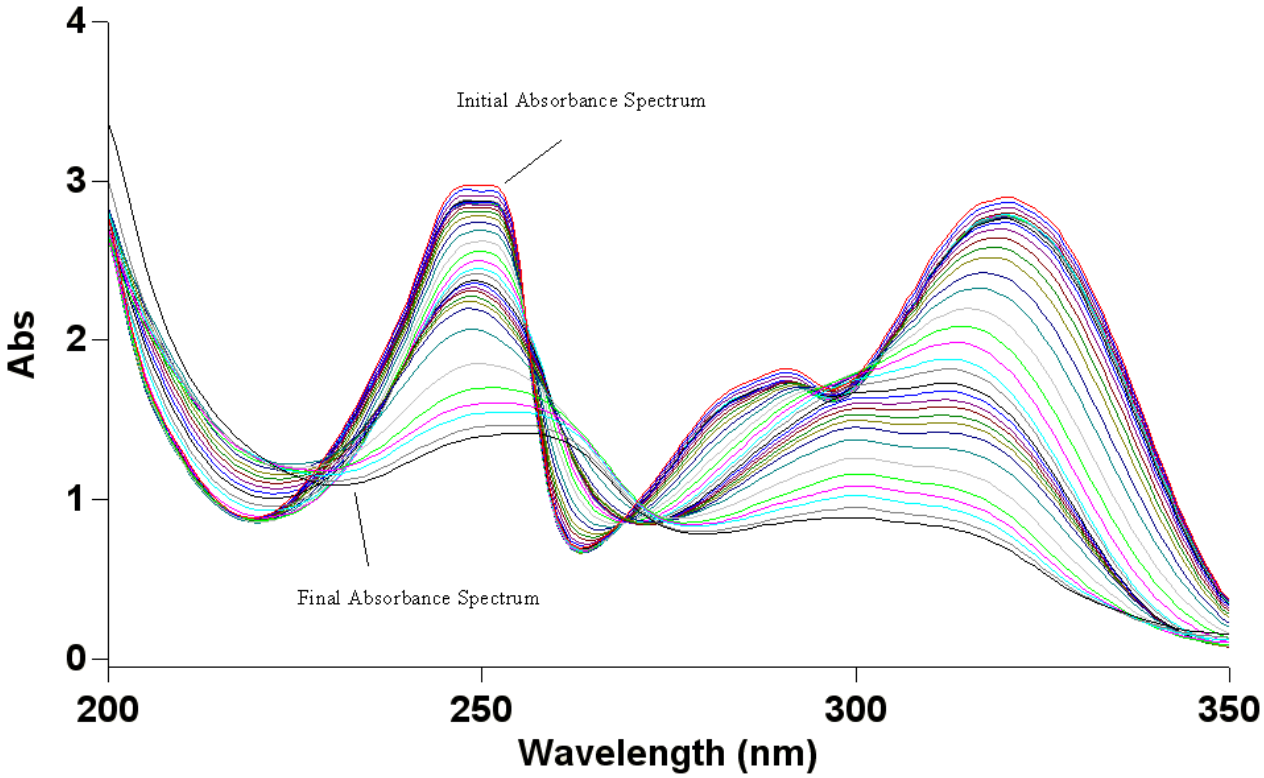

Figure 59: Absorbance versus wavelength (nm) spectra from the titration of the 1:1 solution of cobalt(II) and DIPY at concentrations of $2 \times 10^{-4} M$ at 25.0 ± 0.1 °C with 0.1 M NaOH with a pH range of approximately 2 to 11.

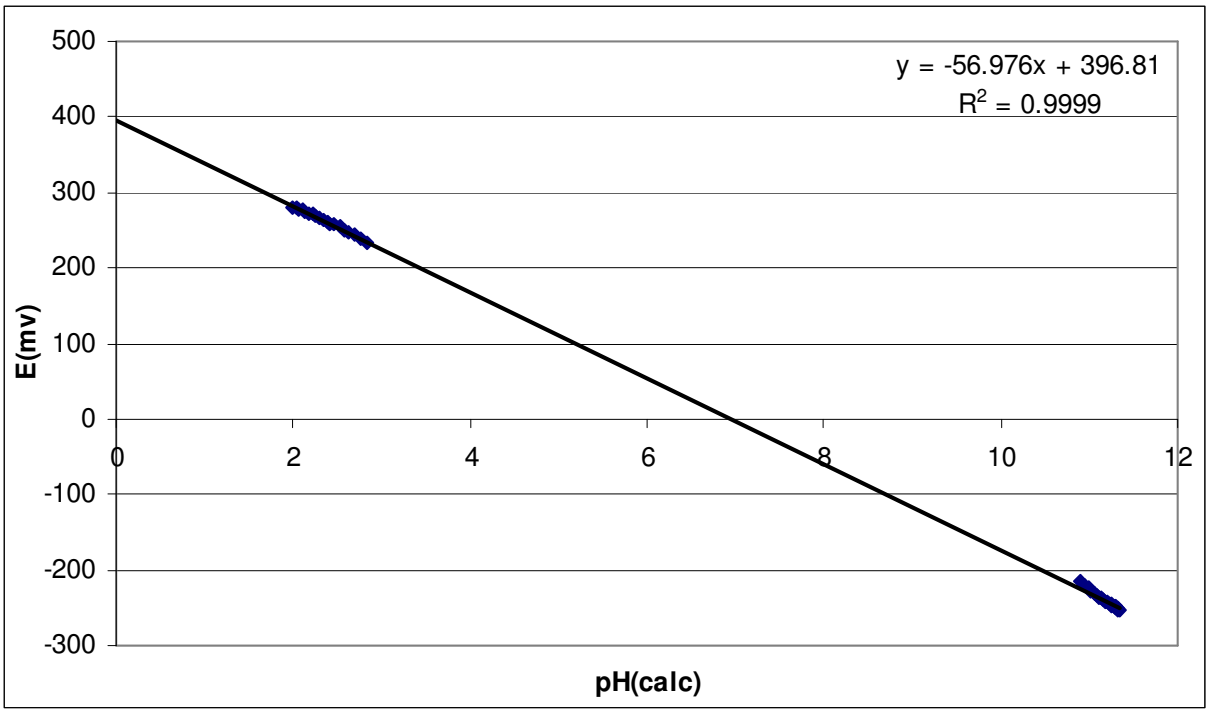

Figure 60: Plot of the correlation between E (mV) and the calculated pH used to calculate E^0 for the titration of the 1:1 cobalt(II) and DIPY solution at concentrations 2 x 10^{-4} *M* at 25.0 ± 0.1 °C with 0.1 *M* NaOH.

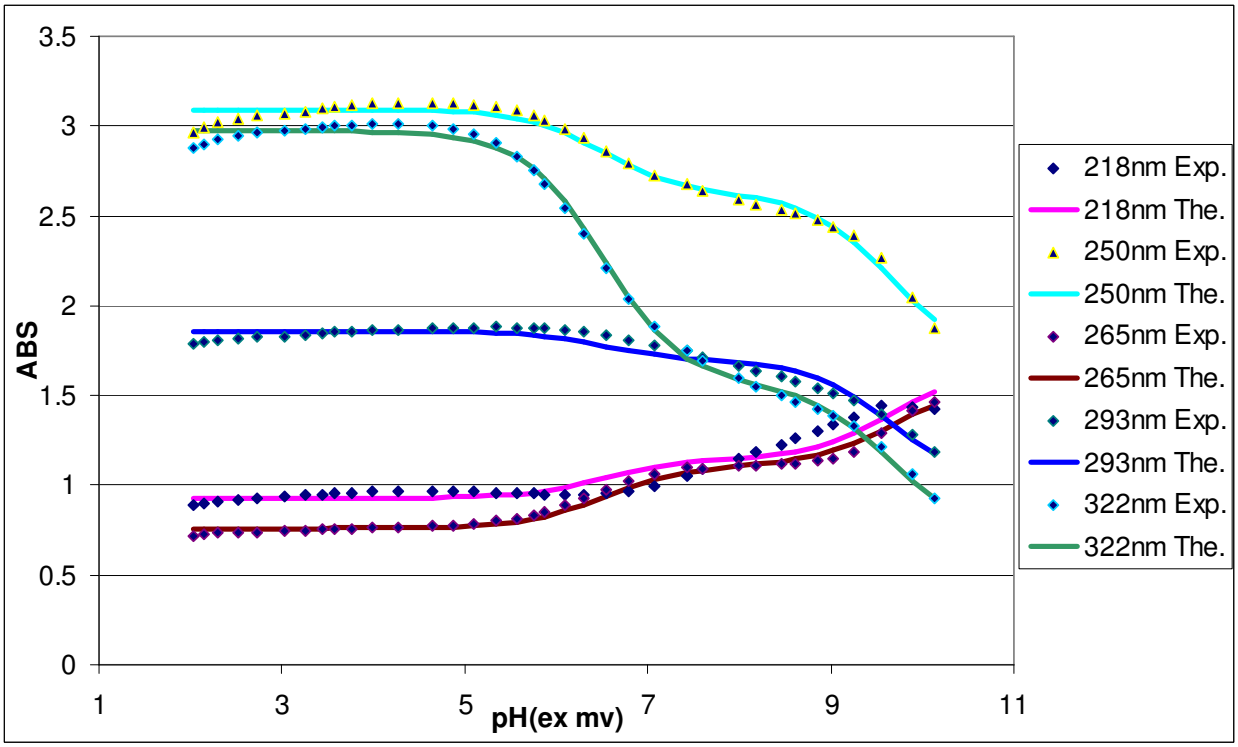

Figure 61: Experimental absorbance data (Exp.) fitted with calculated values (The.) for the titration of 1:1 cobalt(II) and DIPY solution at concentrations of 2 x 10^{-4} *M*.

Copper(II)-DIPY Results:

Copper(II) has an ionic radius of 0.57Å which classifies it as a fairly small metal ion. Three different titration experiments were run with copper(II) and DIPY resulting in three different log K_1 values. The absorbance data from these titrations were fitted together to result in a collective log K_1 for the copper(II)-DIPY complex. The UV absorbance spectrum for the 1:1 copper(II) and DIPY titration experiment in which the concentrations were both at 2 x 10^{-3} M is shown in Figure 62. This spectrum was run from wavelengths 350 to 800nm as the absorbance of such a concentrated solution would be too high to accurately measure at the standard range of 200 to 350nm. Absorbance values were recorded for the wavelengths 405, 450, 600, and 700nm. A plot of correlation between E (mV) and the calculated pH, which was used to calculate E^0, is shown in Figure 63. A graph with the experimental absorbance data fitted with calculated values to determine the protonation constants for the 1:1 copper(II) and DIPY solution is shown in Figure 64. By using equations 1-15 the log K_1 for the copper(II)-DIPY complex was found to be 7.10. The second titration experiment was of 1:1 copper(II) and DIPY at concentrations of 2 x 10^{-4} M and its UV absorbance spectrum can be seen in Figure 65. This spectrum was recorded in the standard wavelength range and the standard pre selected wavelengths. The plot of correlation between E (mV) and the calculated pH used to calculate E^0 is shown in Figure 66. The graph with the experimental absorbance data fitted with calculated values to determine the protonation constants for this 1:1 copper(II) and DIPY solution is shown in Figure 67. Again by using the equations 1-15 the log K_1 for this copper(II)-DIPY complex was found to be 7.42. The third and final titration experiment was of 1:1 copper(II) and DIPY at

concentrations of 2 x 10^{-5} M and its UV absorbance spectrum can be seen in Figure 68. This spectrum was recorded in the standard wavelength range and the standard pre selected wavelengths. The plot of correlation between E (mV) and the calculated pH used to calculate E^0 is shown in Figure 69. The graph with the experimental absorbance data fitted with calculated values to determine the protonation constants for this 1:1 copper(II) and DIPY solution is shown in Figure 70. Again by using the equations 1-15 the log K_1 for this copper(II)-DIPY complex was found to be 6.35. The equilibria observed from these titrations are described below at the pH they occurred.

$(DIPY)H^+ + H^+ \leftrightarrows (DIPY)H_2^{2+}$ (pH = 2.53)

$Cu(DIPY)^{2+} + H^+ \leftrightarrows Cu^{2+} + (DIPY)H^+$ (pH = 4.53)

$Cu(DIPY)^{2+} + 2OH^- \leftrightarrows Cu(DIPY)(OH)_2$ (pH = 6.98)

Lastly the absorbance data for these three titrations were globally fitted with one another to produce a collective value for the log K_1 for the copper(II)-DIPY complex of 7.34. This value was calculated as follows,

$$\text{Log } K_1 = 6.87 - 4.53 - \log(0.00001)$$

where 6.87 is the pK_a of the free ligand, 4.53 is the pK_1 equilibrium of complex formation and 0.00001 represents the amount of free metal ion at the midpoint of the equilibrium where Cu(II) is displaced from DIPY.

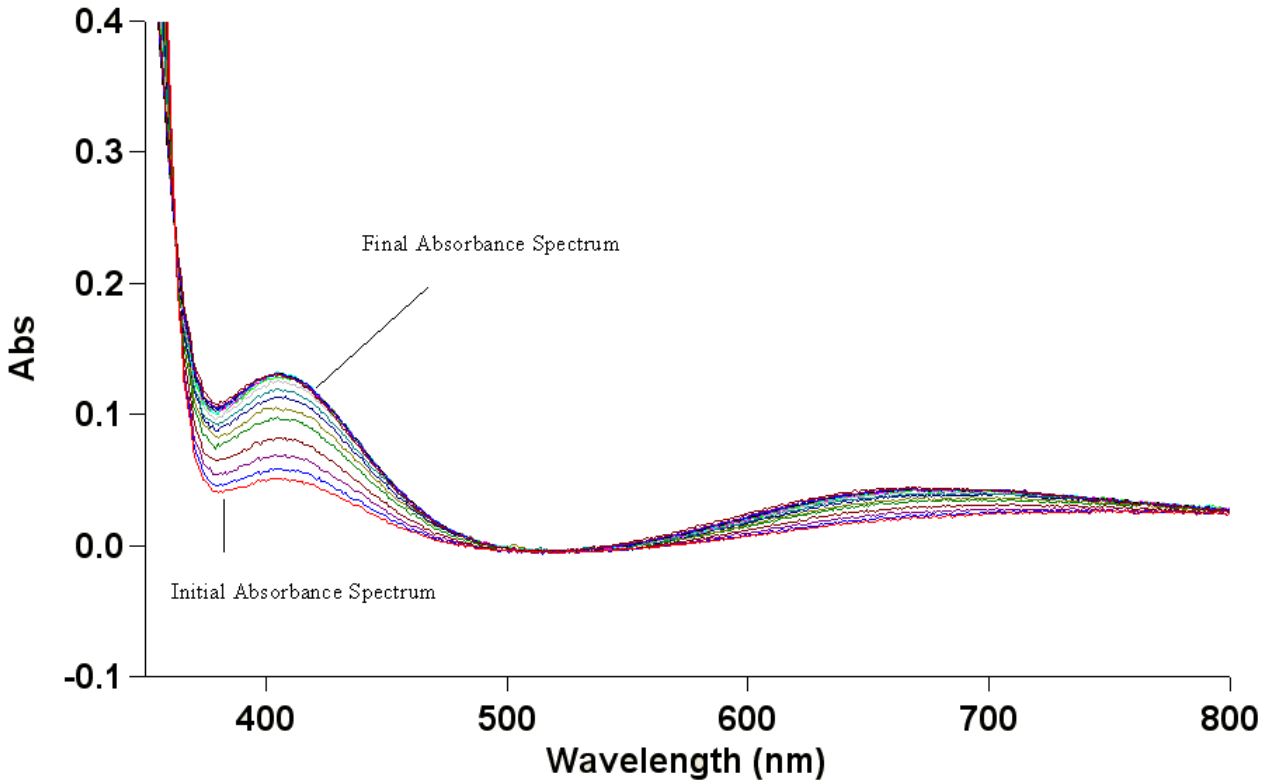

Figure 62: Absorbance versus wavelength (nm) spectra from the titration of the 1:1 solution of copper(II) and DIPY at concentrations of 2×10^{-3} *M* at 25.0 ± 0.1 °C with 0.1 *M* NaOH with a pH range of approximately 2 to 6.5.

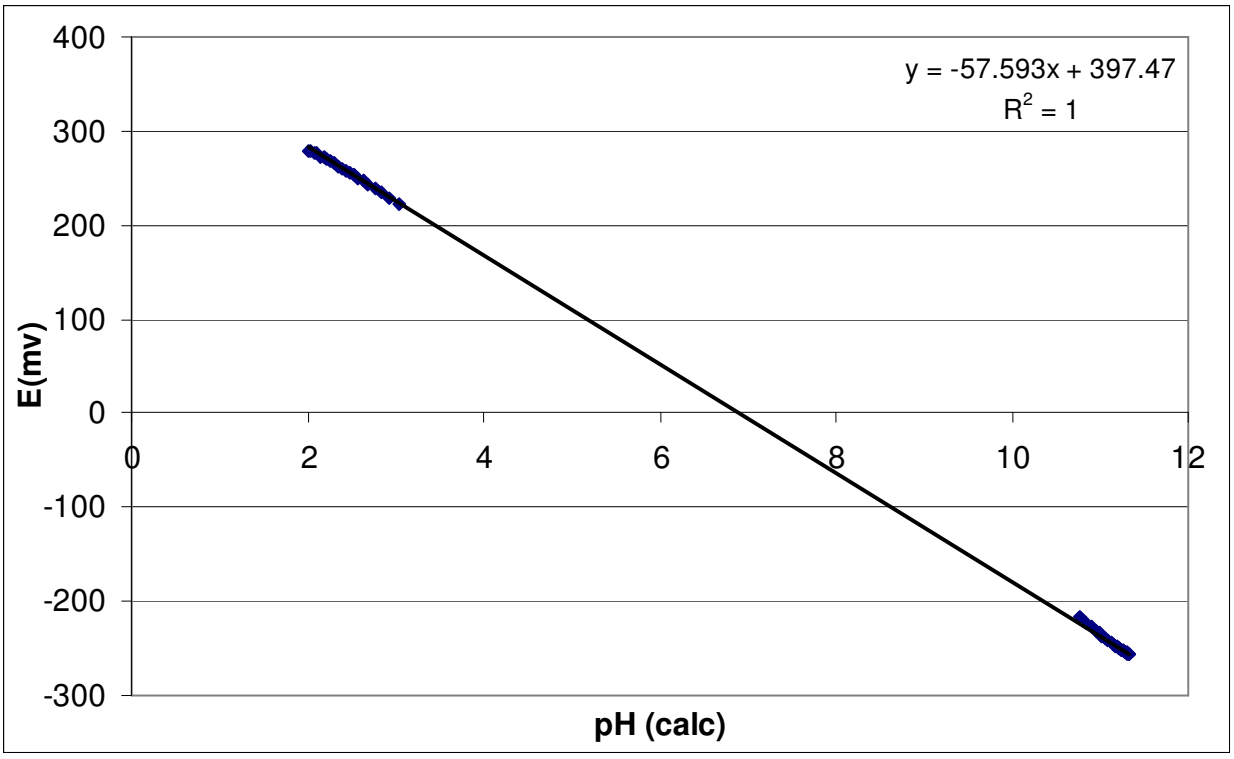

Figure 63: Plot of the correlation between E (mV) and the calculated pH used to calculate E^0 for the titration of the 1:1 copper(II) and DIPY solution at concentrations 2 x 10^{-3} *M* at 25.0 ± 0.1 °C with 0.1 *M* NaOH.

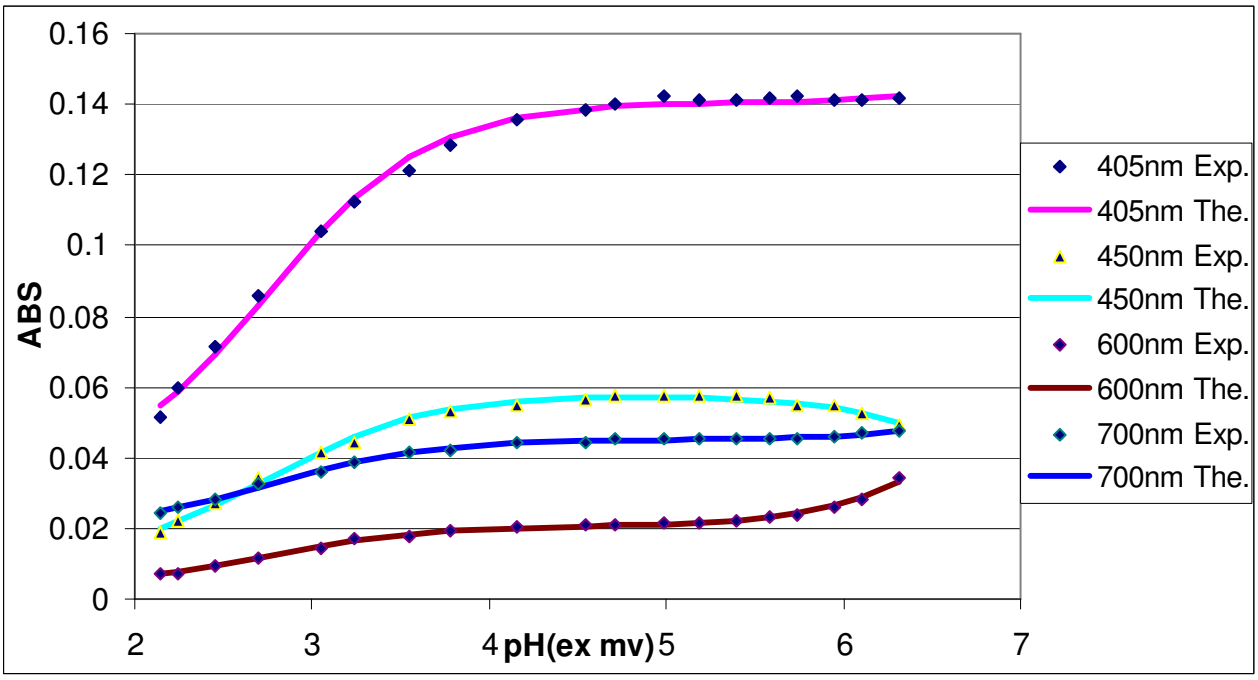

Figure 64: Experimental absorbance data (Exp.) fitted with calculated values (The.) for the titration of 1:1 copper(II) and DIPY solution at concentrations of 2 x 10^{-3} *M*.

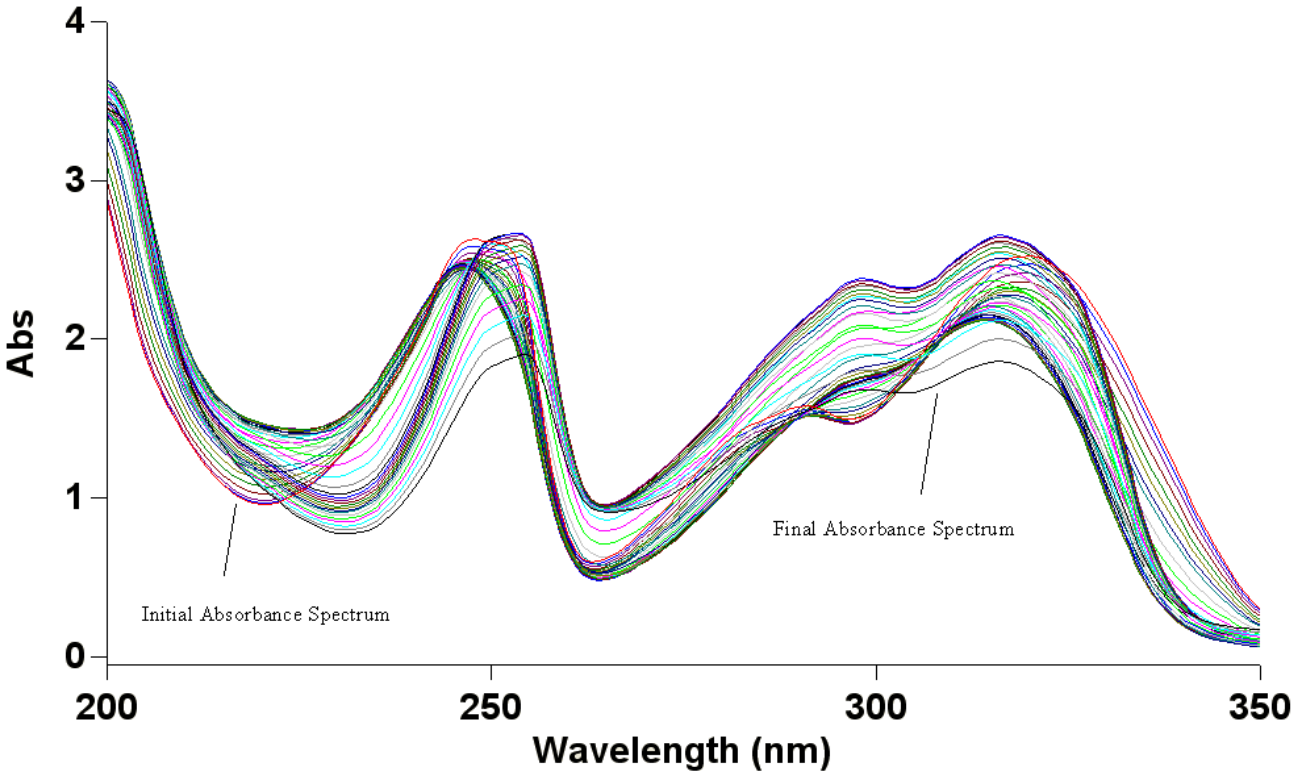

Figure 65: Absorbance versus wavelength (nm) spectra from the titration of the 1:1 solution of copper(II) and DIPY at concentrations of 2×10^{-4} *M* at 25.0 ± 0.1 °C with 0.1 *M* NaOH with a pH range of approximately 2 to 11.

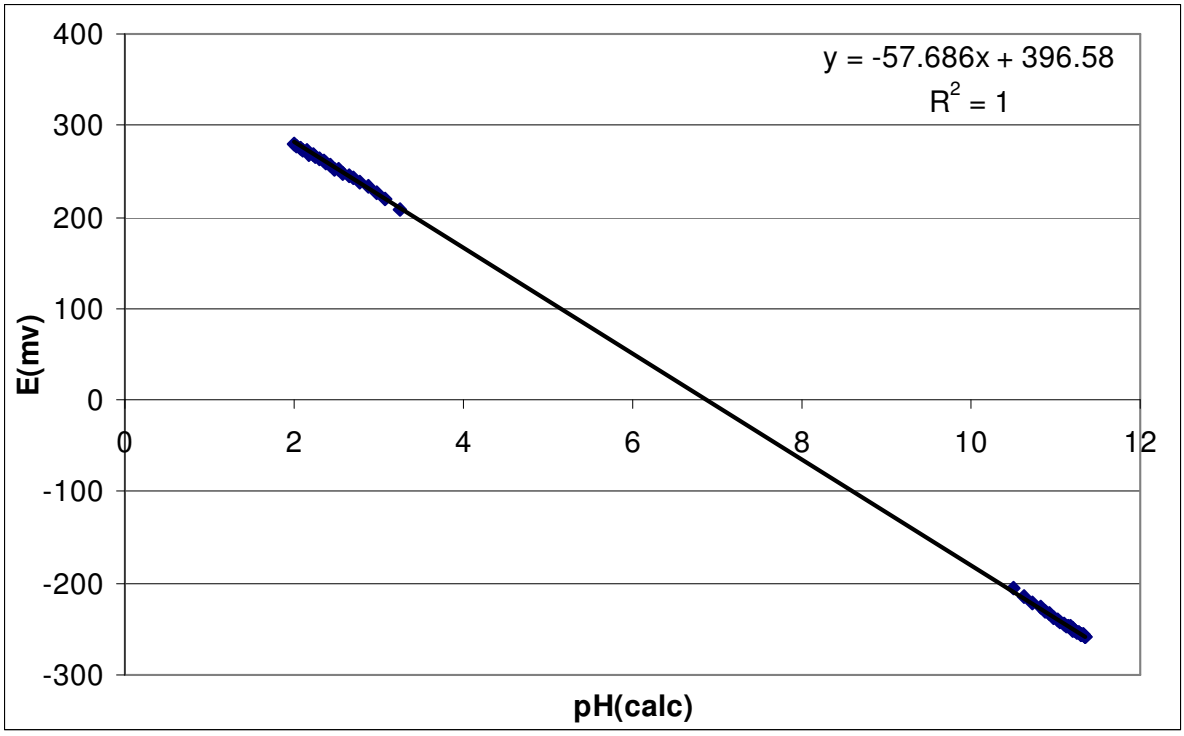

Figure 66: Plot of the correlation between E (mV) and the calculated pH used to calculate E^0 for the titration of the 1:1 copper(II) and DIPY solution at concentrations 2 x 10^{-4} *M* at 25.0 ± 0.1 °C with 0.1 *M* NaOH.

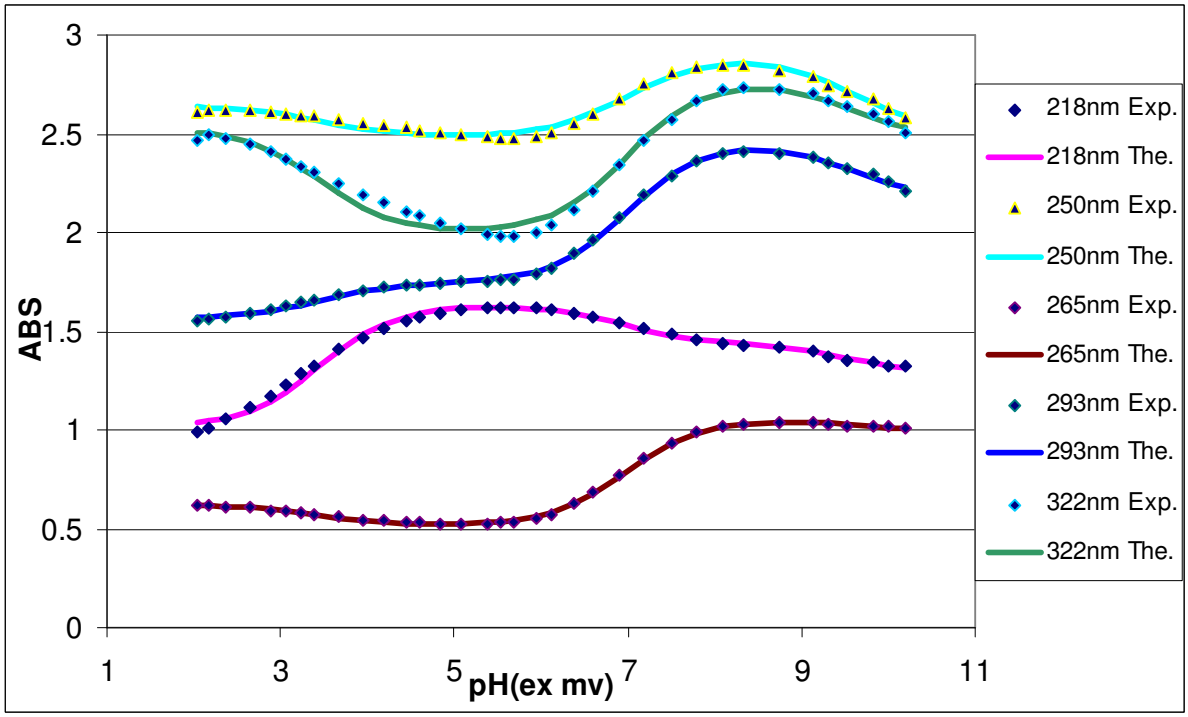

Figure 67: Experimental absorbance data (Exp.) fitted with calculated values (The.) for the titration of 1:1 copper(II) and DIPY solution at concentrations of 2 x 10^{-4} *M*.

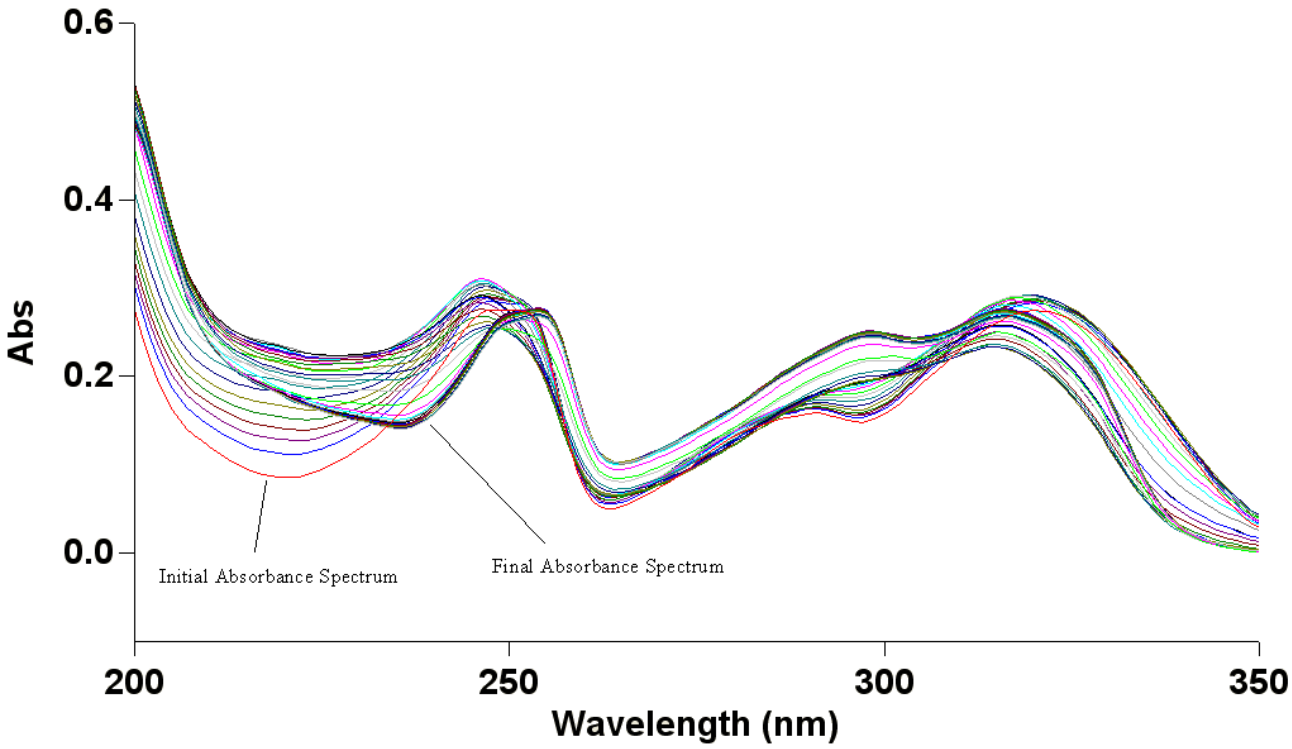

Figure 68: Absorbance versus wavelength (nm) spectra from the titration of the 1:1 solution of copper(II) and DIPY at concentrations of 2×10^{-5} *M* at 25.0 ± 0.1 °C with 0.1 *M* NaOH with a pH range of approximately 2 to 9.

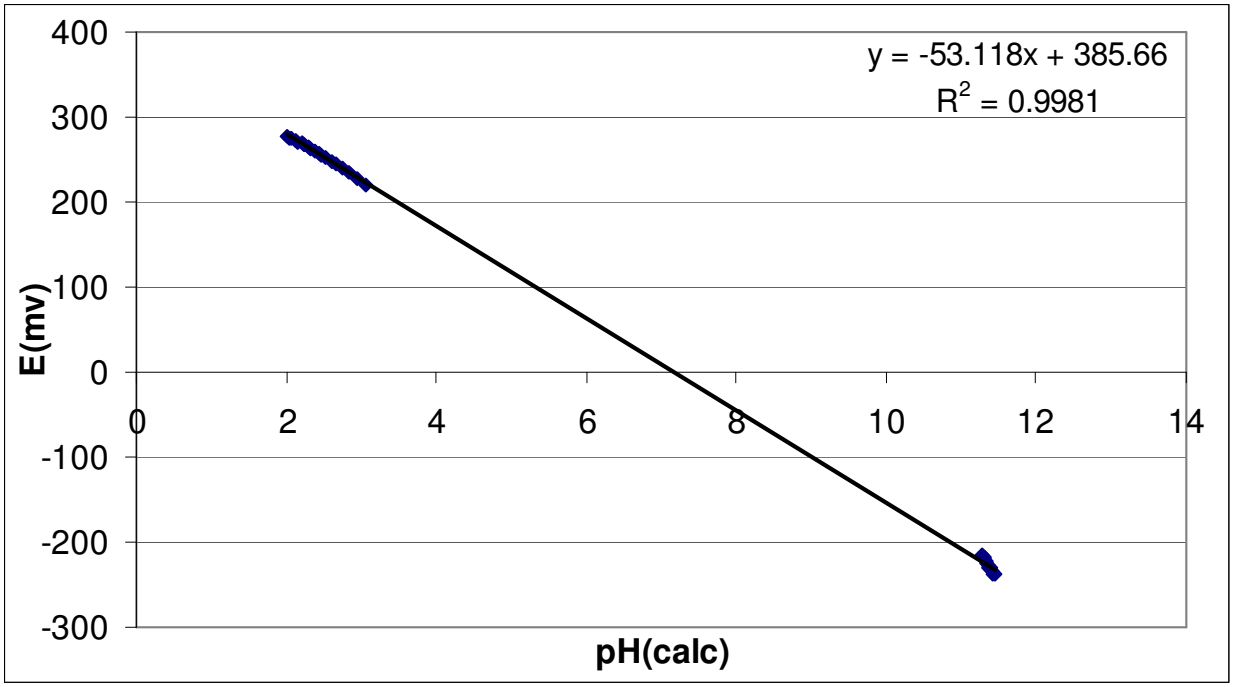

Figure 69: Plot of the correlation between E (mV) and the calculated pH used to calculate E^0 for the titration of the 1:1 copper(II) and DIPY solution at concentrations 2 x 10^{-5} *M* at 25.0 ± 0.1 °C with 0.1 *M* NaOH.

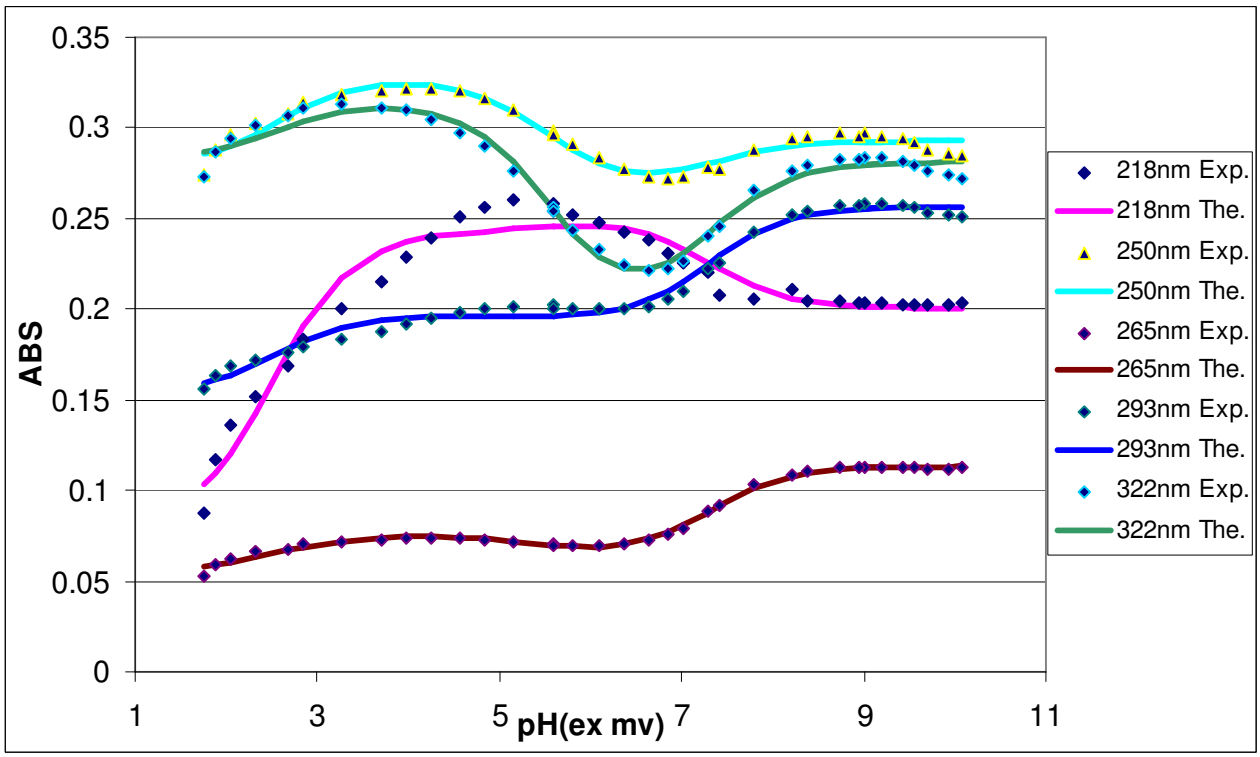

Figure 70: Experimental absorbance data (Exp.) fitted with calculated values (The.) for the titration of 1:1 copper(II) and DIPY solution at concentrations of 2 x 10^{-5} *M*.

Gallium(III)-DIPY Results:

Gallium(III) has an ionic radius of 0.62Å which would classify it as a fairly small metal ion. The UV absorbance spectrum for the 1:1 gallium(III) and DIPY titration experiment where the concentration was 2 x 10^{-5} M for both is shown in Figure 71. A plot of correlation between E (mV) and the calculated pH, which was used to calculate E^0, is shown in Figure 72. A graph with the experimental absorbance data fitted with calculated values to determine the protonation constants for the gallium(III) and DIPY solution is shown in Figure 73. By using equations 1-15 the pK_1 for this titration was calculated to be 6.92 which was almost identical to the pK_1 of the free ligand (6.87). This means that the log K_1 for the gallium(III)-DIPY complex is virtually zero. This can be explained by the fact that Ga(III) is easily hydrolyzed. The pk_a of DIPY is rather high (6.87) and Ga(III) becomes hydrolyzed at a pH lower then this point inhibiting it from complexing with DIPY.

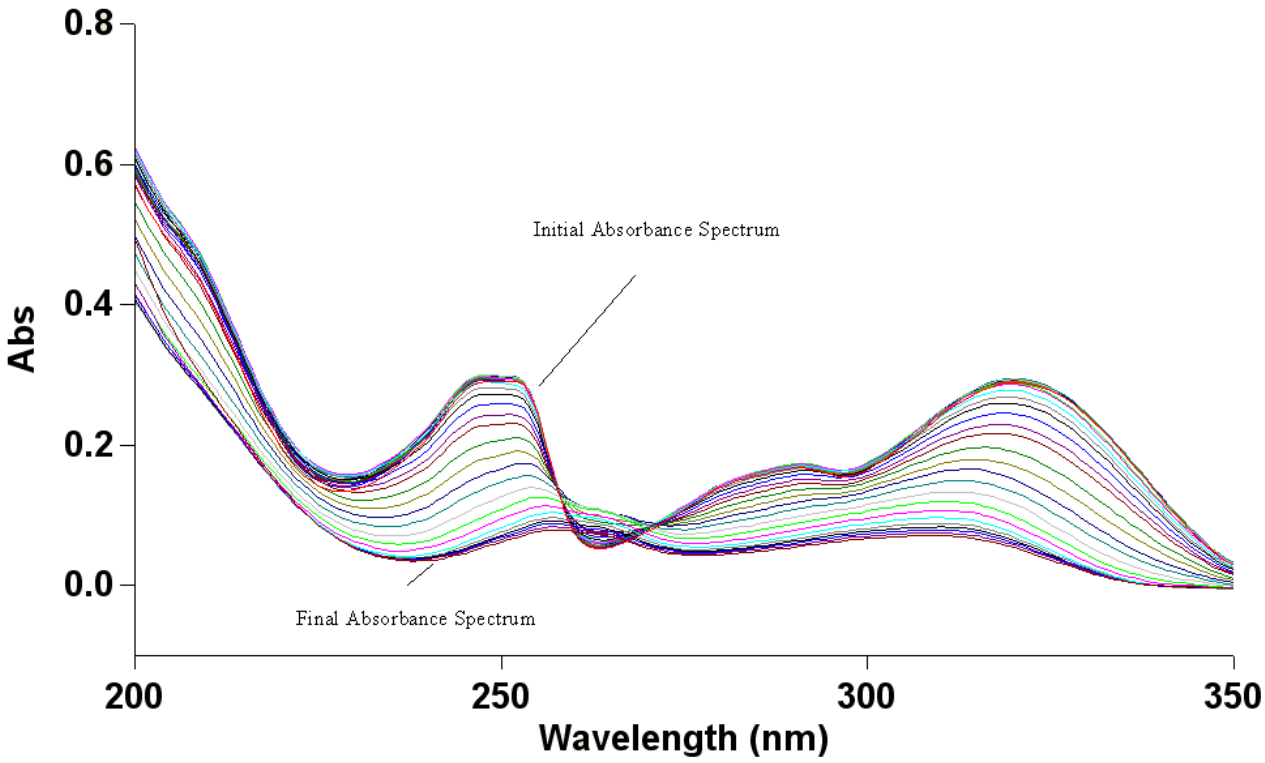

Figure 71: Absorbance versus wavelength (nm) spectra from the titration of the 1:1 solution of gallium(III) and DIPY at concentrations of 2×10^{-5} *M* at 25.0 ± 0.1 °C with 0.1 *M* NaOH with a pH range of approximately 2 to 10.

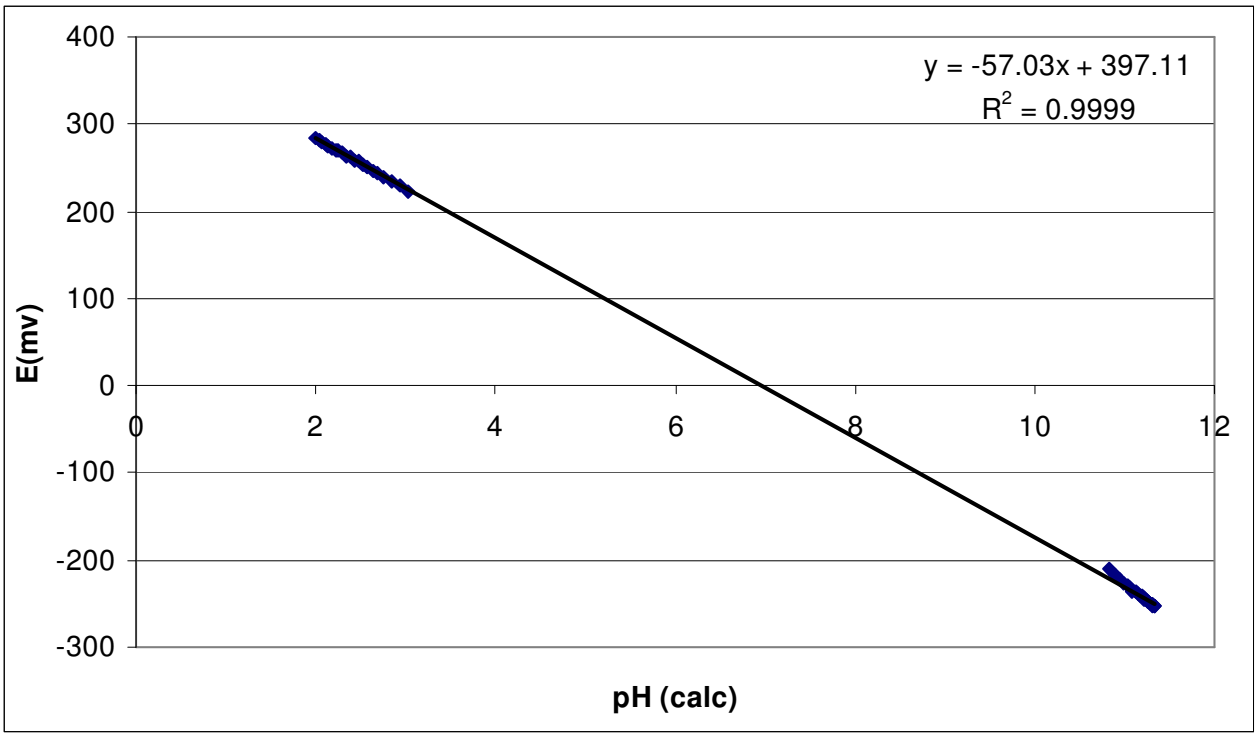

Figure 72: Plot of the correlation between E (mV) and the calculated pH used to calculate E^0 for the titration of the 1:1 gallium(III) and DIPY solution at concentrations of 2 x 10^{-5} *M* at 25.0 ± 0.1 °C with 0.1 *M* NaOH.

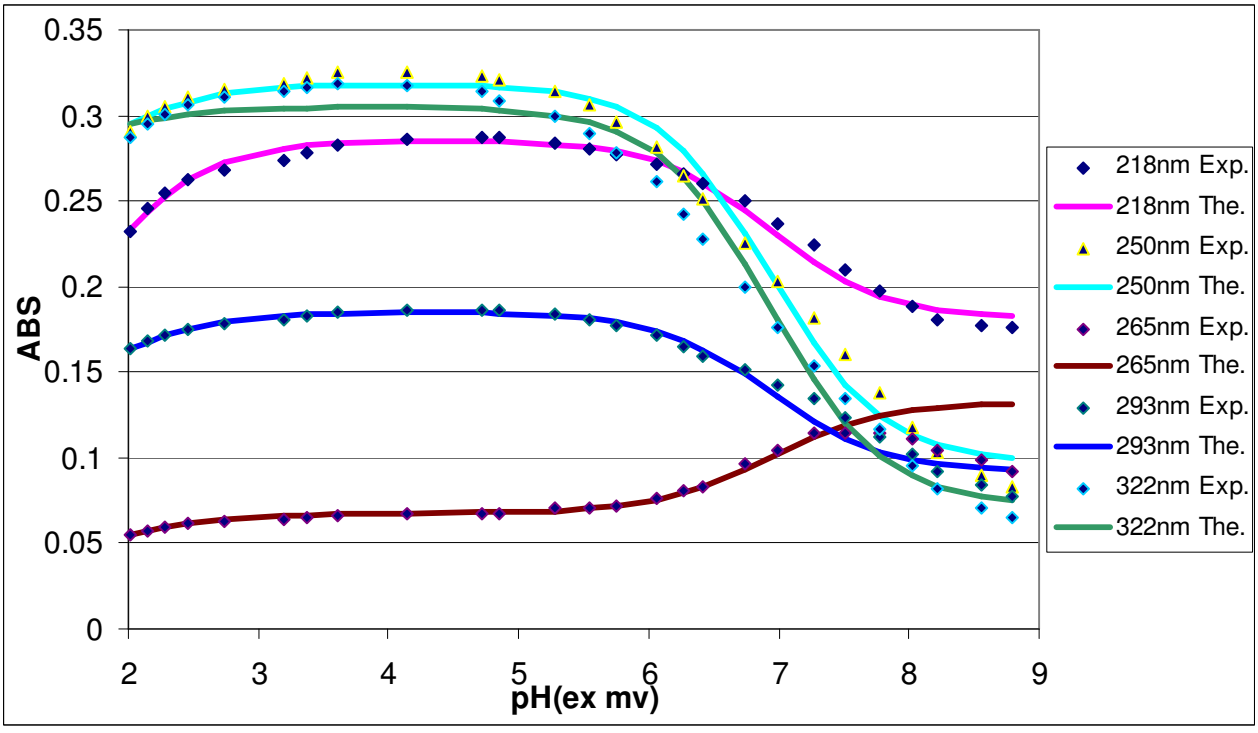

Figure 73: Experimental absorbance data (Exp.) fitted with calculated values (The.) for the titration of 1:1 gallium(III) and DIPY solution at concentrations of 2 x 10^{-5} *M*.

Nickel(II)-DIPY Results:

Nickel(II) has an ionic radius of 0.69Å which classifies it as a medium sized metal ion. Two different titration experiments were run with nickel(II) and DIPY resulting in two different log K_1 values. The absorbance data from these titrations were fitted together to result in a collective log K_1 for the nickel(II)-DIPY complex. The UV absorbance spectrum for the first 1:1 nickel(II) and DIPY titration experiment in which the concentrations were both at 2 x $10^{-4} M$ is shown in Figure 74. A plot of correlation between E (mV) and the calculated pH, which was used to calculate E^0, is shown in Figure 75. A graph with the experimental absorbance data fitted with calculated values to determine the protonation constants for the 1:1 nickel(II) and DIPY solution is shown in Figure 76. By using equations 1-15 the log K_1 for the nickel(II)-DIPY complex was found to be 6.21. The UV absorbance spectrum for the second 1:1 nickel(II) and DIPY titration experiment in which the concentrations were both at 2 x $10^{-5} M$ is shown in Figure 77. A plot of correlation between E (mV) and the calculated pH, which was used to calculate E^0, is shown in Figure 78. The graph with the experimental absorbance data fitted with calculated values to determine the protonation constants for this 1:1 nickel(II) and DIPY solution is shown in Figure 79. Again by using equations 1-15 the log K_1 for the nickel(II)-DIPY complex was this time found to be 5.46. The equilibria observed from these titrations are described below at the pH they occurred.

$Ni(DIPY)^{2+} + H^+ \leftrightarrows Ni^{2+} + (DIPY)H^+$ (pH = 5.72)

$Ni(DIPY)^{2+} + OH^- \leftrightarrows Cu(DIPYH_{-1})$ (pH = 7.10)

The absorbance data for these two titrations were globally fitted with one another to produce a collective value for the log K_1 for the nickel(II)-DIPY complex of 6.15. This value was calculated as follows,

$$\text{Log } K_1 = 6.87 - 5.72 - \log(0.00001)$$

where 6.87 is the pK_a of the free ligand, 5.72 is the pK_1 equilibrium of complex formation and 0.00001 represents the amount of free metal ion at the midpoint of the equilibrium where Ni(II) is displaced from DIPY.

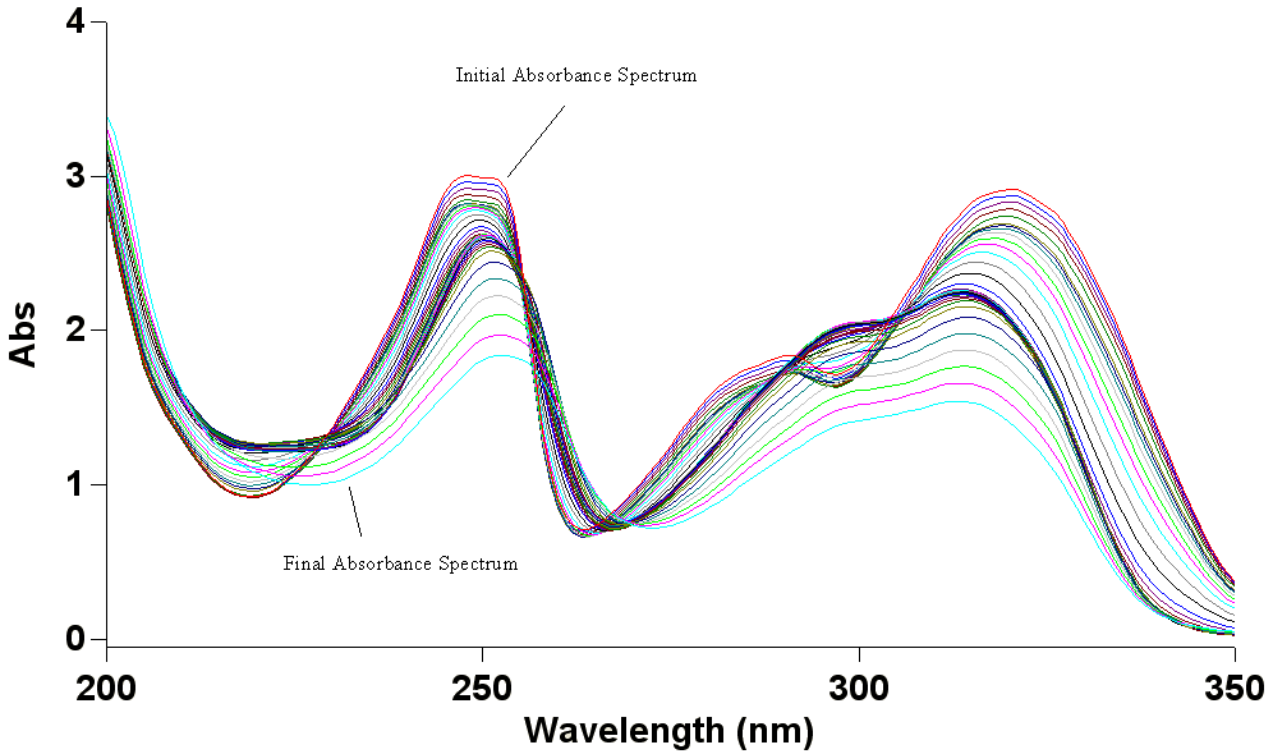

Figure 74: Absorbance versus wavelength (nm) spectra from the titration of the 1:1 solution of nickel(II) and DIPY at concentrations of $2 \times 10^{-4} M$ at 25.0 ± 0.1 °C with 0.1 M NaOH with a pH range of approximately 2 to 11.

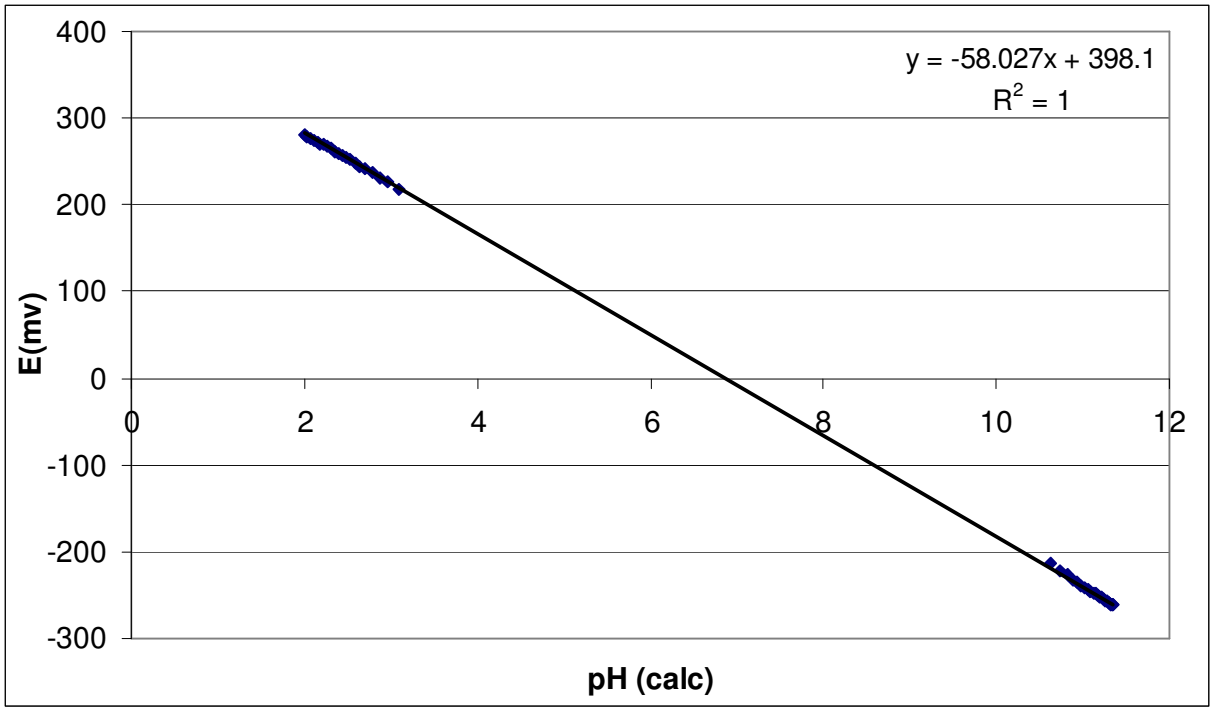

Figure 75: Plot of the correlation between E (mV) and the calculated pH used to calculate E^0 for the titration of the 1:1 nickel(II) and DIPY solution at concentrations of 2 x 10^{-4} *M* at 25.0 ± 0.1 °C with 0.1 *M* NaOH .

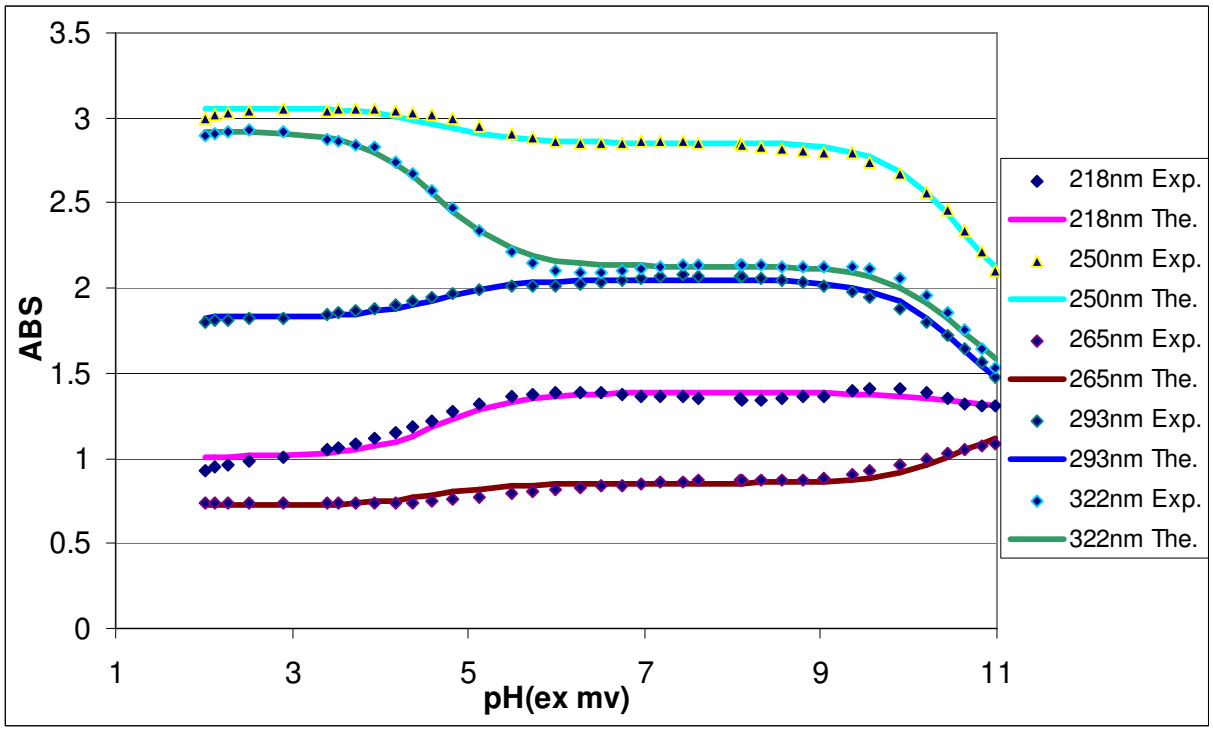

Figure 76: Experimental absorbance data (Exp.) fitted with calculated values (The.) for the titration of 1:1 nickel(II) and DIPY solution at concentrations of 2 x 10^{-4} *M*.

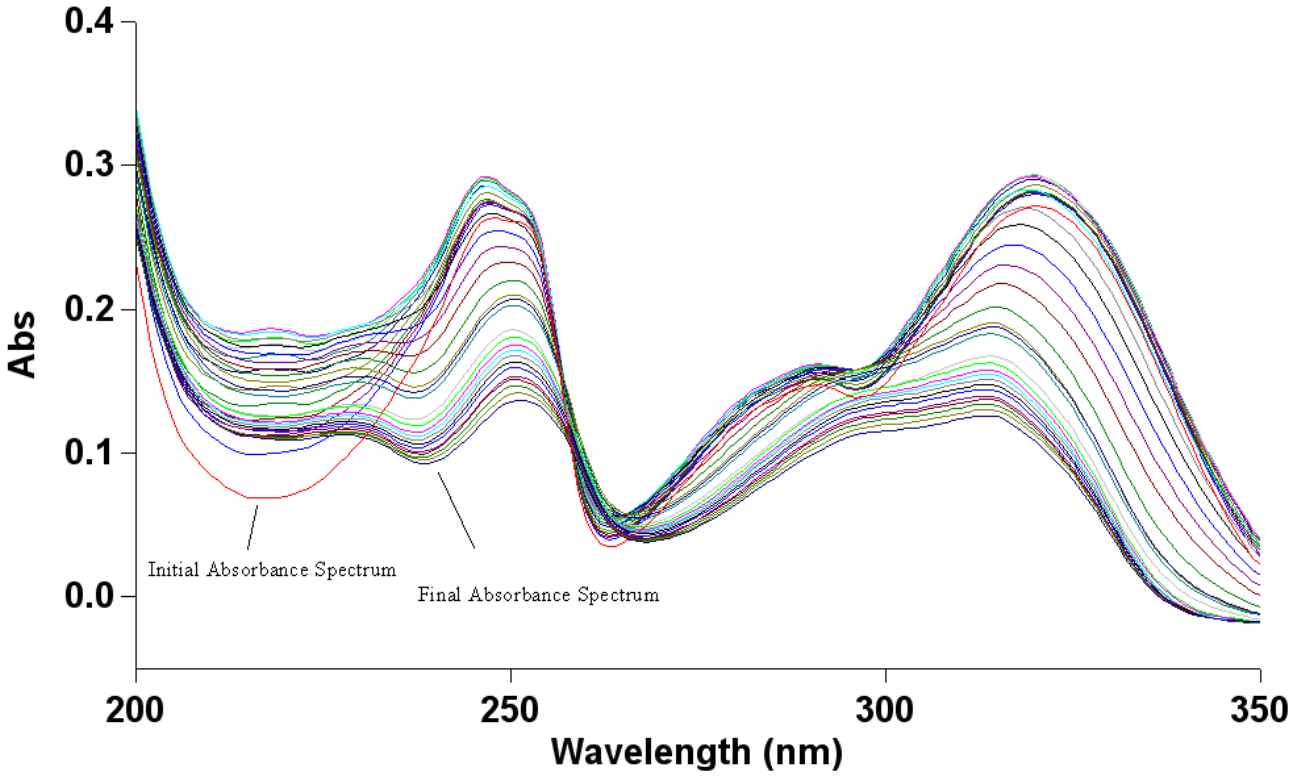

Figure 77: Absorbance versus wavelength (nm) spectra from the titration of the 1:1 solution of nickel(II) and DIPY at concentrations of 2×10^{-5} *M* at 25.0 ± 0.1 °C with 0.1 *M* NaOH with a pH range of approximately 2 to 9.

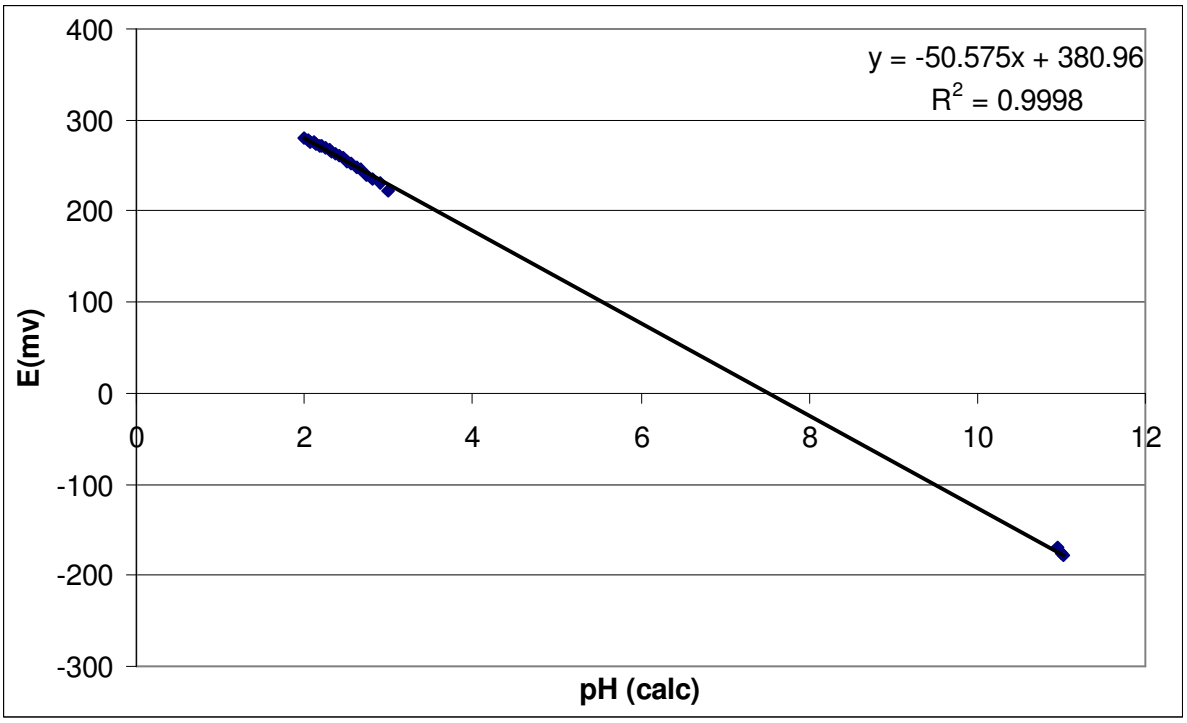

Figure 78: Plot of the correlation between E (mV) and the calculated pH used to calculate E^0 for the titration of the 1:1 nickel(II) and DIPY solution at concentrations of $2 \times 10^{-5} M$ at 25.0 ± 0.1 °C with 0.1 M NaOH .

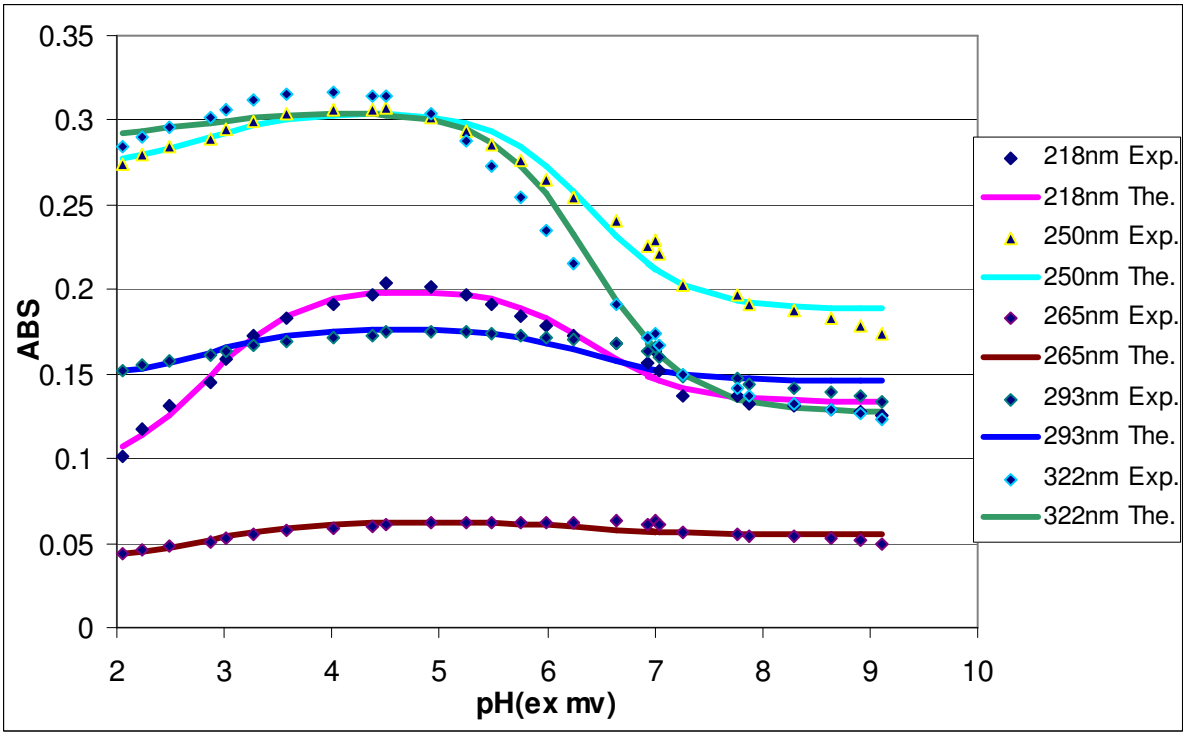

Figure 79: Experimental absorbance data (Exp.) fitted with calculated values (The.) for the titration of 1:1 nickel(II) and DIPY solution at concentrations of $2 \times 10^{-5} M$.

Zinc(II)-DIPY Results

Zinc(II) has an ionic radius of 0.74Å which classifies it as a medium sized metal ion. Two different titration experiments were run with zinc(II) and DIPY resulting in two different log K_1 values. The absorbance data from these titrations were fitted together to result in a collective log K_1 for the zinc(II)-DIPY complex. The UV absorbance spectrum for the 1250:1 zinc(II) and DIPY titration experiment in which the concentrations were 2 x 10^{-2} M and 1.6 x 10^{-5} M respectively is shown in Figure 80. A plot of correlation between E (mV) and the calculated pH, which was used to calculate E^0, is shown in Figure 81. A graph with the experimental absorbance data fitted with calculated values to determine the protonation constants for the 1250:1 zinc(II) and DIPY solution is shown in Figure 82. By using equations 1-15 the log K_1 for the zinc(II)-DIPY complex was found to be 3.39. The UV absorbance spectrum for the 50:1 zinc(II) and DIPY titration experiment in which the concentrations were 1 x 10^{-3} M and 2 x 10^{-5} M respectively is shown in Figure 83. A plot of correlation between E (mV) and the calculated pH, which was used to calculate E^0, is shown in Figure 84. A graph with the experimental absorbance data fitted with calculated values to determine the protonation constants for the 50:1 zinc(II) and DIPY solution is shown in Figure 85. By using equations 1-15 the log K_1 for the zinc(II)-DIPY complex was found to be 3.59. The equilibria observed from these titrations are described below at the pH they occurred.

$$Zn(DIPY) + H^+ \leftrightarrows Zn(DIPY)H^+ \qquad (pH = 2.45)$$

$$Zn(DIPY)^{2+} + H^+ \leftrightarrows Zn^{2+} + (DIPY)H^+ \qquad (pH = 6.35)$$

The absorbance data for these two titrations were globally fitted with one another to produce a collective value for the log K_1 for the zinc(II)-DIPY complex of 3.52. This value was calculated as follows,

$$\text{Log } K_1 = 6.87 - 6.35 - \log(0.001)$$

where 6.87 is the pK_a of the free ligand, 6.35 is the pK_1 equilibrium of complex formation and 0.001 represents the amount of free metal ion at the midpoint of the equilibrium where Zn(II) is displaced from DIPY.

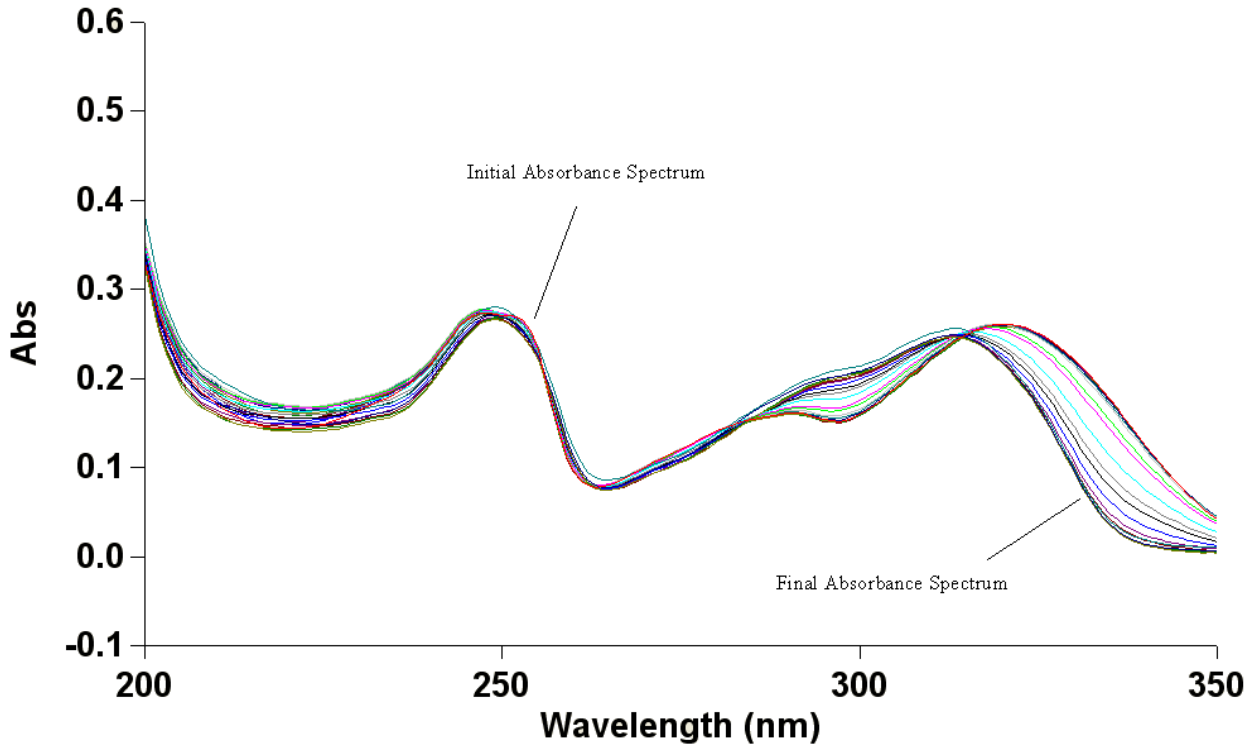

Figure 80: Absorbance versus wavelength (nm) spectra from the titration of the 1250:1 solution of zinc(II) and DIPY at concentrations of $2 \times 10^{-2} M$ and $1.6 \times 10^{-5} M$ respectively at 25.0 ± 0.1 °C with 0.1 M NaOH with a pH range of approximately 2 to 7.

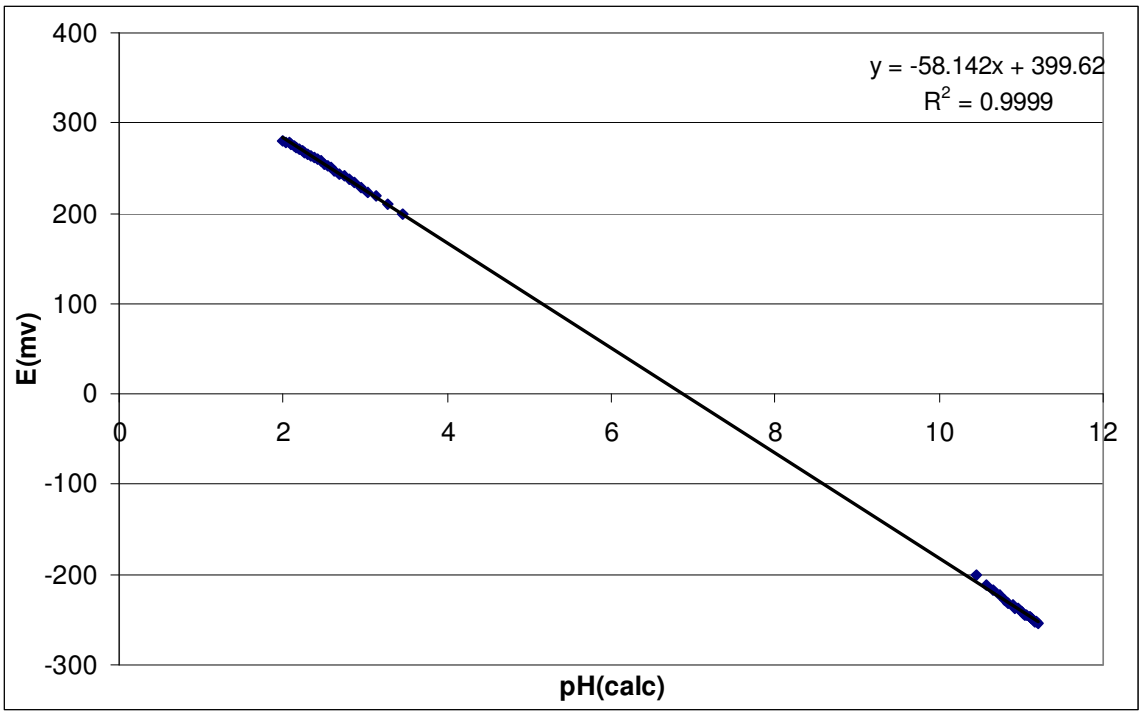

Figure 81: Plot of the correlation between E (mV) and the calculated pH used to calculate E^0 for the titration of the 1250:1 solution of zinc(II) and DIPY at concentrations of $2 \times 10^{-2} M$ and $1.6 \times 10^{-5} M$ respectively at 25.0 ± 0.1 °C with 0.1 *M* NaOH.

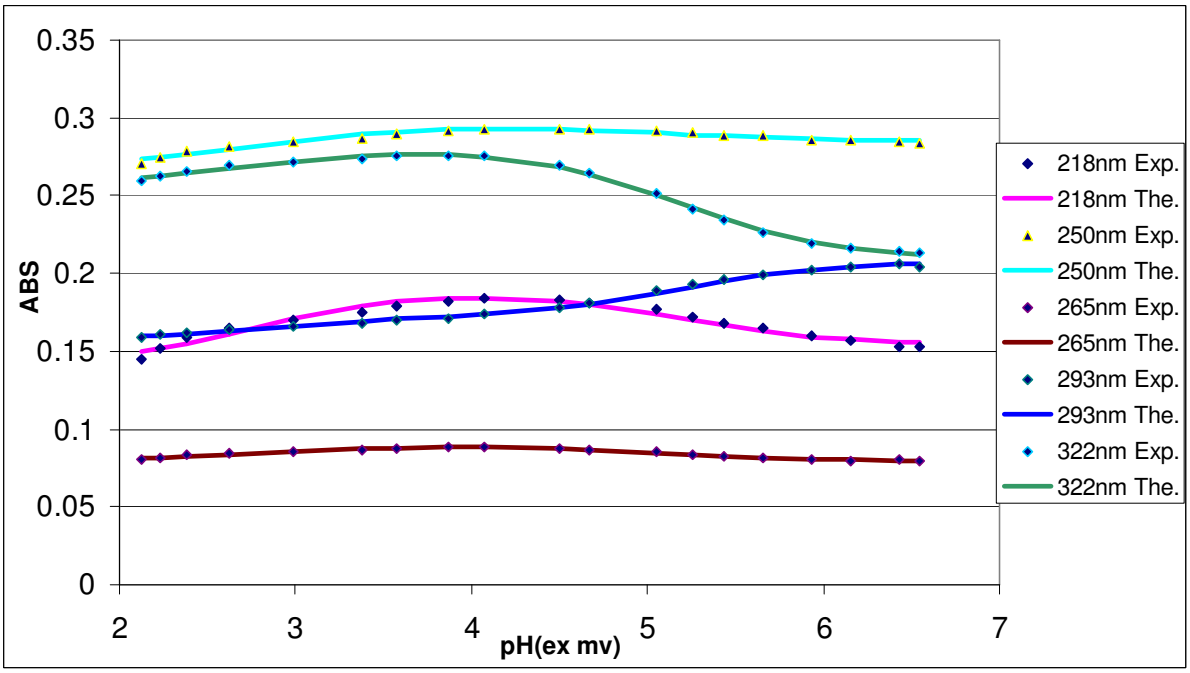

Figure 82: Experimental absorbance data (Exp.) fitted with calculated values (The.) for the titration of 1250:1 solution of zinc(II) and DIPY at concentrations of $2 \times 10^{-2} M$ and $1.6 \times 10^{-5} M$ respectively at 25.0 ± 0.1 °C with 0.1 *M* NaOH.

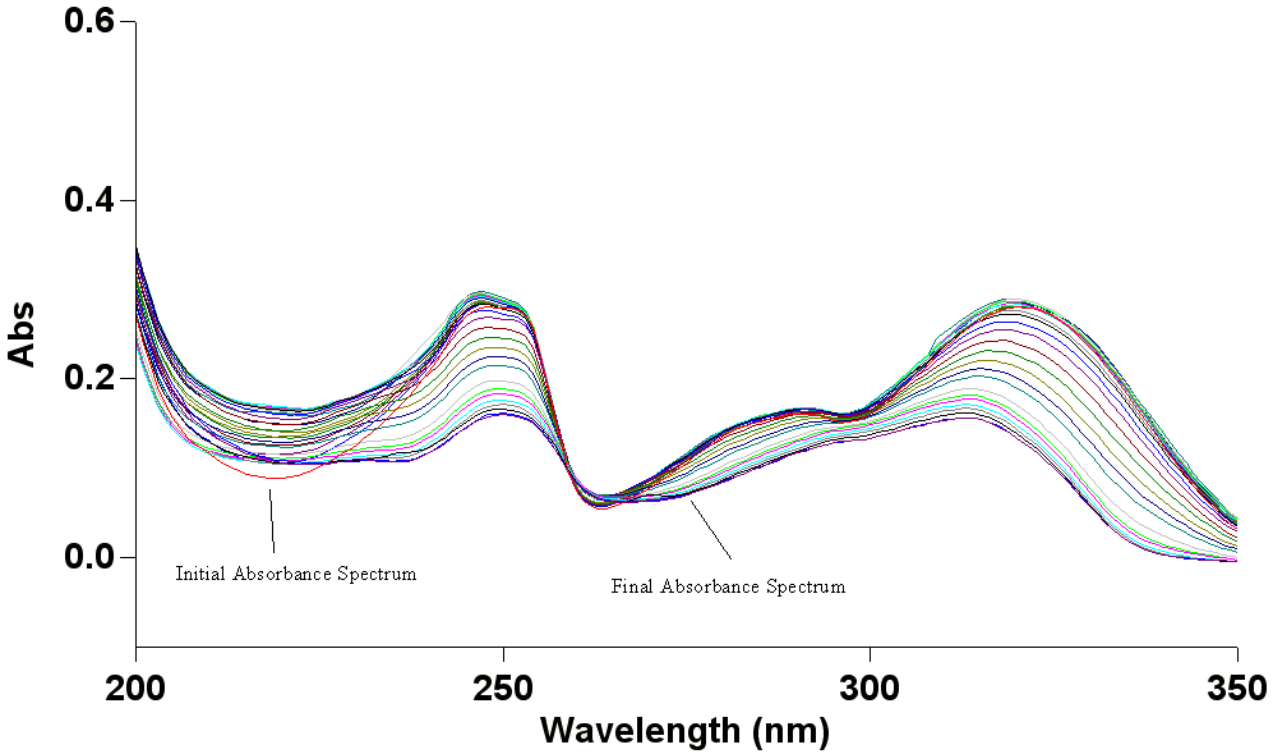

Figure 83: Absorbance versus wavelength (nm) spectra from the titration of the 50:1 solution of zinc(II) and DIPY at concentrations of $1 \times 10^{-3} M$ and $2 \times 10^{-5} M$ respectively at 25.0 ± 0.1 °C with 0.1 *M* NaOH with a pH range of approximately 2 to 7.

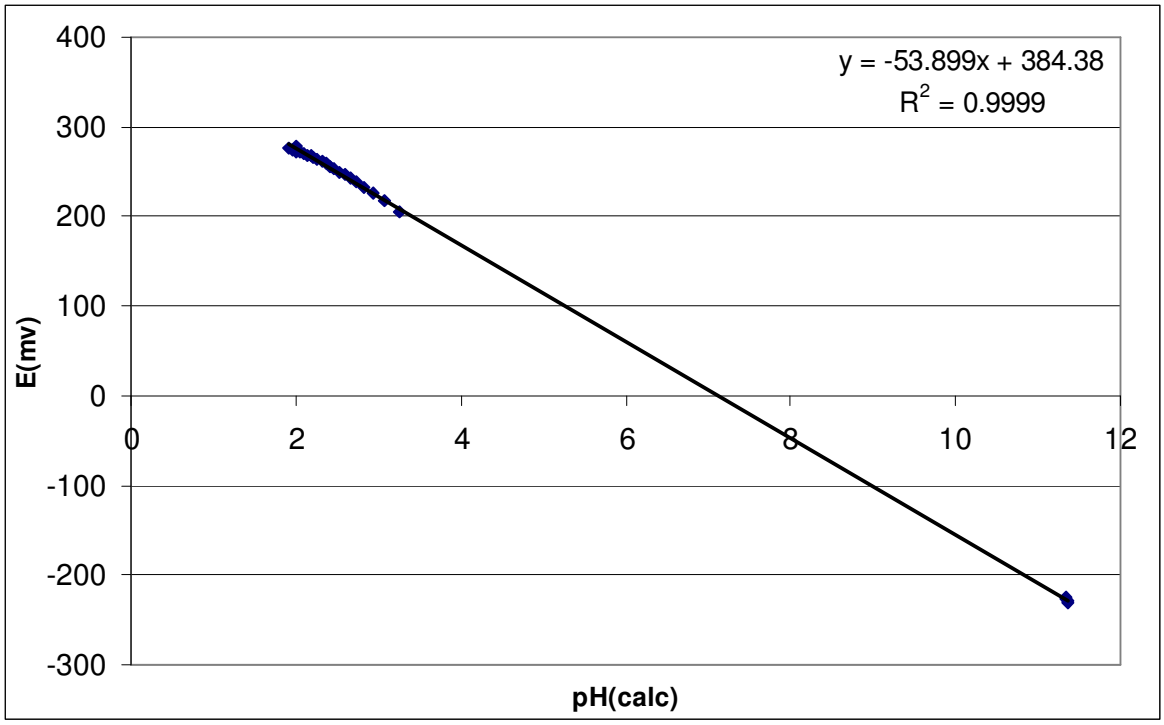

Figure 84: Plot of the correlation between E (mV) and the calculated pH used to calculate E^0 for the titration of the 50:1 solution of zinc(II) and DIPY at concentrations of 1 x 10^{-3} *M* and 2 x 10^{-5} *M* respectively at 25.0 ± 0.1 °C with 0.1 *M* NaOH.

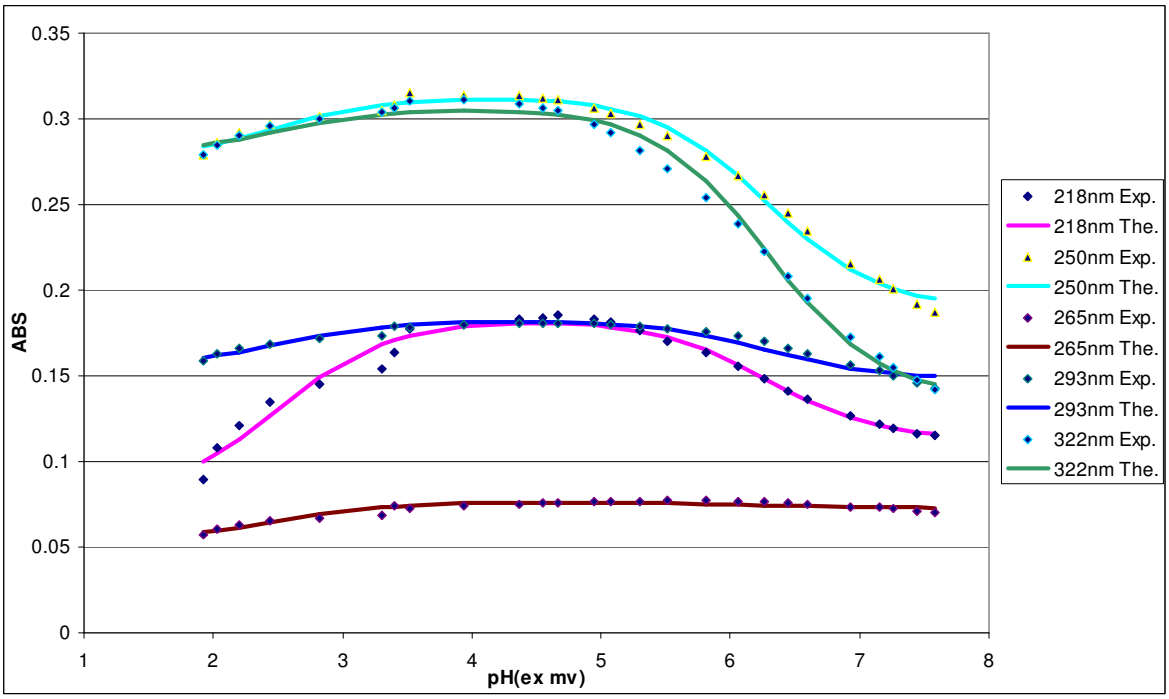

Figure 85: Experimental absorbance data (Exp.) fitted with calculated values (The.) for the titration of 50:1 solution of zinc(II) and DIPY at concentrations of 1 x 10^{-3} *M* and 2 x 10^{-5} *M* respectively at 25.0 ± 0.1 °C with 0.1 *M* NaOH.

Synthesis of PDA

The synthesis of 1,10-phenanthroline-2,9-dicarboxaldehyde (PDALD) yielded 0.681 g (2.88 mmol) of product for a 62.61% yield. The product was obtained as yellow crystals after filtration. This PDALD product was not tested for purity as any product not oxidized by the first reaction will be in the second step of the reaction. The PDALD collected was used to produce 1,10-phenanthroline-2,9-dicarboxylic acid (PDA). The reaction produced 0.527 g (1.965 mmol) of PDA for a 68.23% yield. The melting point for the product was found to be 239-242°C which is in close agreement to the literature value[21] of 238°C. An IR analysis was preformed on the product and the spectrum obtained can be seen in Figure 86. The spectrum shows a large peak at 1721cm^{-1} corresponding to the C=O stretch of the carboxylic acid. A broad peak is also seen at around 3500 cm^{-1} resulting from the water molecule in the crystal lattice. This IR analysis paired with the accurate melting point obtained combine to sufficiently prove that PDA was produced from this reaction.

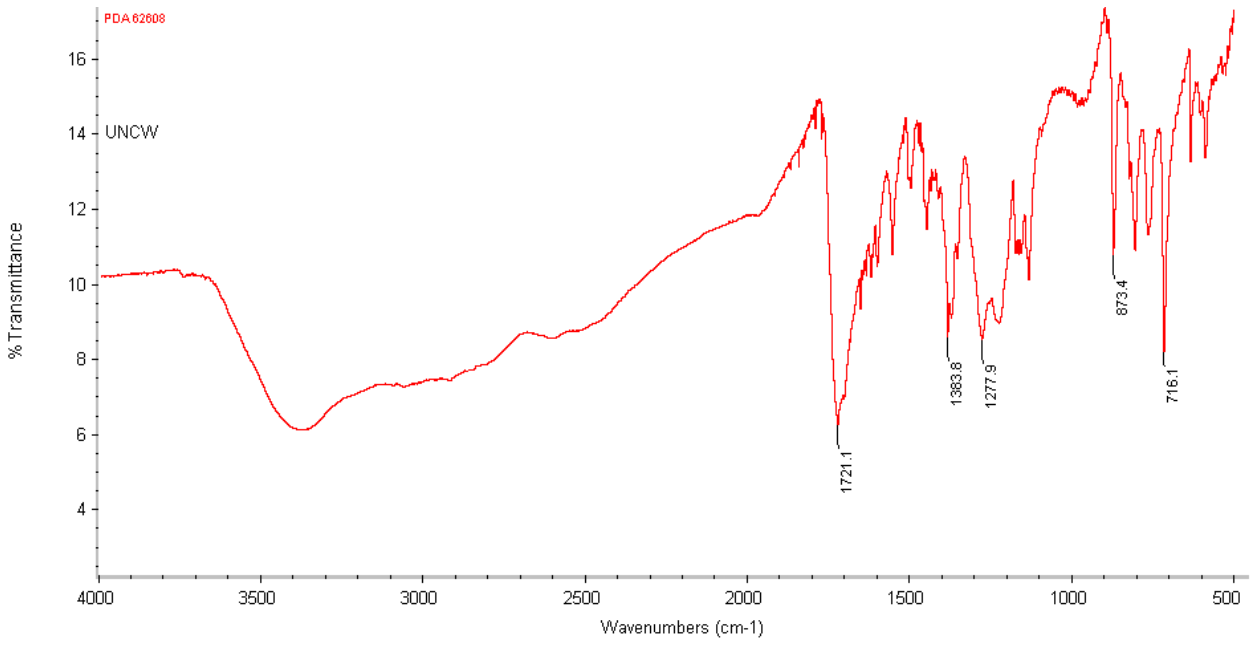

Figure 86: IR spectrum of 1,10-phenanthroline-2,9-dicarboxylic acid (PDA) product as a KBr pellet.

UV-Vis Spectrophotometric Titrations Involving PDA

UV/Vis spectroscopy was used as an analytical tool to determine the stability constants (log K_1) of the metal-PDA complexes. Absorbance scans were preformed from 200 to 350nm and were taken after each titrant addition of NaOH. Absorbance data was taken at selected wavelengths of 211, 235, 260, 286, and 320nm. Absorbance spectra of the free ligand at varying pH at these wavelengths can be seen in Figure 87. Peak shifts were seen for these absorbances upon complexation of PDA with a metal ion.

In order to determine the protonation constants for this ligand, PDA, a titration experiment was performed at 25.0 ± 0.1 °C at 0.1 *M* ionic strength (0.1 *M* $HClO_4$). Figure 88 shows absorbance versus wavelength (nm) scans at pH values of approximately 2 to 9. A plot of correlation between E (mV) and the calculated pH, which was used to calculate E^0, is shown in Figure 89. Absorbance data for the selected wavelengths were used to generate a plot of absorbance versus pH(ex mv). This plot is shown in Figure 90. The points drawn in are the experimental values and the solid lines are theoretical curves of absorbance versus pH calculated for the constants corresponding to the observed protonation equilibria. The theoretical curves of absorbance versus pH in Figure 90 were fitted to the experimental points using the SOLVER tool of the program EXCEL[22]. The standard deviations of these protonation constants were calculated using the SOLVSTAT macro provided in reference 22. The protonation constants for PDA were calculated using the absorbance data and pH values from this plot. Like the two previous ligands, PDA also has two protonation events pK_1 and pK_2. The calculated protonation constants of pK_1 and pK_2 were 4.91 and 2.31, respectively. An illustration of the proposed

protonation equilibria for PDA can be seen in Figure 91. These protonation constants were determined by using equations 1-7.

a.)

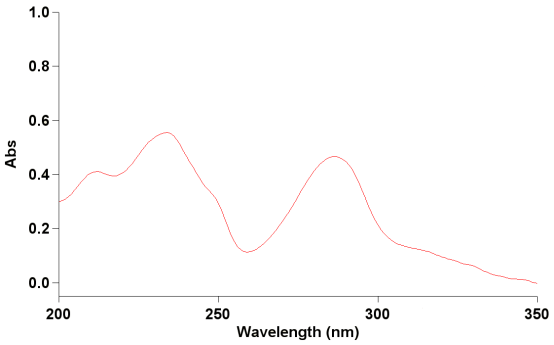

b.)

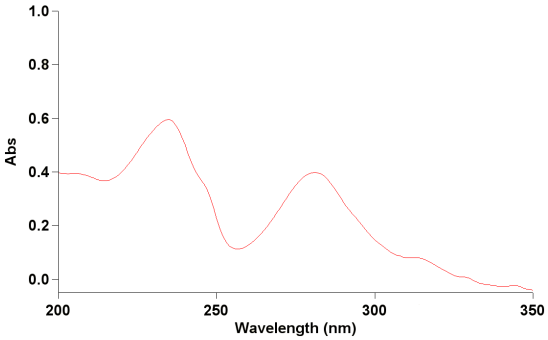

c.)

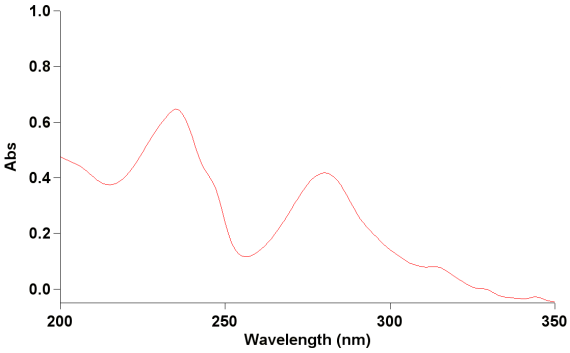

d.)

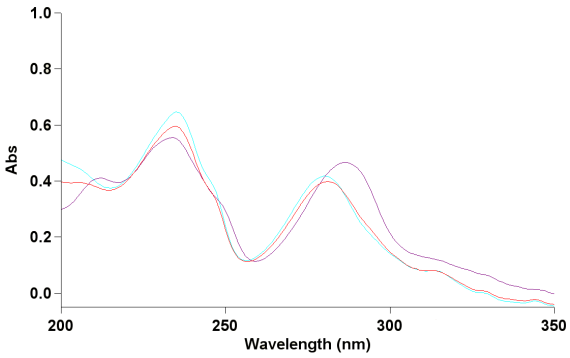

Figure 87: Plots of absorbance versus wavelength (nm) spectra at varying pH of 2 x 10^{-5} *M* PDA at 25.0 ± 0.1 °C with 0.1 *M* NaOH. a.) pH = 2.02, b.) pH = 5.27, c.) pH = 8.68, d.) overlay of pH 2.02, 5.27, and 8.68 spectra.

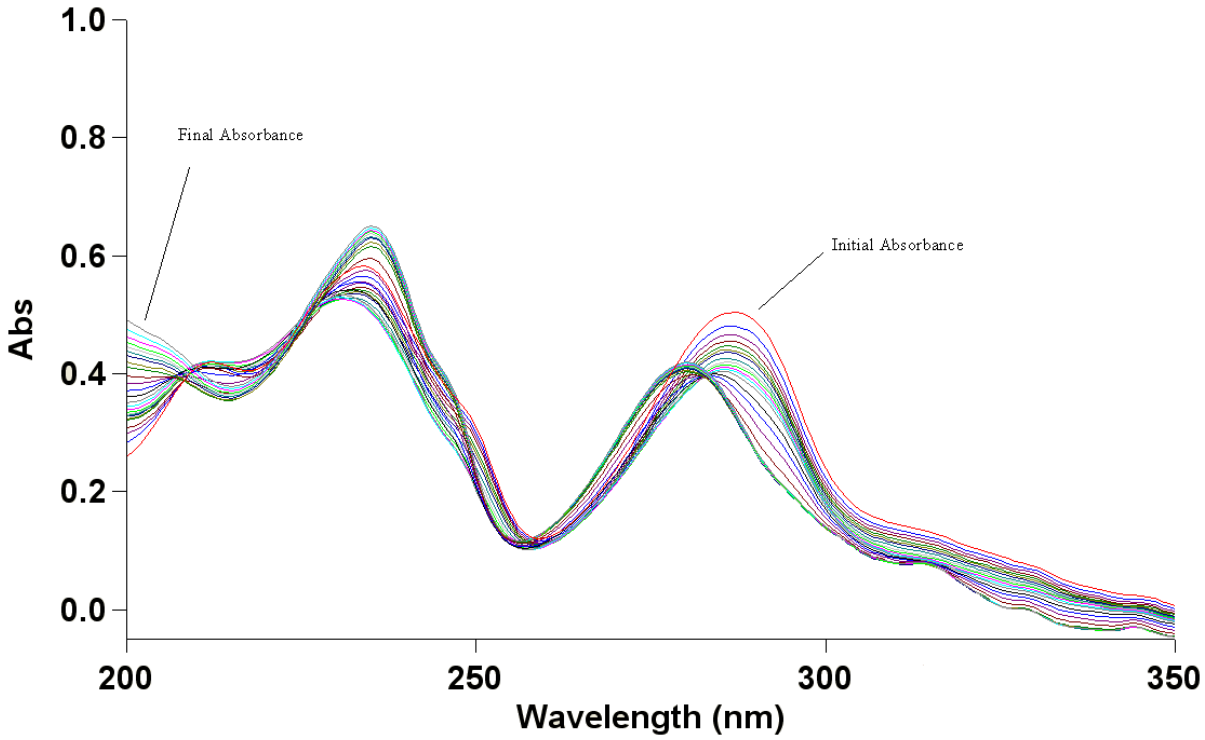

Figure 88: Absorbance versus wavelength (nm) spectra from the titration of 2 x 10^{-5} *M* PDA at 25.0 ± 0.1 °C with NaOH with a pH range of approximately 2 to 9.

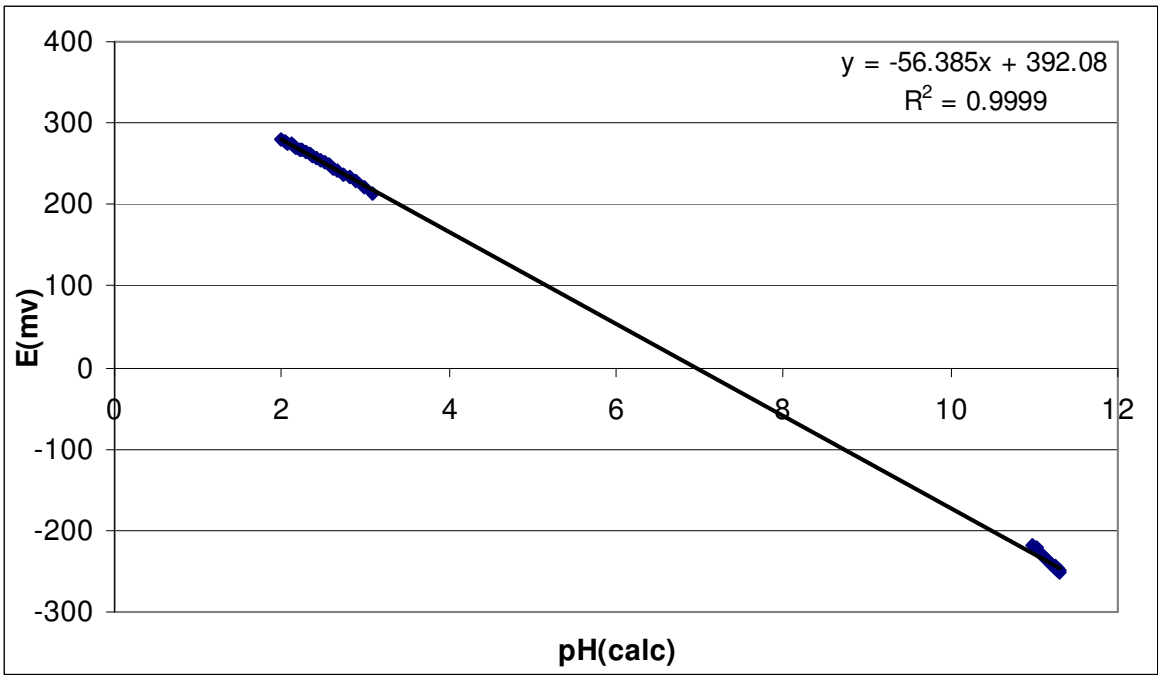

Figure 89: Plot of the correlation between E (mV) and the calculated pH used to calculate E^0 for the titration of 2 x 10^{-5} *M* PDA at 25.0 ± 0.1 °C with NaOH.

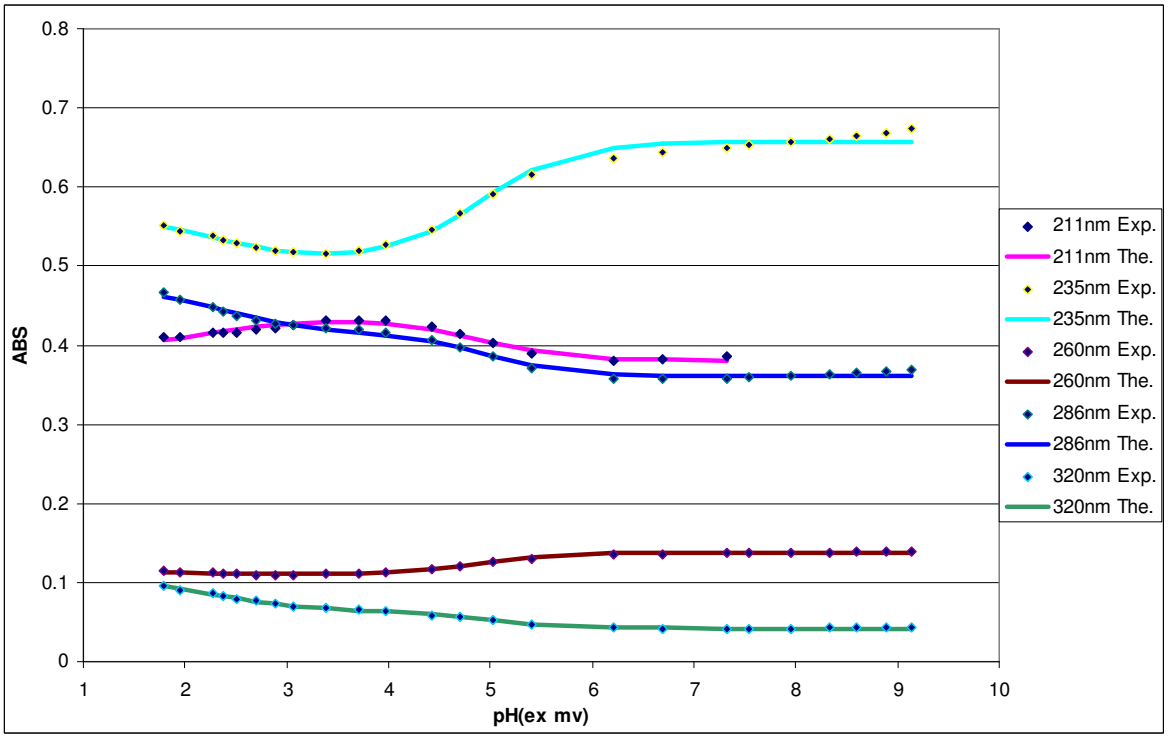

Figure 90: Experimental absorbance data (Exp.) fitted with calculated values (The.) to determine the protonation constants of 2 x 10^{-5} *M* PDA.

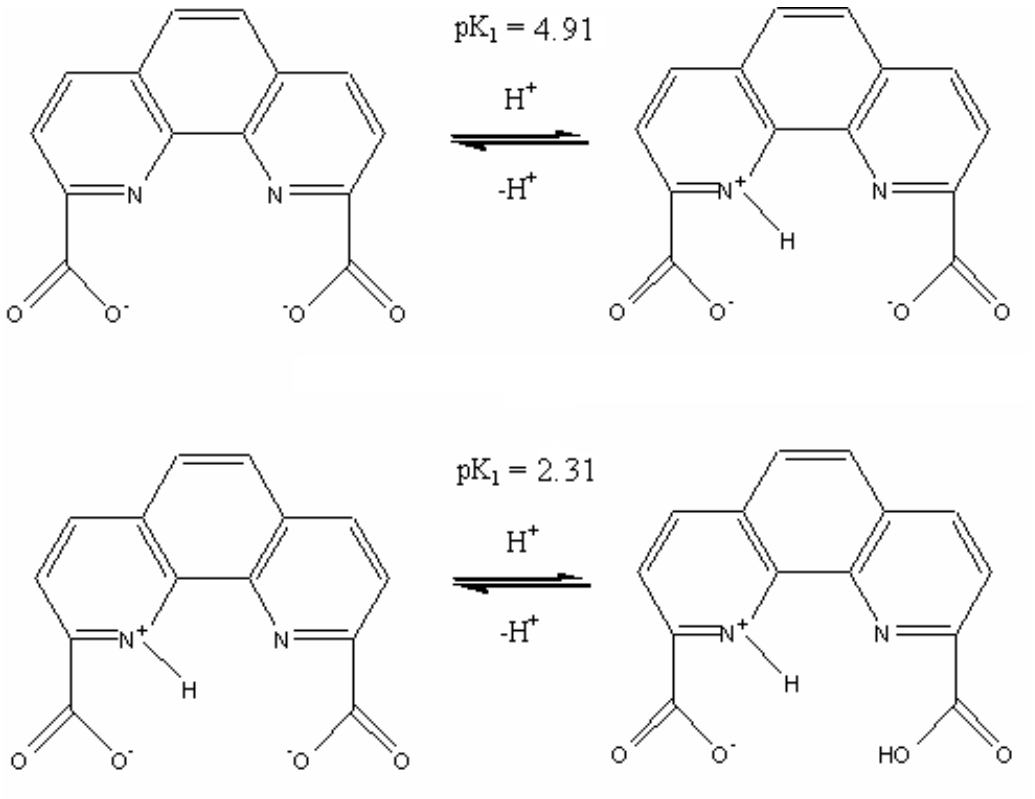

Figure 91: The proposed protonation equilibria for 1,10-phenanthroline-2, 9-dicarboxylic acid (PDA).

Titrations Involving Metal Ion Complexation with PDA

In these titrations, unless stated otherwise, the same procedure was performed for each metal-ligand complex at the same wavelengths as done with the free ligand. The equations 1-15 can again be used here to determine the log K_1 for metal ion stability since PDA has the same number of protonation events as 8PQ and DIPY.

Indium(III)-PDA Results:

Indium(III) has an ionic radius of 0.8Å which would classify it as a medium sized metal ion. The UV absorbance spectrum for the 1:1 indium(III) and PDA titration experiment where the concentration was 2 x 10^{-5} M for both is shown in Figure 92. A plot of correlation between E (mV) and the calculated pH, which was used to calculate E^0, is shown in Figure 93. Absorbance values were recorded for the wavelengths 211, 235, 248, 259, 286, and 293nm. These wavelengths were chosen as they exhibited at a large variance in absorbance due to complexation. A graph with the experimental absorbance data fitted with calculated values to determine the protonation constants for the indium(III) and PDA solution is shown in Figure 94. From this data 3 successive pH-dependent equilibria were observed.

$$\mathrm{In(PDA)^+ + OH^- \leftrightarrows In(PDA)OH} \qquad \text{(pH = 5.89)}$$

$$\mathrm{In(PDA)(OH) + OH^- \leftrightarrows [In(PDA)(OH)_2]^-} \qquad \text{(pH = 8.31)}$$

$$\mathrm{[In(PDA)(OH)_2]^- + OH^- \leftrightarrows In(OH)_3 + PDA^{2-}} \qquad \text{(pH = 10.90)}$$

Using log K_w = 13.78, the log K_1 [OH^-] of the In-PDA complex can be described as follows.

$$In(PDA)+ + OH^- \leftrightarrows In(PDA)OH \qquad (\log K_1\ [OH^-] = 7.89)$$

$$In(PDA)(OH) + OH^- \leftrightarrows [In(PDA)(OH)_2]^- \qquad (\log K_2\ [OH^-] = 5.47)$$

$$[In(PDA)(OH)_2]^- + 2\ OH^- \leftrightarrows [In(OH)_4]^- + PDA^{2-} \qquad (\log K_{3,4}\ [OH^-] = 2.88)$$

The value of $\log \beta_4\ [OH^-]$ for indium(III) is 33.9 and from this value a $\log K_1$ for PDA with indium(III) can be calculated by using the equation shown below.

$$\log K_1 = 33.9 - (2 \text{ x } (2.88) + 5.47 + 7.89) + 5$$

The values in the equation can be identified where 33.9 corresponds to the value of $\log \beta_4\ [OH^-]$ for indium(III) and 5 is the negative log of the amount of free ligand at the isosbestic point. Using this equation the $\log K_1$ for PDA with indium(III) was found to be 19.78. This $\log K_1$ value is in close agreement with the previously recorded value of 19.7.[17,18]

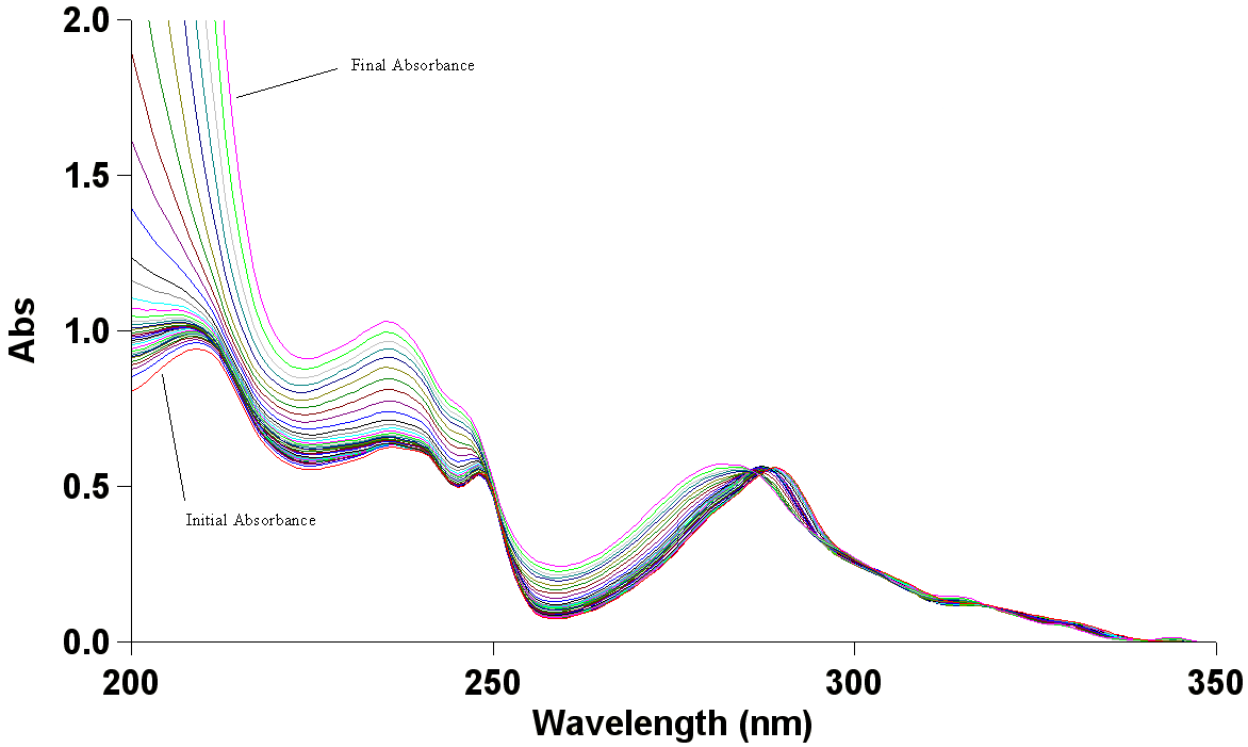

Figure 92: Absorbance versus wavelength (nm) spectra from the titration of the 1:1 solution of indium(III) and PDA both at concentrations of 2 x 10^{-5} *M* at 25.0 ± 0.1 °C with NaOH with a pH range of approximately 2 to 12.

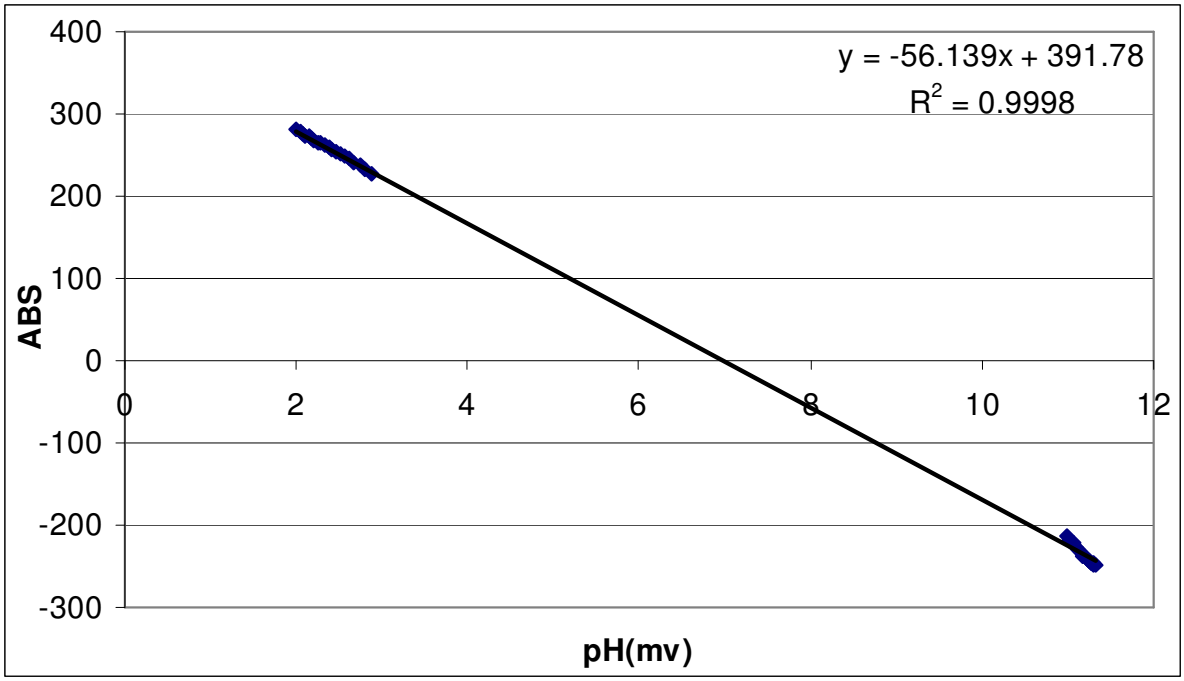

Figure 93: Plot of the correlation between E (mV) and the calculated pH used to calculate E^0 for the titration of a 1:1 solution of indium(III) and PDA both at concentrations of 2 x 10^{-5} *M* at 25.0 ± 0.1 °C with NaOH.

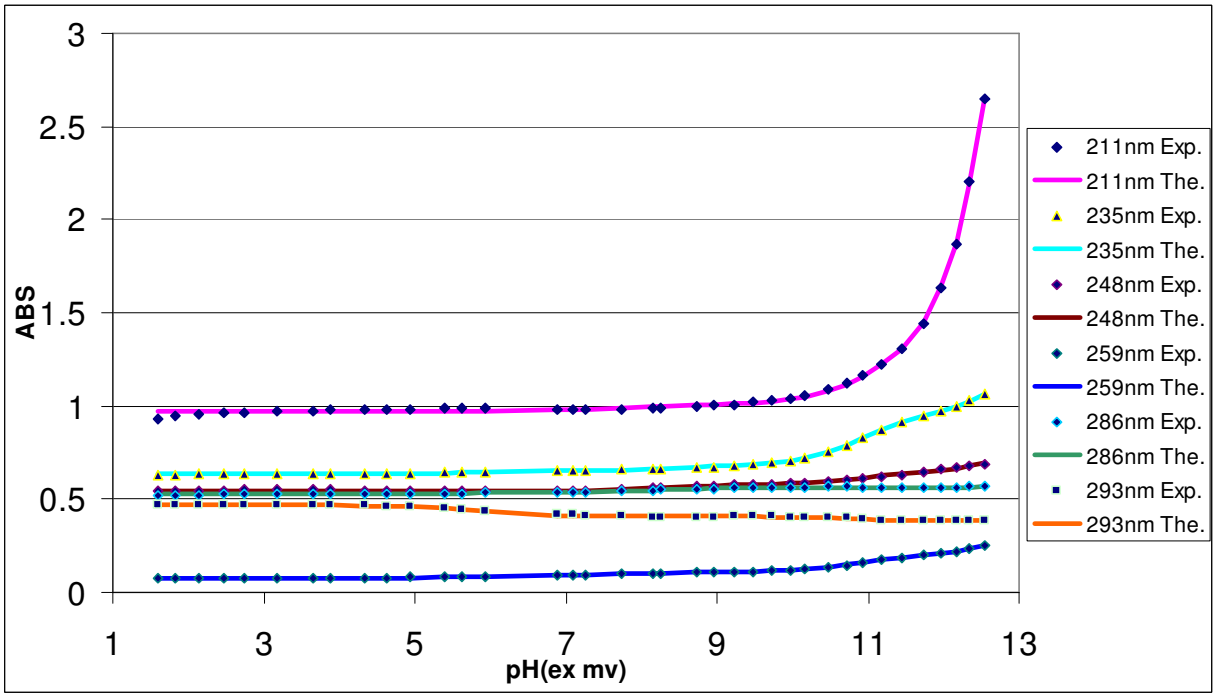

Figure 94: Experimental absorbance data (Exp.) fitted with calculated values (The.) for the titration of a 1:1 solution of indium(III) and PDA both at concentrations of 2 x 10^{-5} *M* at 25.0 ± 0.1 °C with 0.1 *M* NaOH.

Uranyl(VI)-PDA Results:

Uranyl(VI) has an effective ionic radius in the plane of about 1Å which would classify it as a large metal ion. Due to uranyl(VI)'s slow kinetics determining the formation constant for the uranyl-PDA complex proved difficult. Two different types of titrations were performed in order to determine the formation constant of PDA with uranyl(VI). Metal competition titrations where two metal solutions were added to a PDA solution and allowed to come to equilibrium, observing the complex that was formed. Solutions of PDA and uranyl(VI) were also titrated with NaOH in an attempt to determine p*K*a values. The UV absorbance spectrum for the 48 hour 1:1 uranyl(VI) and PDA titration experiment where the concentration was 2 x 10^{-5} *M* for both is shown in Figure 95. The final absorbance of this spectrum can be said to be what the PDA-uranyl(VI) complex looks like at equilibrium.

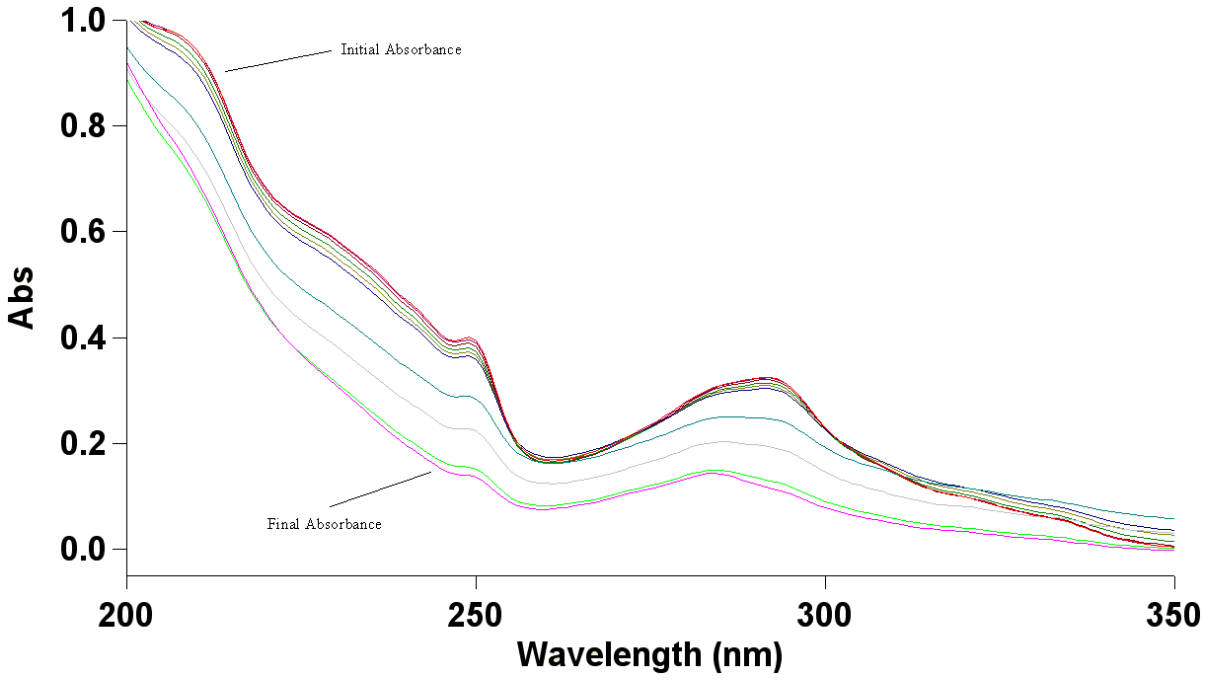

Figure 95: Absorbance versus wavelength (nm) spectra for the 1:1 solution of uranyl(VI) and PDA both at concentrations of 2 x 10^{-5} *M* at 25.0 ± 0.1 °C titrated with NaOH to a pH of approximately 3.3 and observed for 48 hours.

The UV absorbance spectrum for the 24 hour 1:1000:1 uranyl(VI), Cd(II), and PDA titration where concentrations of 2 x 10^{-5} M, 2 x 10^{-2} M, and 2 x 10^{-5} M respectively is shown in Figure 96. As it can be seen, the final absorbance of this titration is very similar to that of Figure 95. The log K_1 value of Cd(II) with PDA was previously found to be 12.87.[18] This titration shows that the log K_1 value of uranyl(VI) with PDA is greater then 12.87.

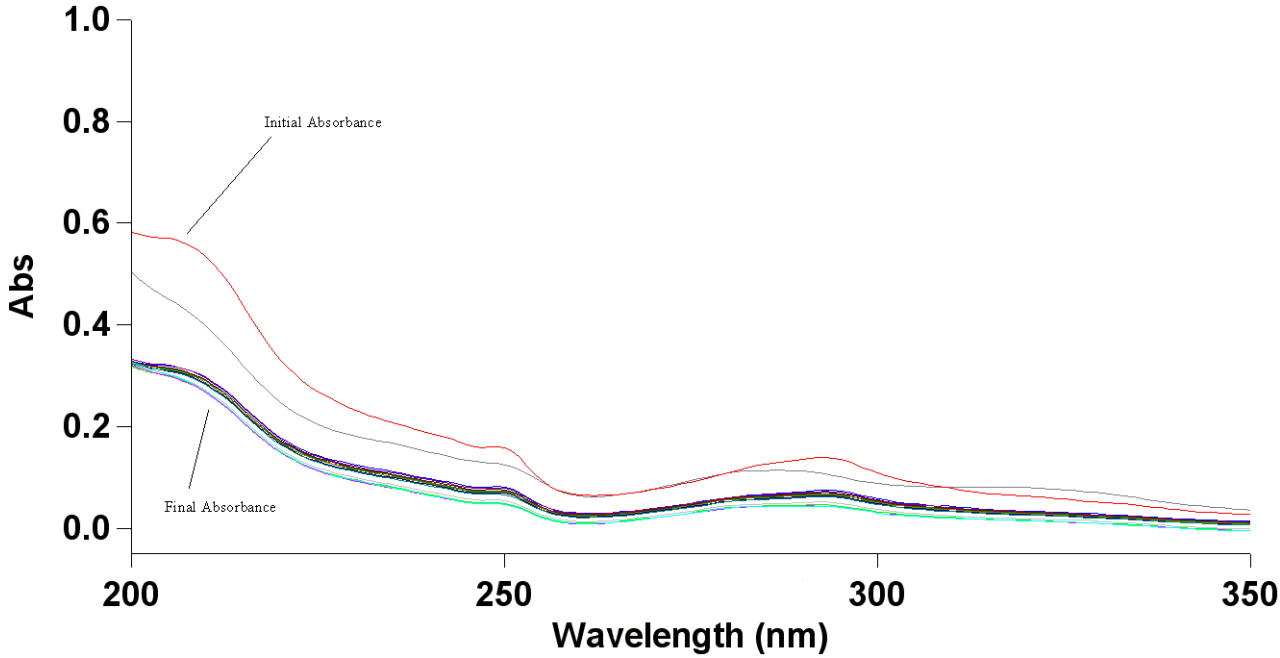

Figure 96: Absorbance versus wavelength (nm) spectra for the 1:1000:1 solution of uranyl(VI), Cd(II), and PDA at concentrations of 2 x 10^{-5} M, 2 x 10^{-2} M, and 2 x 10^{-5} M respectively at 25.0 ± 0.1 °C titrated with NaOH to a pH of approximately 3.4 and observed for 24 hours.

The UV absorbance spectrum for the 24 hour 1:1:1 uranyl(VI), gadolinium(III), and PDA titration where concentrations were all 2 x 10^{-5} M is shown in Figure 97. As it can be seen, the final absorbance of this titration is very similar to that of Figure 95. The log K_1 value of Gd(III) with PDA was previously found to be 14.84.[18] This titration shows that the log K_1 value of uranyl(VI) with PDA is greater then 14.84.

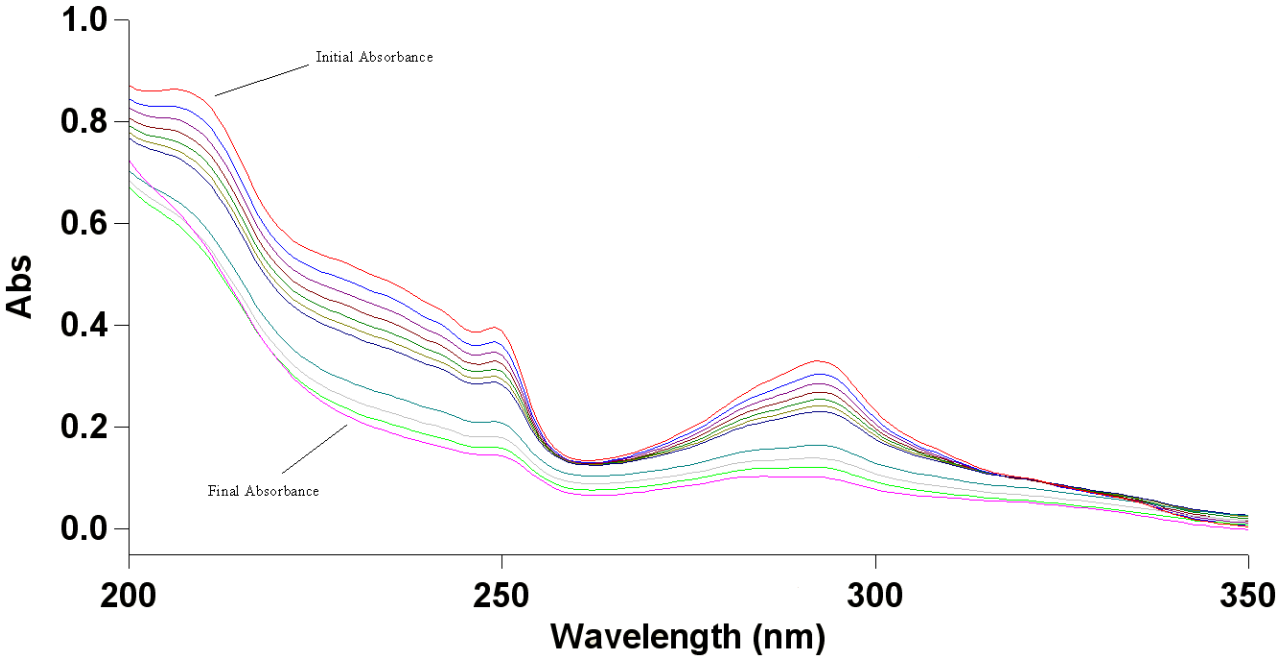

Figure 97: Absorbance versus wavelength (nm) spectra for the 1:1:1 solution of uranyl(VI), gadolinium(III), and PDA all at concentrations of 2 x 10^{-5} M, at 25.0 ± 0.1 °C titrated with NaOH to a pH of approximately 3.85 and observed for 24 hours.

The UV absorbance spectrum for the 24 hour 1:1:1 uranyl(VI), In(III), and PDA titration, where uranyl(VI) was added first, and the concentrations were all 2 x $10^{-5} M$ is shown in Figure 98. The UV absorbance spectrum for the 24 hour 1:1:1 uranyl(VI), In(III), and PDA titration, where In(III) was added first, and the concentrations were all 2 x $10^{-5} M$ is shown in Figure 99. As it can be seen, the final absorbance of the titration where uranyl(VI) was added first is very similar to that of Figure 95. However, the final absorbance of the titration where In(III) was added first does not look like the final absorbance in Figure 95. From previous titrations the log K_1 value of In(III) with PDA was found to be 19.78. These titrations seem to suggest that the log K_1 value of uranyl(VI) with PDA is in the order of 19.78.

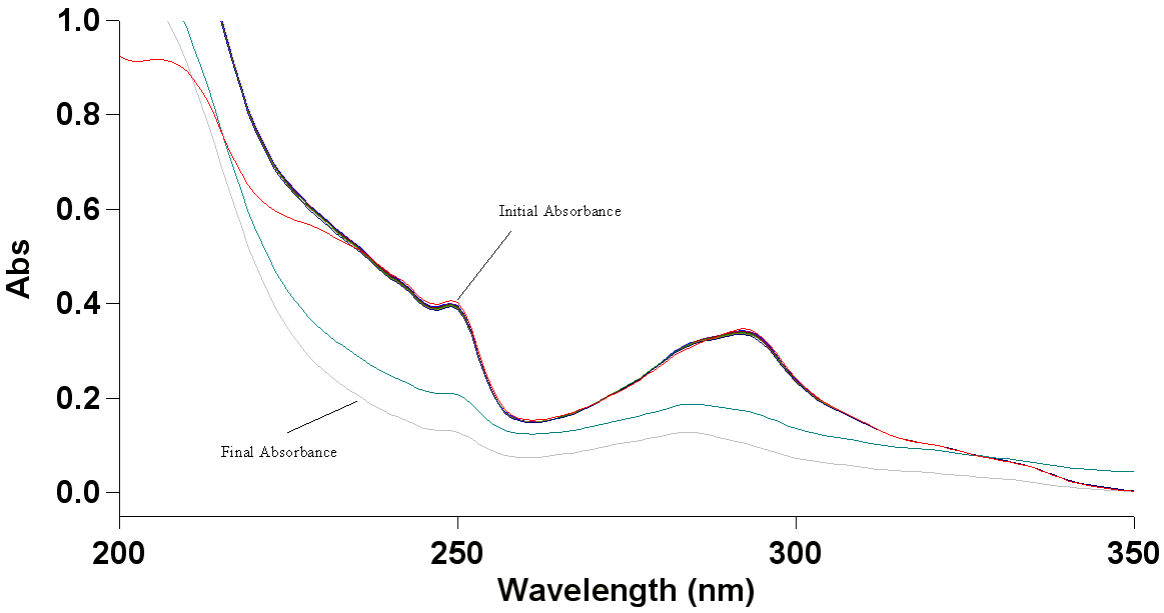

Figure 98: Absorbance versus wavelength (nm) spectra for the 1:1:1 solution of uranyl(VI), In(III), and PDA, where uranyl(VI) was added first, all at concentrations of 2 x 10^{-5} *M*, at 25.0 ± 0.1 °C titrated with NaOH to a pH of approximately 4.38 and observed for 24 hours.

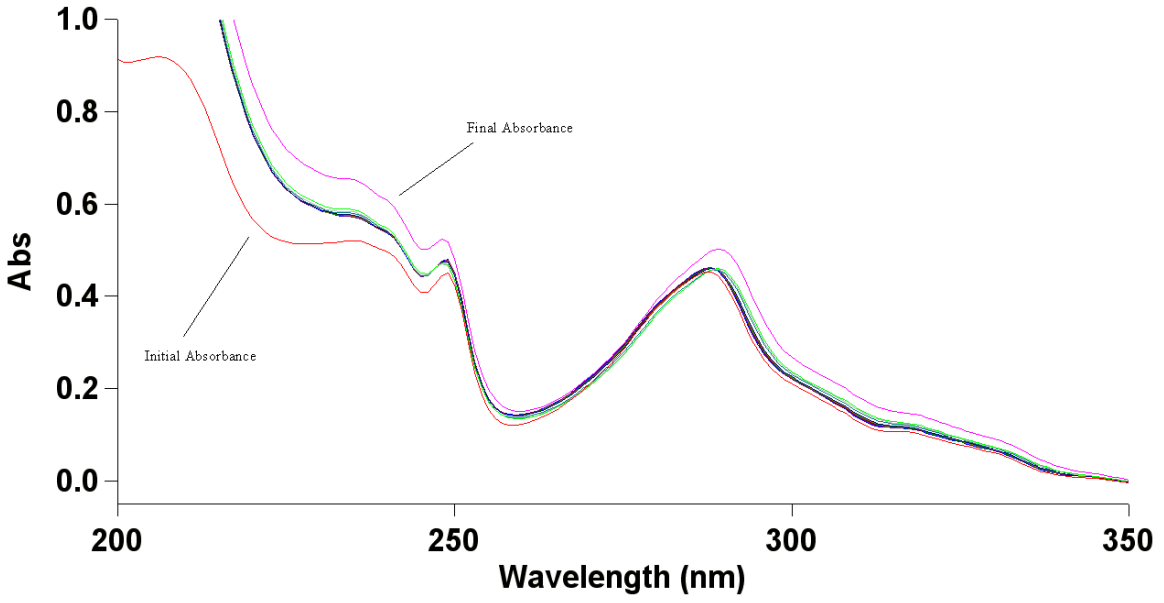

Figure 99: Absorbance versus wavelength (nm) spectra for the 1:1:1 solution of uranyl(VI), In(III), and PDA, where In(III) was added first, all at concentrations of 2 x 10^{-5} *M*, at 25.0 ± 0.1 °C titrated with NaOH to a pH of approximately 3.9 and observed for 24 hours.

The UV absorbance spectrum for the 1:1 uranyl(VI) and PDA titration experiment where the concentration was 2 x $10^{-6} M$ for both is shown in Figure 100. A plot of correlation between E (mV) and the calculated pH, which was used to calculate E^0, is shown in Figure 101. Absorbance values were recorded for the wavelengths 211, 235, 248, 286, and 300 nm. These wavelengths were chosen as they exhibited a large variance in absorbance due to complexation. A graph with the experimental absorbance data fitted with calculated values to determine the protonation constants for the uranyl(VI) and PDA solution is shown in Figure 102. From this data 3 successive pH-dependent equilibria were observed.

$$UO_2(PDA)^+ + OH^- \leftrightarrows UO_2(PDA)OH \qquad (pH = 8.54)$$

$$UO_2(PDA)(OH) + OH^- \leftrightarrows [UO_2(PDA)(OH)_2]^- \qquad (pH = 10.13)$$

$$[UO_2(PDA)(OH)_2]^- + OH^- \leftrightarrows UO_2(OH)_3 + PDA^{2-} \qquad (pH = 12.72)$$

Using $\log K_w = 13.78$, the $\log K_1\ [OH^-]$ of the UO_2-PDA complex can be described as follows.

$$UO_2(PDA)^+ + OH^- \leftrightarrows UO_2(PDA)OH \qquad (\log K_1\ [OH^-] = 7.89)$$

$$UO_2(PDA)(OH) + OH^- \leftrightarrows [UO_2(PDA)(OH)_2]^- \qquad (\log K_2\ [OH^-] = 5.47)$$

$$[UO_2(PDA)(OH)_2]^- + OH^- \leftrightarrows UO_2(OH)_3 + PDA^{2-} \qquad (\log K_{3,4}\ [OH^-] = 2.88)$$

The value of $\log \beta_3 [OH^-]$ for uranyl(VI) is 21.75 and from this value a $\log K_1$ for PDA with uranyl(VI) can be calculated by using the equation shown below.

$$\log K_1 = 21.75 - (1.06 + 3.65 + 5.24) + 6$$

The values in the equation can be identified where 21.75 corresponds to the value of $\log \beta_3 [OH^-]$ for uranyl(VI) and 6 is the negative log of the amount of free ligand at the

isosbestic point. Using this equation the log K_1 for PDA with uranyl(VI) was found to be 17.8. This log K_1 value is not in very close agreement with the previous findings that the value should be in the order of 19.78.

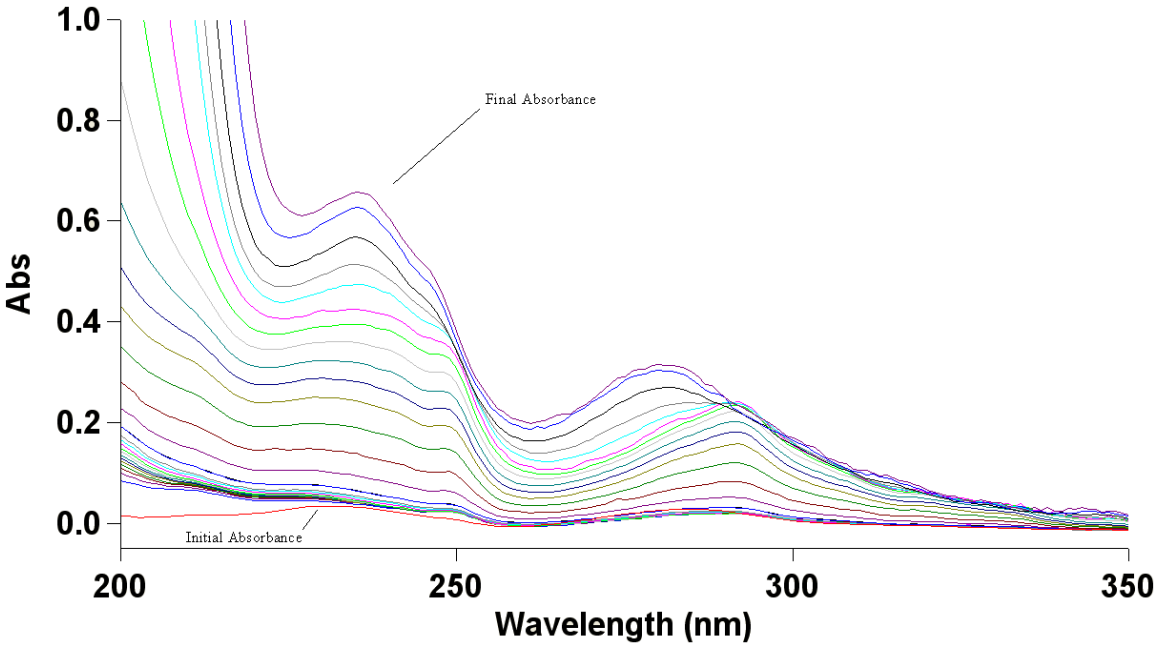

Figure 100: Absorbance versus wavelength (nm) spectra from the titration of the 1:1 solution of uranyl(VI) and PDA both at concentrations of 2 x 10^{-6} M at 25.0 ± 0.1 °C with NaOH with a pH range of approximately 2.5 to 12.

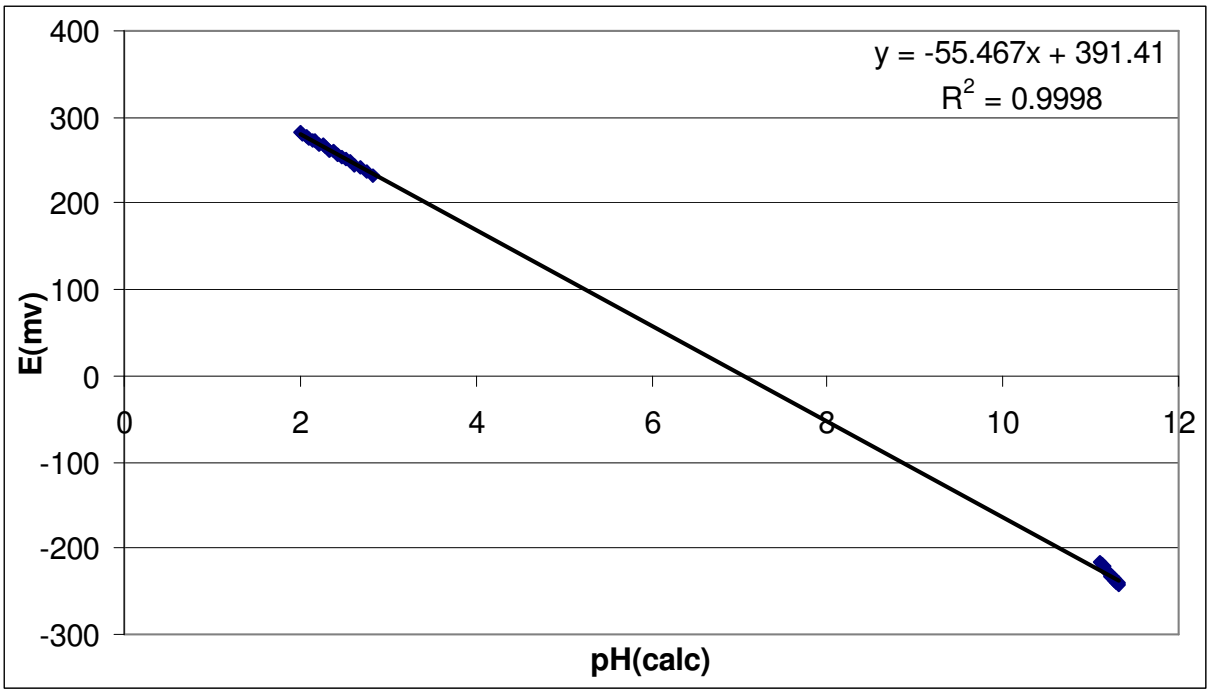

Figure 101: Plot of the correlation between E (mV) and the calculated pH used to calculate E^0 for the titration of a 1:1 solution of uranyl(VI) and PDA both at concentrations of 2 x 10^{-6} *M* at 25.0 ± 0.1 °C with NaOH.

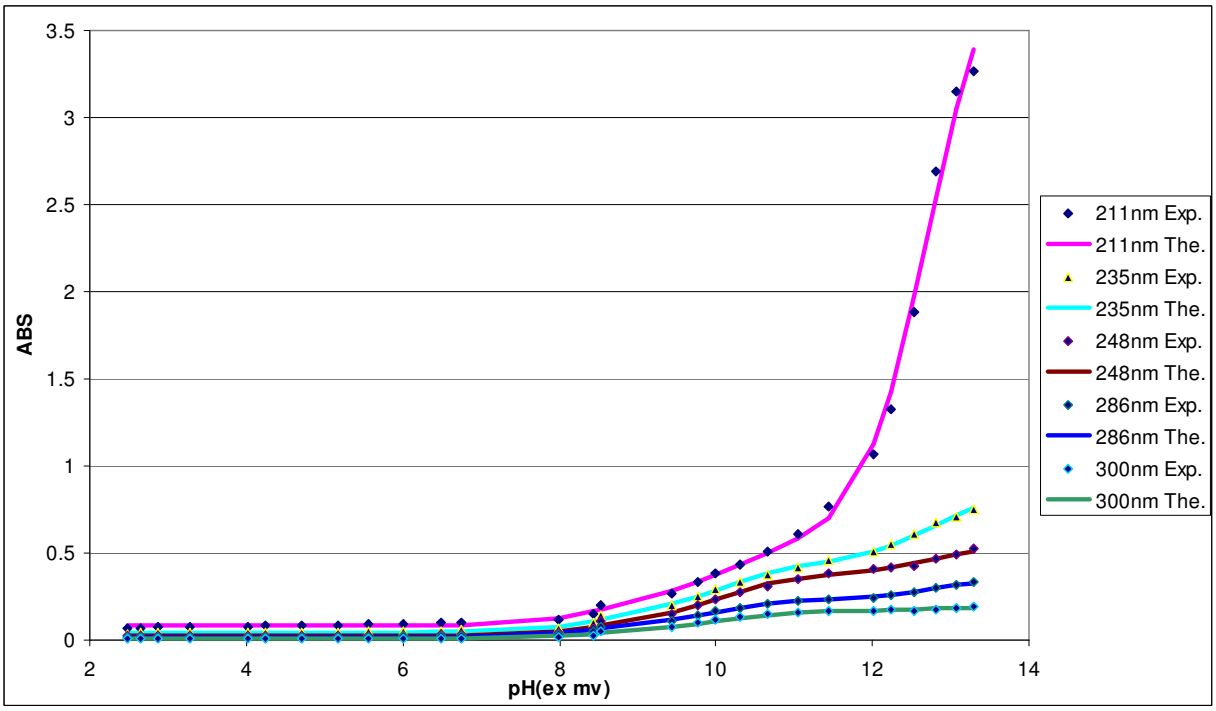

Figure 102: Experimental absorbance data (Exp.) fitted with calculated values (The.) for the titration of a 1:1 solution of uranyl(VI) and PDA both at concentrations of 2 x 10^{-6} *M* at 25.0 ± 0.1 °C with NaOH.

CONCLUSIONS

Macrocycles have often been used in coordination chemistry to enhance the thermodynamic stability of the complexes formed, as well as the metal ion selectivity of ligands. The ability to enable selective chelation is of great importance to inorganic chemistry. This can be done by using ligand donor atoms with higher affinities for the target metal ion which closely match the number of ligand donor atoms with the coordination number of that metal ion. A size-selective framework for the donor atoms of the ligand can also be introduced to the structure to increase selectivity. UV-Vis absorption spectrophotometry proved to be an effective technique for the detection of metal-8PQ complexes in aqueous solutions as a function of pH. Absorption bands for 8PQ in the UV region facilitated the detection of metallation and demetallation of 8PQ.

The ligand 8-(2-Pyridyl)Quinoline (8PQ) did not exhibit a great deal of selectivity toward a specific type of metal ion. In general the formation constants, log K_1 values, obtained for 8PQ with various metal ions were low. The results did show that, in general, as radii of metal ions decreased the formation constants with 8PQ increased. This is a trend that was expected to be seen as 8PQ forms six-membered chelate rings. Also, an increase in log K_1 values was observed when 8PQ was paired with metal ions that could form complexes of low coordination number such as the tetrahedral Cu(I) or square planar Pd(II). Pd(II) is unique in this set of ions in being a very strong Lewis acid, as evidenced by the very high value of log K_1 for BIPY which is 19.8. By observing the trends between 8PQ and BIPY enabled the prediction of log K_1 value of Pd(II) with 8PQ to be 16.4. The graph comparing the differences in log K_1 values of 8PQ and bipyridine can be seen in Figure 13 on page 38. The results of this UV-Vis study of 8PQ prove that

in most cases it is a weak ligand that shows slightly increased selectivity over bipyridine for forming complexes with larger metal ions. These results are counterintuitive as it was expected that 8PQ would show increased selectivity over bipyridine for forming complexes with smaller metal ions. A partial explanation for these results is that fact that 8PQ prefers to be in its *cis* conformation rather then its *trans* conformation which are depicted in Figure 103 below. The *trans* conformation is energetically favored by approximately 3kcal/mol over its *cis* conformation. As 8PQ needs to be in the *cis* formation to complex metal ions its preference to be in the *trans* formation has the effect of lowering its binding constants. This helps to explain why 8PQ was a weaker ligand then was expected.

Figure 103: Images of the *cis* (right) and *trans* (left) conformations of the ligand 8PQ.

UV-Vis absorption spectrophotometry also proved to be an effective technique for the detection of metal-DIPY complexes in aqueous solutions as a function of pH. The absorption bands for DIPY in the UV region facilitated the detection of metallation and demetallation of DIPY. The ligand 2,2'-dipyridyl Amine (DIPY) exhibited a moderate amount of selectivity towards smaller metal ions (0.7-0.5Å). As the metal ion size decreased from 0.9Å to 0.5Å the formations constants with DIPY increased in a nearly

linear fashion. The lone exceptions were Al(III) and Ga(III) which can be explained by the extremely low affinity of Al(III) for N donors and the tendency of Ga(III) to hydrolyze at a relatively low pH. Observing the trends between DIPY and BIPY enables the prediction of log K_1 values of metal ions that were not studied based on their ionic radii. The graph comparing the differences in log K_1 values of DIPY and bipyridine can be seen in Figure 46 on page 78. The results of this UV-Vis study of DIPY prove that it is selective toward small metal ions and exhibits an increase in selectivity over BIPY toward small metal ions. These results are exactly what were expected to be seen for a small six-member chelate ring like DIPY.

UV-Vis absorption spectrophotometry also proved to be an effective technique for the detection of metal-PDA complexes in aqueous solutions as a function of pH. The absorption bands for PDA in the UV region facilitated the detection of metallation and demetallation of PDA. The determination for the formation constant of the PDA-UO_2 (VI) complex proved to be difficult due to the slow kinetics of UO_2 (VI). However, by pairing it with other metal ions, their respective log K_1 values could be compared. The log K_1 value for UO_2 (VI) proved to be greater then those of Cd(II) and Gd(III) which are 12.87 and 14.84 respectively. Comparing UO_2 (VI) with In(III) gave mixed results. This was interpreted to mean that the two metal ions had very similar log K_1 values with PDA. As In(III) was found to have a log K_1 value of 19.78, it is believed that log K_1 value for the PDA-UO_2 (VI) complex is close to, and likely slightly higher than that of the PDA-In(III) complex. This makes the PDA-UO_2 (VI) complex the strongest known uranyl(VI) complex.

LITERATURE CITED

1. Hancock, R. D. and A. E. Martell, *Chem. Rev*., **1989**. *89*. 1875.

2. Guo, Zijian and Peter Sadler. *Angew. Chem. Int. Ed.*, **1999**. *38*. 1512-1531.

3. Pierre, V. C., M. Botta, S. Aime, K. N. Raymond, *J. Am. Chem. Soc.* **2006**. 128. 5344-5345.

4. Kroak, R. W., T. A. Waldeman, R. W. Atcher, and O. A. Gansow, *Trends. Biotechnol.*, **1985**. *4.* 259.

5. Grynkiewicz, G., M. Poenie, and R. J. Tsien, *J. Biol. Chem.*, **1985**. *260*. 3440.

6. Lim, N. C., V. J. Schuster, M. C. Porto, M. A. Tanudra, L. Yao, H. C. Freake, C. Bruckner, *Inorg. Chem.* **2005**. 44. 2018-2030.

7. Cram, D.J., "The design of molecular hosts, guests, and their complexes." Nobel Lecture, **1987**.

8. Pedersen, C.J., *J. Am. Chem. Soc.,* **1967**. *89*. 2495-2496.

9. Pedersen, C.J., *J. Am. Chem. Soc.*, **1967**. *89*. 7017-7036.

10. Dietrich, B. and J. M. Lehn, *Tetrahedron Lett.*, **1969**. 2885-2888.

11. Dietrich, B. and J. M. Lehn, *Tetrahedron Lett.*, **1969**. 2889-2892.

12. Cabbiness, D.K., D. W. Margerum, *J. Am. Chem. Soc.*, **1969**. *91*. 6540.

13. Lehn, J.M., *Acc. Chem. Res.*, **1978**. *11*. 49.

14. Hancock, R. D., *J. Chem. Ed*., **1992**. *69*. 615.

15. Shannon, R. D., *Acta Crystallogr*., **1976**. A32. 751.

16. Hancock, R. D., *Accounts Chem. Res*., **1990**. *26*. 875.

17. Melton, D. L., VanDerveer, D. G., and R. D. Hancock, *Inorg. Chem.*, **2006**. *45*. 9306.

18. Dean, N. E., Hancock, R. D., Cahill, C. L., and M. Frisch, *Inorg. Chem.,* **2008**. *47*. 2000.

19. Pearson, Ralph G., *J. Am. Chem. Soc.*, **1963**. 85. 3533-3539.

20. Delis, Johannes G. P.; Rep, Marco; Ruelke, Richard E.; van Leeuwen, Piet W. N. M.; Vrieze, Kees; Fraanje, Jan; Goubitz, Kees, *Inorganica Chimica Acta*., **1996**. 250(1-2). 87-103.

21. Chandler, C. J., Leslie W. Deady, and James A. Reiss, *J. Heterocyclic Chem.*, **1981**. 18. 599-601.

22. E. J. Billo, *EXCEL for Chemists*, Wiley-VCH, New York, 2001.

APPENDIX

8PQ 8-(2-Pyridyl)Quinoline

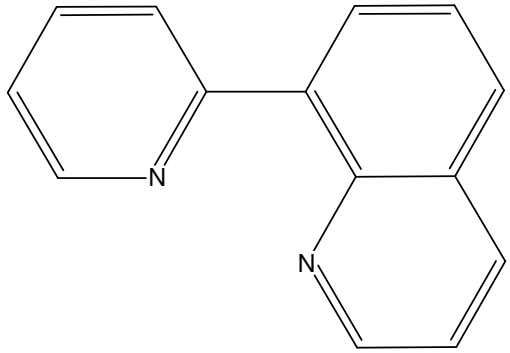

DIPY 2,2'-Dipyridal Amine

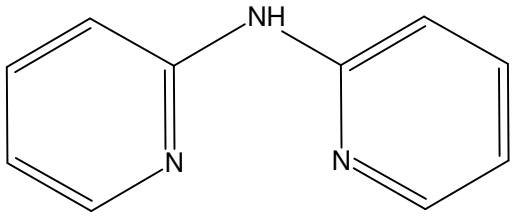

PDA 1,10-Phenanthroline-2, 9-Dicarboxylic Acid